

**Anticariogenic properties of *Dodonaea viscosa* var. *angustifolia* derived
flavone stabilized nanoparticles**

Mpho Audrey Sebelemetja



Degree of Master of Science in Medicine by research only

Dissertation submitted to the Faculty of Health Sciences, University of the Witwatersrand, Johannesburg, in fulfilment of the requirements for the degree of Master of Science in Medicine

Johannesburg 2019

DECLARATION

I, Mpho Audrey Sebelemetja declare that this dissertation is my own work. It is being submitted for the degree of Master of Science in Medicine at the University of Witwatersrand, Johannesburg. It has not been submitted before for any degree or examination at this or any other University.

I declare that this thesis has the approval of The Committee for Research on Human Subjects (Medical). Ethical clearance (W-CJ-170713).

.....

Student signature

.....

Date

DEDICATION

To Prof M Patel (Supervisor), your passion for teaching and sharing knowledge is beyond measure. You are truly an inspiration.

To my family and friends, your love and support for me gives me strength.

PUBLICATIONS AND PRESENTATIONS

Poster presentation

- 100 years of excellence Wits Faculty of Health sciences 2018 Research Day and Postgraduate Expo. 6TH September 2018. Wits Medical school, Parktown Johannesburg.

Oral presentation (Flash talk/ Oral and poster)

- International Association for Dental Research South African Division, 48th Scientific meeting – Oral Presentation and Poster 30-31st August 2018 Muldersdrift lodge, Johannesburg.
- 9th Cross Faculty Postgraduate Symposium- Flash Talk/ Poster presentation 29-30th October 2018. Wits West campus Braamfontein, Johannesburg. Won a second prize in the faculty category.

ABSTRACT

Introduction

Dental caries is the most important oral infection. It is caused by *Streptococcus mutans* due to its ability to form biofilm and the production of acids in the oral cavity. Many oral hygiene products containing antimicrobial chemicals have been used to control and prevent dental caries. Medicinal plants have also been investigated for their ability to prevent dental caries. *Dodonaea viscosa var. angustifolia*, has been found to have this property. However, beneficial concentrations are difficult to maintain in the oral cavity due to continual saliva flow which can be overcome using nanoparticles. The aim of this study was to investigate the anti-cariogenic properties of *Dodonaea viscosa var. angustifolia* (DVA) derived flavone stabilized nanoparticles.

Methods and materials

Stock cultures of *Streptococcus mutans* were obtained from the Oral microbiology laboratory and the DVA plant was collected from Mkhunyanne Eco Reserve in Mpumalanga, South Africa. The leaves were dried and milled to powder. The crude extract was prepared from DVA dried leaves using methanol, which were fractionated to produce six fractions. Fraction F 5 was further fractionated to subfraction F 5.1 and F 5.2. A flavone containing subfraction (subfraction F 5.1) was selected. Subfraction F5.1 was chosen as the main agent due to its antimicrobial activities. Subfraction F5.1 was found to have anti-streptococcus. mutans activity, anti-acidogenic and anti-aciduric properties (Patel et al., 2009; Naidoo et al., 2012 and Ngabaza et al., 2017). Poly lactic-co-glycolic acid (PLGA) and poly ethylene glycol (PEG) were polymerized to form diblock copolymers. These copolymers were then used to synthesize PLGA-PEG nanoparticles, stabilized with the DVA derived subfraction and crude extract. Ten nanoparticles were prepared using PLGA-PEG copolymers. The synthesized products were then used to screen for antimicrobial activity to obtain minimum inhibitory concentrations (MIC) and minimum bactericidal concentration (MBC) using a microtitre broth dilution technique. The most active nanoparticles were chosen and characterized. Further tests were done using the best active nanoparticle mixture (PLGA-PEG subfraction stabilized nanoparticles), subfraction F 5.1 (flavone) and unattached PLGA-PEG nanoparticles (blank). The effect of acid production and biofilm production of the chosen nanoparticles were determined using acid production assay and biofilm production assay

respectively. The subfraction release profile (substantivity) from the nanoparticle's matrix was determined at physiological pH (7.4) and cariogenic pH (5.5) over a period of 12 hours. The cytotoxicity of PLGA-PEG subfraction stabilized nanoparticles was determined using human hepatic cells. Results were analyzed using Wilcoxon sum test (Mann-Whitney) and student T-test.

Results

The ten nanoparticles were divided into two groups depending on the molecular weight: Five nanoparticles were prepared using higher molecular weight (two surface adsorbed nanoparticles, two surface/ encapsulated nanoparticles and one blank nanoparticles) and five nanoparticles were prepared from lower molecular weight (two surface adsorbed nanoparticles, two surface/ encapsulated nanoparticles and one blank nanoparticles). Each group consisted of crude nanoparticles and flavone nanoparticles. The results showed that the ten groups of synthesized nanoparticles had a degree of antimicrobial activity. The median MIC/MBC values of the ten nanoparticles ranged from 25 mg/ml to 1.56 mg/ml. Subfraction stabilized nanoparticles were chosen, and MIC/MBC was repeated.

The nanoparticles retained the known anti-streptococcus. *mutans* property of flavone. PLGA-PEG Subfraction F 5.1 stabilized nanoparticles and blank nanoparticles had a median MIC value of 1.56 mg/ml and 6.25 mg/ml respectively. Sub-inhibitory concentrations of the flavone (P=0.02), subfraction stabilized nanoparticles (P=0.02) and blank nanoparticles (P=0.03) significantly reduced the acid production in *S. mutans*.

Biofilm formation was reduced in all tests with the highest reduction in F 5.1 and lowest reduction in blank nanoparticles. The lowest sub-inhibitory concentration of subfraction F 5.1 stabilized nanoparticles (0.20 mg/ml) reduced biofilm formation by 84.0% after 6 hours of incubation and 85.8% after 24 hours. The lowest sub-inhibitory concentration of blank nanoparticles (0.78 mg/ml) reduced biofilm formation by 35.5% after 6 hours of incubation and 33.8% after 24 hours. The retention and slow release profiles of subfraction F 5.1 stabilized nanoparticles showed good substantivity, with 60% and 40% of the flavone being released over a period of 12 hours at pH of 5.5 and 7.4 respectively. The cytotoxicity profile of subfraction F 5.1 stabilized nanoparticles showed that the nanoparticles are safe to use.

Conclusion

Nanoparticles stabilized with subfraction F 5.1 from the plant DVA which is well known to have anti-streptococcus. *mutans* properties have shown improved potency against *S. mutans* due to the slow release of the subfraction drug from the nanoparticles over a period of 12 hours at a physiological pH (7.4) and at cariogenic pH (5.5). The slow release of the flavone from the nanoparticles showed good substantivity. These results suggest that PLGA-PEG stabilized DVA flavone nanoparticles have the potential to be used as an anti-cariogenic agent.

ACKNOWLEDGEMENTS

I would like to thank my supervisor, Prof. Mrudula Patel (Department of Oral Biological Sciences, University of the Witwatersrand) for giving me the opportunity to pursue my research under her guidance throughout the research and expertise in the field of Microbiology.

My co-supervisor Dr Sharon Moeno (Department of Oral Biological Sciences, University of the Witwatersrand) for her guidance and expertise in the field of Chemistry.

Mrs Zandiswa Gulube (Department of Oral Biological Sciences, University of the Witwatersrand) for her assistance with ordering of laboratory supplies.

Laboratory trainees Malefaso and Matladi (Department of Oral Biological Sciences, University of the Witwatersrand) for their assistance in the laboratory with preparation of media.

I would also like to thank Dr Mpho Ngoepe, Maxwell Thatyana and Khumbulani Mnqiwu (Department of Oral Biological Sciences, University of the Witwatersrand) for their assistance with statistical analysis of all the results and their help in chemistry analysis for the nanoparticles prepared in this study.

.

TABLE OF CONTENTS

Contents	
DECLARATION	ii
DEDICATION	iii
PUBLICATIONS AND PRESENTATIONS	iv
ABSTRACT	v
ACKNOWLEDGEMENTS	viii
TABLE OF CONTENTS	ix
List of figures	xvi
List of tables	xix
List of abbreviations and acronyms	xxii
CHAPTER 1	1
Introduction	1
1. Literature Review	3
1.1. Dental caries	3
1.2. Factors influencing the development of dental caries	5
1.2.1. Host factors (Teeth and saliva)	6
1.2.2. Microorganisms	7
1.2.2.1. <i>Streptococcus mutans</i>	8
1.2.2.2. <i>Lactobacillus</i> spp.	10
1.2.3. Diet	10
1.2.4. Quantity and frequency of consumption	11
1.3. Prevention of dental caries	11
1.3.1 Saliva	12
1.3.2 Sucrose intake	13
1.3.3. Antimicrobial agents used in prevention of caries	14
1.3.3.1. Fluoride	14

1.3.3.2. Chlorhexidine gluconate.....	15
1.3.3.3. Triclosan	16
1.4 Treatment of dental caries	16
1.5. Pharmacologic effects of plants.....	16
1.6. <i>Dodonaea viscosa var. angustifolia</i> (DVA).....	17
1.6.1. Chemical constituents of DVA.....	18
1.6.2 Structure of a flavonoid	18
1.6.3. Classification of Flavonoids	19
1.6.4. Study flavonoid- Flavone	22
1.7. Nanotechnology and delivery systems	22
1.7.1. Nanomaterials.....	23
1.7.1.1. Metallic nanoparticles.....	23
1.7.1.2. Polymeric Nanoparticles.....	23
1.7.2. Study polymers:.....	24
1.7.2.1. Poly (lactic-co-glycolic acid) polymers.....	24
1.7.2.2. Poly (ethylene) glycol polymers (PEG).....	26
1.7.2.3. PEG-PLGA copolymers	27
1.8. Cytotoxicity of nanoparticles.....	28
1.9 Aim.....	29
1.10 Objectives	29
1.11. Dissertation plan.....	30
CHAPTER 2	31
2.1. Materials and methods	31
2.1.1 Test Cultures and inocula	31
2.1.2. Plant material.....	31
2.2. Extraction and purification	31
2.2.1. Column chromatography	32

2.2.2. Thin layer chromatography	33
2.2.3. Purification of F 5.1	33
2.4. Identification of subfraction F 5.1	34
2.4.1. Ultra violet visible spectroscopy (UV-vis).....	34
2.4.2. Fourier Transform Infrared spectroscopy analysis (FTIR).....	34
2.4.3 Gas Chromatography-Mass Spectroscopy.....	34
2.5. Synthesis of beneficial nanoparticles	35
2.5.1 Synthesis of copolymers	35
2.5.2. Synthesis of nanoparticles	37
2.5.3. Purification of nanoparticles.....	38
2.6. Characterization of nanoparticles	38
2.6.1. UV-vis spectroscopy of nanoparticles	38
2.6.2 Fourier Transform Infrared spectroscopy analysis (FTIR) - Nanoparticles	39
2.6.3. Transmission Electron Microscopy and Scanning Electron Microscopy.....	39
2.6.4. Dynamic Light Scattering (Zeta sizer)	39
2.6.5. Determination of drug loading and drug entrapment efficiency	39
2.7. <i>In vitro</i> drug release study	40
2.8. Minimum inhibitory concentrations and Minimal bactericidal concentrations.....	40
2.9. Effect of chemical constituents on acid formation by <i>S. mutans</i>	41
2.10. Effect of chemical constituents on biofilm formation by <i>S. mutans</i>	42
2.11. Cytotoxicity assay.....	42
2.11.1. Cell culturing	42
2.11.2. Determination of cell count and viability	43
2.11.3. Seeding of cells into the microtitre plate and exposures	44
CHAPTER 3	45
RESULTS.....	45
3.1. Extraction and purification	45

3.1.1. Extraction.....	45
3.1.2. Column chromatography	45
3.1.3. Thin layer chromatography	46
3.2. Characterisation of subfraction F 5.1	46
3.2.1. UV-vis spectroscopy analysis of subfraction F 5.1	46
3.2.2 Fourier transform infrared spectroscopy (FTIR) analysis of Subfraction F 5.1	47
3.2.3 Gas Chromatography-Mass Spectrometry analysis of subfraction F 5.1	48
3.3. Synthesis of nanoparticles	49
3.4. Characterisation of synthesized nanoparticles.....	50
3.4.1 UV-vis spectroscopy analysis of synthesized nanoparticles	50
3.4.2. Fourier Transform Infrared spectroscopy analysis of nanoparticles	51
3.4.3. Particle size and morphology	54
3.4.3.1. Transmission electron microscopy	54
Table 3.7: Summary of the measurements obtained from Image J analysis of subfraction F 5.1 stabilized nanoparticles (using Image: Figure 3.10)	56
.....	56
Figure 3.10: Histogram of the distribution of nanoparticles (using image 3.7)	56
3.4.3.2. Scanning electron microscopy.....	57
3.4.4. The influence of pH on Zeta size and Zeta potential.....	59
3.4.4.1. The influence of pH Zeta size and Zeta potential of PLGA-PEG blank nanoparticles.....	59
3.4.4.2. The influence of pH on Zeta size and Zeta potential of PLGA-PEG F 5.1 nanoparticles.....	60
3.4.4.3. The influence of pH on Zeta potential of PLGA-PEG copolymers, PLGA-PEG blank nanoparticles and subfraction F 5.1 nanoparticles.....	62
3.5. Drug (Subfraction F 5.1) entrapment analyses	63
3.5.1. Determination of drug loading and drug entrapment	63
3.5.2. Drug release profile	64

3.5.3. Release kinetics model of nanoparticles.....	66
3.6. Antimicrobial study	69
3.6.1. Screening of subfraction F 5.1 and crude extract	69
3.6.2. Screening of prepared nanoparticles.....	69
3.6.3. Screening of selected nanoparticles.....	72
3.7. The effect of beneficial compounds on acid production by <i>S. mutans</i>	73
3.7.1. The effect of subfraction F 5.1 on acid production	73
3.7.2. The effect of subfraction F 5.1 nanoparticles on acid production	78
3.7.3. The effect of blank nanoparticles on acid production by <i>S. mutans</i>	82
3.7.4. Summary of the effects of compounds on the acid production assay	86
3.8. The effect of beneficial compounds on biofilm production by <i>S. mutans</i>	88
3.8.1 The effect of subfraction F 5.1 on biofilm production by <i>S. mutans</i>	88
3.8.2. The effect of subfraction F 5.1 surface stabilized nanoparticles on biofilm formation by <i>S. mutans</i>	92
3.8.3. The effect of blank nanoparticles on biofilm formation by <i>S. mutans</i>	96
3.8.4: Summary of the effect of compounds on biofilm formation by <i>S. mutans</i>	100
3.9. Cytotoxicity study.....	102
3.9.1. The effect of subfraction F 5.1 on the viability of cells	102
3.9.2. The effect of subfraction F 5.1 stabilized nanoparticles on the viability of cells.	104
3.9.3 The effect of blank nanoparticles on the viability of cells.	106
3.9.4. Summary of the cytotoxicity effects of compounds on Hep2 cells	108
CHAPTER 4	109
DISCUSSION	109
4.1. Fractionation of crude extract.....	110
4.2 Characterisation of subfraction F 5.1	110
4.3. Synthesis of Nanoparticles	111
4.4. Characterisation of nanoparticles	111
4.4.1. UV-vis spectroscopy and FTIR	111

4.4.2. Particle size and morphology	112
4.4.3. Zeta potential and size distribution (Poly Dispersity Index)	112
4.5. Drug entrapment analyses	114
4.5.1. Drug loading and drug entrapment	114
4.5.2. Release profiles of F 5.1 from nanoparticles	114
4.6. MIC/MBC.....	116
4.7. Acid production of subfraction 5.1 and prepared nanoparticles.....	117
4.8. Biofilm formation of subfraction 5.1 and the beneficial nanoparticles	118
4.9. Cytotoxicity study of subfraction F 5.1 and the prepared nanoparticles	119
4.10. Clinical implications.....	121
CHAPTER 5	123
5.1. CONCLUSION	123
5.2. Limitations to the study	124
5.3. Future research	125
CHAPTER 6	126
REFERENCES.....	126
CHAPTER 7	136
APPENDICES.....	136
Appendix I: Preparation of media and its composition	136
Appendix II: Ethical clearance letter	139
Appendix III: Modification of Ethical clearance waiver	140
Appendix IV: Cell count worksheet	141
Appendix V: Fourier Transform Infrared spectroscopy analyses PLGA-PEG Copolymers	142
Appendix VI: Fourier Transform Infrared spectroscopy analyses F5.1	143
Appendix VII: Fourier Transform Infrared spectroscopy analyses of Blank nanoparticles	144

Appendix VIII: Fourier Transform Infrared spectroscopy analyses PLGA-PEG F5.1NPs	145
Appendix IX: Abstract for the conference presentation.....	146

List of figures

Figure 1.1:	Factors that are involved in the dental caries process (Helwitz, 2007)	5
Figure 1.2:	The important functions of saliva (Amerongen and Veerman, 2012)	7
Figure 1.3:	The basic structure of a flavonoid (Panche <i>et al.</i> , 2016)	19
Figure 1.4:	The classification of flavonoids (Panche <i>et al.</i> , 2016)	19
Figure 1.5:	The structure of PLGA and its monomers (Gentile <i>et al.</i> , 2014)	25
Figure 1.6:	Plan of dissertation	30
Figure 2.1:	Schematic diagram of the synthesis of copolymers.....	36
Figure 2.2:	Summary of the synthesis of nanoparticles	38
Figure 3.1:	Spectrum bands of subfraction F 5.1 observed using UV-vis spectroscopy...47	
Figure 3.2:	Fourier Transform infrared spectroscopy analysis of subfraction F 5.1.....47	
Figure 3.3:	Gas chromatography-mass spectroscopy chromatogram of Subfraction F 5.1	49
Figure 3.4:	The spectrum bands of 50:50 PLGA-PEG nanoparticles attached with subfraction F 5.1	51
Figure 3.5:	Fourier Transform Infrared spectroscopy analysis of PLGA-PEG copolymers	52
Figure 3.6:	Fourier Transform Infrared spectroscopy analysis of F 5.1 stabilized nanoparticles	53
Figure 3.7:	Transmission electron micrograph of PLGA-PEG copolymers	55
Figure 3.8:	Transmission electron micrograph of PLGA-PEG blank nanoparticles	55
Figure 3.9:	Transmission electron micrograph of PLGA-PEG subfraction F 5.1 nanoparticles.....	55
Figure 3.10:	Histogram of size distribution of nanoparticles	56
Figure 3.11:	Scanning electron micrograph of PLGA-PEG copolymers	58
Figure 3.12:	Scanning electron micrograph of PLGA-PEG blank nanoparticles	58

Figure 3.13: Scanning electron micrograph of PLGA-PEG subfraction F 5.1 stabilized nanoparticles	58
Figure 3.14: The effect of pH on size and PDI PLGA-PEG blank nanoparticles	60
Figure 3.15: The effect of pH on size and PDI of subfraction F 5.1 nanoparticles	61
Figure 3.16: The influence of pH on Zeta potential of PLGA-PEG blank nanoparticles and subfraction F 5.1 nanoparticles	62
Figure 3.17: Standard curve for the concentrations of subfraction F 5.1	65
Figure 3.18: The amount of drug (F 5.1) released from nanoparticles over a period of 12 hours	68
Figure 3.19: The percentage drug (F 5.1) dissolution from nanoparticles over a period of 12 hours	68
Figure 3.20: The effect of subfraction F 5.1 on acid production of <i>S. mutans</i> in acid assay	77
Figure 3.21: The effect of subfraction F 5.1 on the growth of <i>S. mutans</i> in acid production	77
Figure 3.22: The effect of subfraction F 5.1 nanoparticles on acid production of <i>S. mutans</i> in acid assay	81
Figure 3.23: The effect of subfraction F 5.1 nanoparticles on growth of <i>S. mutans</i> in acid assay	81
Figure 3.24: The effect of blank nanoparticles on acid production of <i>S. mutans</i> in acid assay	85
Figure 3.25: The effect of blank nanoparticles on growth of <i>S. mutans</i> in acid assay.....	85
Figure 3.26: The effect of subfraction F 5.1 on biofilm formation <i>S. nutans</i> after 6 and 24 hours of exposure	91
Figure 3.27: The effect of subfraction F 5.1 nanoparticles on biofilm formation by <i>S. nutans</i> after 6 and 24 hours of exposure	95
Figure 3.28: The effect of blank nanoparticles on biofilm production by <i>S. nutans</i> after 6 and 24 hours of exposure	99
Figure 3.29: Viability of cells exposed to F 5.1 expressed as percentage.....	104

Figure 3.30: Viability of cells exposed to F 5.1 nanoparticles expressed as percentage...106

Figure 3.31: Viability of cells exposed to blank nanoparticles expressed as percentage...108

List of tables

Table 1.1:	Prevalence of dental caries and untreated caries by age group in South Africa (Singh, 2011)	4
Table 1.2:	Flavonoids of <i>Dodonaea viscosa</i> (Rani <i>et al.</i> , 2009).....	21
Table 2.1:	Ratios of the solvents used in the elution process of crude extract.....	32
Table 2.2:	The mass and molecular weights of polymers used to synthesise copolymers	36
Table 3.1:	The percentage yield of methanolic crude extract.....	45
Table 3.2:	Absorption vibration bands observed in subfraction F 5.1.....	48
Table 3.3:	Prepared nanoparticles and their measurements.....	50
Table 3.4:	Yields obtained from synthesis of subfraction F 5.1 surface adsorbed nanoparticles	50
Table 3.5:	Fourier Transform Infrared spectroscopy analysis of PLGA-PEG copolymer.....	53
Table 3.6:	Fourier Transform Infrared spectroscopy analysis of subfraction F 5.1 nanoparticles	54
Table 3.7:	Summary of the measurements obtained from Image J analysis of subfraction F 5.1 stabilized nanoparticles (using Image: Figure 3.8)	56
Table 3.8:	The influence of pH Zeta size and Zeta potential of PLGA-PEG blank nanoparticles	59
Table 3.9:	The influence of pH on Zeta size and Zeta potential of PLGA-PEG F 5.1 nanoparticles	61
Table 3.10:	Summary of particle size and surface charge of PLGA-PEG copolymers, blank nanoparticles and subfraction F 5.1 stabilized nanoparticles (F5.1/NPs)	63
Table 3.11:	Concentrations of subfraction F 5.1 calculated from the absorbances obtained from UV-vis spectroscopy	64
Table 3.12:	The amount of F 5.1 released from nanoparticles over a period of 12 hours...	66
Table 3.13:	Mathematical release model of F 5.1 from the nanoparticles.....	67

Table 3.14:	Antimicrobial screening of crude extract, subfraction F 5.1 against <i>Streptococcus mutans</i> strains	69
Table 3.15:	Antimicrobial screening of 50:50 and 85:15 PLGA-PEG nanoparticles against <i>Streptococcus mutans</i> strains	71
Table 3.16:	Antimicrobial activity of synthesised nanoparticles against <i>S. mutans</i>	72
Table 3.17:	Concentrations of the beneficial compounds used in acid assay and biofilm assay.....	73
Table 3.18:	The effect of subfraction F 5.1 on acid production by <i>S. mutans</i>	75
Table 3.19:	The effect of subfraction F 5.1 on the growth of <i>S. mutans</i> in acid assay.....	76
Table 3.20:	The effect of subfraction F 5.1 nanoparticles on acid production on <i>S. mutans</i>	79
Table 3.21:	The effect of subfraction F 5.1 nanoparticles on the growth of <i>S. mutans</i> in Acid production	80
Table 3.22:	The effect of blank nanoparticles on acid production by <i>S. mutans</i>	83
Table 3.23:	The effect of blank nanoparticles on the growth of <i>S. mutans</i> in Acid assay.....	84
Table 3.24:	The statistical comparison between control and tests in acid assay.....	87
Table 3.25:	The effect of sub-inhibitory concentrations of subfraction F 5.1 on biofilm formation by <i>S. mutans</i>	89
Table 3.26:	The log conversion of bacterial count of <i>S. mutans</i> in biofilm formation: subfraction F 5.1	90
Table 3.27:	The percentage reduction in biofilm production by <i>S. mutans</i> : F 5.1	91
Table 3.28:	The effect of sub-inhibitory concentrations of subfraction F 5.1 stabilized nanoparticles on biofilm formation by <i>S. mutans</i>	93
Table 3.29:	Log conversion of Bacterial counts in biofilm formation by <i>S. mutans</i> : Subfraction F 5.1 stabilized nanoparticles	94

Table 3.30:	The percentage reduction in biofilm by <i>S. mutans</i> : subfraction F 5.1 stabilized nanoparticles	95
Table 3.31:	The effect of sub-inhibitory concentrations of blank nanoparticles on biofilm formation by <i>S. mutans</i>	97
Table 3.32:	Log conversion of Bacterial counts in biofilm formation by <i>S. mutans</i> : Blank nanoparticles	98
Table 3.33:	The percentage reduction in biofilm production by <i>S. mutans</i> : Blank nanoparticles	99
Table 3.34:	Statistical comparison between control and tests in biofilm formation by <i>S. mutans</i>	101
Table 3.35:	Cytotoxicity assay absorption values of subfraction F 5.1	103
Table 3.36:	Cytotoxicity assay absorption values of subfraction F 5.1 nanoparticles.....	105
Table 3.37:	Cytotoxicity assay absorption values of blank nanoparticles.....	107

List of abbreviations and acronyms

ATCC:	American Type Culture Collection
ATR:	Acid tolerance response
CFU/ml:	Colony forming units per millilitre
CO ₂ :	Carbon dioxide
DCM:	Dichloromethane
DEF:	Dichloromethane/ ethyl acetate/ formic acid
DMEM:	Dulbecco's modified eagle medium
DMSO:	Dimethyl sulphoxide
DVA:	<i>Dodonaea viscosa var. angustifolia</i>
EMW:	Ethyl acetate/ methanol/ water
eV:	Electron volt
FBS:	Fetal bovine serum
FTIR:	Fourier transform infrared spectroscopy
GA:	Glycolic acid
GC-MS:	Gas chromatography - Mass spectrophotometer
GTF:	Glucosyltransferase
HEP:	Human epithelial cells
INT:	Iodotetrazolium dye
kDa:	Kilodalton
kV:	Kilovolt
LA:	Lactic acid
MBC:	Minimum bactericidal concentration
MePEG:	Methoxy Poly ethylene glycol

mg/ml:	milligrams per millilitre
MIC:	Minimum inhibitory concentration
MRC:	Medical research council
mTorr:	Milli Torr
MTT:	3-(4-5-dimethyl thiazol-2-yl)-2-,5-diphenyl tetrazolium bromide
nm:	nanometre
NMR:	Nuclear magnetic resonance
NPs:	Nanoparticles
PBS:	Phosphate buffered saline
PEG:	Poly ethylene glycol
PLGA:	Poly-lactic-co-glycolic acid
PLGA-PEG:	Poly-lactic-co-glycolic acid- Poly ethylene glycol copolymer
PVA:	Polyvinyl alcohol
rpm:	Revolutions per minute
<i>S. mutans</i> :	<i>Streptococcus mutans</i>
TEA:	Toluene/ ethanol/ ammonium hydroxide
TLC:	Thin layer chromatography
TSB:	Tryptic soy broth
UV:	Ultra violet light
UV-vis:	Ultra violet spectrometer

CHAPTER 1

Introduction

The most densely populated site of the body is the oral cavity which contains approximately 700 species of microorganisms. Recently developed molecular biological techniques have been used for the isolation of these oral cavity microorganisms. A microbial consortium also known as dental plaque or oral biofilm is usually found at the oral surfaces where these microorganisms form colonies (Kilian *et al.*, 2016). These microorganisms live in harmony however, if opportunity is given, they can cause infections such as dental caries and periodontal diseases.

Dental caries and periodontal diseases are the most detrimental oral infections that pose a major health problem globally. A prevalence of up to 90% has been observed in school aged children and the majority of adults are also affected (Palombo, 2011). Two pathogens (*Mutans streptococci* and *Porphyromonas gingivalis*) have been recognised as the microorganisms that are responsible for causing dental caries (Kilian *et al.*, 2016).

Treatment of dental infections imposes an economic burden, with tooth decay and periodontal infections being the most expensive infections that most individuals struggle with during their lifetime (Griffin *et al.*, 2012). As a result, the cost of dental treatments every year amounts to billions of dollars. The public expenditure reported by World Health Organisation to be related to dental care is as high as that 5-10% (Henly-Smith *et al.*, 2013).

Many plants including medicinal plants have anti-microbial effects against oral bacteria, this has drawn attention to the use of these plants. The history of traditional use of plants for various diseases has been seen in many civilisations (Teffo *et al.*, 2010). The major parts of the plants used were fresh or dried roots, stems, leaves and barks. This is due to the plant's structural diversities and their secondary metabolites which offer a wide range of natural antioxidants (Teffo *et al.*, 2010).

Various ailments have been treated using *Dodonaea viscosa* which is a well-known indigenous. Leaves of this plant have been found effective against sore throat, wounds, fever, malaria, angina, cold, arthritis, sinusitis, flu and boils (Khan *et al.*, 2012). In addition, it has been used for oral candidiasis (Patel *et al.*, 2009), rheumatism, skin infections, diarrhoea,

stomach aches, pains of hepatic or splenic origin, uterine colic and other disorders involving smooth muscles (Getie *et al.*, 2003).

Previous studies have shown that the compounds isolated from this plant exhibit antibacterial, antiviral, antifungal and anti-inflammatory activities (Khan *et al.*, 2012). A study by Naidoo *et al.*, (2012) reported that *D. viscosa* has anti-streptococcus. *mutans* properties and can be used as a prophylaxis for oral infections, including dental caries. Further studies on the plant were done to isolate the compound responsible for its antibacterial effects. The compounds were identified as a class of flavones (Ngabaza *et al.*, 2017). A flavone isolated from DVA plant has been shown to have beneficial effects against dental caries which can be improved using nanoparticles. Therefore, Nano-delivery systems for medicinal plant extract should be developed to conquer difficulties such as the microbe's ability to develop resistance and improve effectiveness, stability, absorption, metabolism, excretion and economic feasibility of the extract nanoparticle product.

1. Literature Review

1.1. Dental caries

Dental caries is an endogenous chronic infection caused by the normal commensal oral flora. It is a localised progressive tooth decay which is multifactorial. The disease is brought by interaction of host factors, plaque bacteria and diet (Sima *et al.*, 2016). These factors can be attributed to dietary habits such as ingestion of sugar, the differences in patterns of oral hygiene, variations in the virulence of the dental plaque and changes in the oral protective mechanism including the immune status (Ferrazzano *et al.*, 2009). The occurrence of 99% of carious lesions is observed in permanent teeth and molar teeth as the plaque tends to mature in these areas which are relatively protected from mechanical wear by the tongue, cheeks, and tooth brushing (Metwalli *et al.*, 2013).

Historically, dental caries has been considered as an oral health burden of global importance with high prevalence. Dental caries prevalence worldwide is as high as nearly 100% of the population (Menon *et al.*, 2018). In the United states the prevalence of dental caries is 42% in children with caries occurring in primary teeth. This prevalence of caries has been observed in children aged between 2 and 11 years old. In adults, the worldwide prevalence of dental caries and periodontal disease is 60-90% (Metwalli *et al.*, 2013).

Sixty-eight percent of children aged 12 years in over 184 countries have had decayed/missing/filled (DMFT) tooth according to the country or area profile oral health programme. The oral health programme suggests that, the incidence of caries in developed countries has declined steadily. The same trend has been observed in the South African Oral health profile, the incidence of caries decreased from 2.5 to 1.1% in 2003 (Singh, 2011). The percentage of children in South Africa who need caries treatment range from 45 to 60%. These results were obtained from a prevalence study for caries which was done in all the provinces in South Africa among 4 to 6 years old, 12 years and 15 years old aged children by the World Health organisation (Table 1, Singh, 2011). Although the results show a decrease in prevalence of caries in South Africa, the rate for untreated caries is still high. The results depict what is seen in children only and not adults. The combined rate for treatment required for children together with adults can be ten times higher. The results presented in Table 1.1 suggest that treatment for dental caries is still in high demand amongst South African children.

Table 1.1: The prevalence of dental caries in South Africa in children (Singh, 2011)

	Age group (Years)							
	4-5 *		6 *		12		15	
	(%)		(%)		(%)		(%)	
	Caries	Untreated caries	Caries	Untreated caries	Caries	Untreated caries	Caries	Untreated caries
Weighted National mean	50.6	46.6	60.3	55.1	6.3	5.1	36.9	30.3
Western Cape	77.1	72.0	82.3	75.2	9.6	6.9	61.8	51.6
Northern Cape	-	-	84.1	82.7	16.4	14.8	47.3	44.2
Eastern Cape	58.9	53.7	67.7	63.6	4.1	3.7	49.0	32.7
Free State	60.1	57.8	59.2	56.8	4.9	4.0	36.8	33.3
Kwa-Zulu Natal	52.4	50.8	64.8	59.9	6.2	5.3	38.7	34.9
Gauteng	49.1	37.6	59.7	50.5	4.9	3.9	34.3	26.6
North West	41.0	39.5	52.3	48.2	7.8	7.4	27.5	25.0
Mpumalanga	40.2	35.1	56.2	48.4	10.1	4.8	29.7	26.6
Limpopo	31.3	30.8	37.2	33.8	4.9	4.8	15.8	14.1

***Primary dentition**

Dental caries is an infectious, multifactorial and multi-microbial disease. It is caused by biofilm or plaque associated oral bacteria which metabolise dietary carbohydrates and produce acids. These acids lower the plaque pH to critical pH of 5.5 and below. At this pH, calcium and phosphate carbonate diffuse out (demineralization) of the upper layer of the tooth structure called enamel. Chronic demineralization will eventually result into cavitation or dental caries (Helwitz *et al.*, 2007). In the early stages, demineralization can be reversed through replacement of those lost ions (remineralization). Therefore, the balance between demineralization and remineralization is crucial for the progression of dental caries. When

plaque (biofilm) remains on the surface and matures over a long period, carious lesions develop (Helwitz *et al.*, 2007).

1.2. Factors influencing the development of dental caries

The development of caries is generally dependent on the lifestyle and behavioural factors. The frequent intake of carbohydrates and poor oral hygiene, poor dietary habits, and frequent use of oral medications are some of the factors that lead to the development of caries (Helwitz, 2007). Poverty and social status also influence the risk of caries. Other factors related to caries include the use of orthodontic appliances and dental sealants, or poorly designed dentures. However, the most important factors implicated in the development of dental caries are oral environment (saliva and teeth), microorganisms and diet (Figure 1.1, Helwitz, 2007).

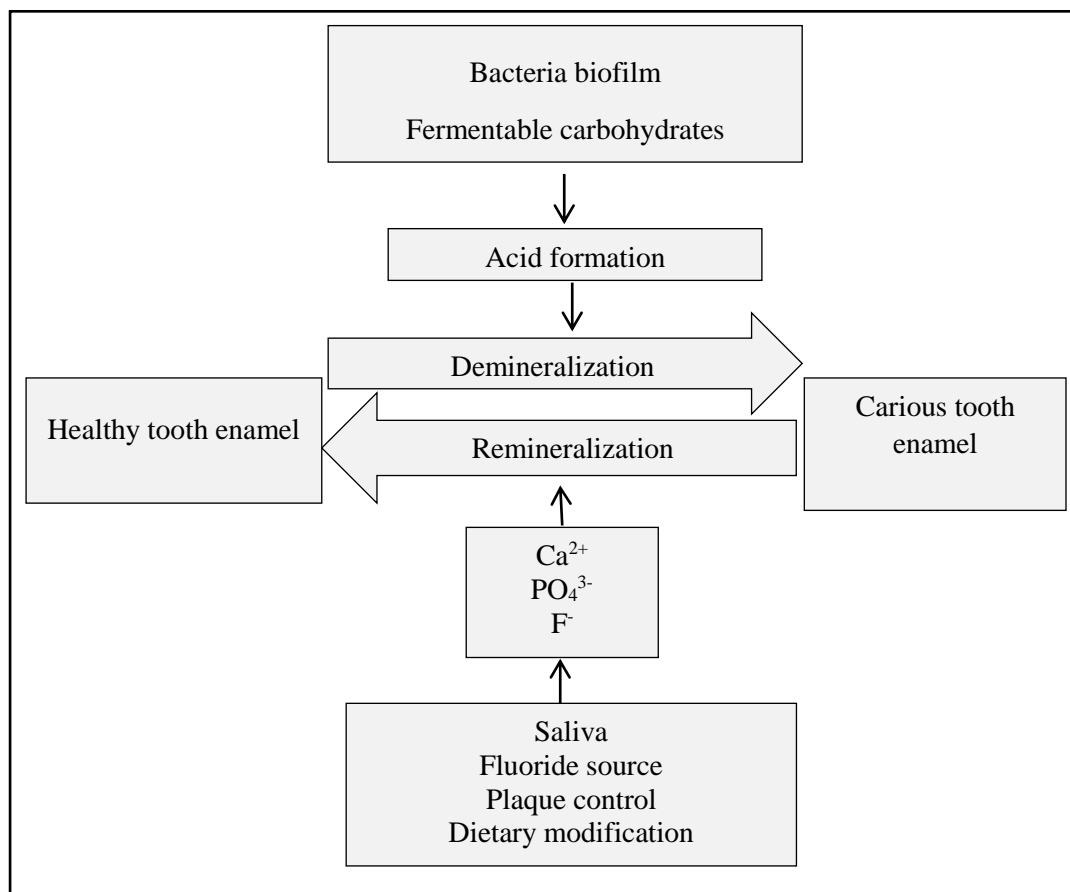


Figure 1.1: Factors that are involved in the dental caries process (Helwitz, 2007)

1.2.1. Host factors (Teeth and saliva)

The oral cavity is made up of four major habitats namely the buccal mucosa, the dorsum of the tongue, the tooth surface and the crevicular epithelium. These are referred to as natural habitats whereas the prosthodontic and orthodontic appliances are referred to as fifth habitat of the oral cavity. The tooth surface is further divided into two main habitats where plaque accumulates, the supragingival and subgingival plaque. The subgingival plaque is found in the shallow crevice that surrounds the teeth located in the gingival surface. The three living tissues (matrix of the teeth, dentin and pulp) are surrounded by the protective calcium phosphate enamel. The teeth are constantly in contact with saliva. The most important and well-established roles that saliva play is keeping the soft and hard tissues healthy, accomplishing mechanical cleansing and protection through various physiological and biochemical mechanisms (Zabokova-Bilbilova *et al.*, 2007).

The major functions of saliva include remineralization, buffering, digestion, lubrication, taste and anti-bacterial properties (Figure 1.2). Saliva constantly bathes teeth in crucial minerals that buffer the mouth's pH. A super saturation of ions in the saliva buffers acidic pH to keep the mouth's pH around neutral (7.0) conditions. One of the strongest indicators of increased caries risk is chronically low salivary flow rate. Saliva remineralizes teeth by bathing teeth in calcium phosphate. It helps restore calcium phosphate minerals to the teeth, healing soft spots and reversing cavities in the beginning stages of decay (Amerongen and Veerman, 2012). Specific and non-specific immunologic actions in saliva help prevent the build-up of microorganisms in the mouth. Saliva also protects the oral mucosa from mechanical damage while speaking, eating and swallowing. It washes food off from the surface of teeth and tissues thereby decreasing the likelihood of mechanical damage and it keeps tissues from drying out (Amerongen and Veerman, 2012).

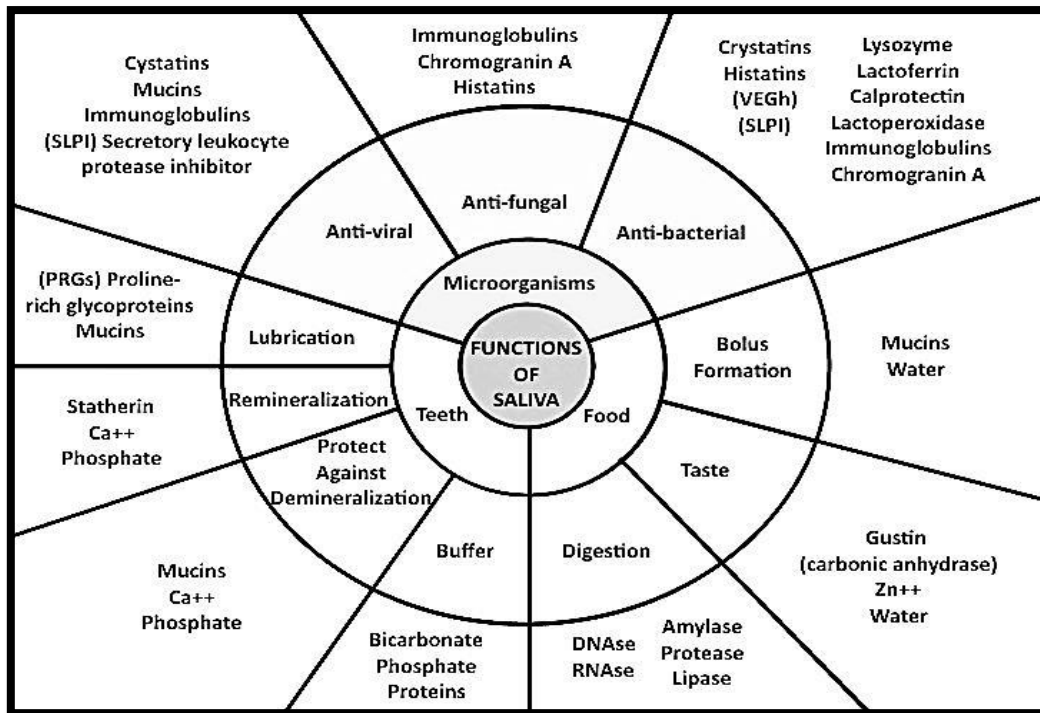


Figure 1.2: The important functions of saliva (Amerongen and Veerman, 2012)

1.2.2. Microorganisms

Gram positive bacteria mainly aciduric and acidogenic, are involved in the development of dental caries. These bacteria include microorganisms such as *Streptococci* (*Streptococcus mutans* and *Streptococcus sobrinus*), *Lactobacilli* and *Actinomyces*. These microorganisms metabolize sucrose and produce organic acids which cause decalcification in teeth and eventually tooth decay by dissolving the calcium phosphate in teeth (Palombo, 2009). *Streptococcus mutans* have been implicated as the primary causative agent of dental caries. It can also synthesize glucan from sucrose by actions of glucosyltransferase (Lim-song *et al.*, 2004). Glucans are extracellular polysaccharides which provide nutrient to the bacteria and adherence moiety.

1.2.2.1. *Streptococcus mutans*

Streptococcus mutans were first isolated from the human carious lesion by J Kilian Clarke in 1924 (Loesche, 1986). Strains of *S. mutans* are usually α (alpha) or non hemolytic on blood agar. They produce acids from a variety of carbohydrates such as N-acetylglucoamine, galactose, maltose and mannitol. The colonies appear yellow, rough, heaped and detachable on sucrose containing agar (Whiley and Beighton, 1998). *Streptococcus mutans* have the ability to adhere and attach to enamel and pellicle through surface proteins thereby producing biofilm.

Colonization of the host by *mutans streptococci* begins after the eruption of the first teeth. Surfaces such as the teeth and plaque are the most preferred sites for colonization. *Streptococcus mutans* is abundant in plaque in carious lesions. The consumption of sucrose increases the level of colonization of *S. mutans* within the plaque. *Mutans streptococci* produce extracellular polysaccharides (EPS) from sucrose that render their attachment to the teeth. Simple carbohydrates are rapidly produced by *Mutans streptococci* from sucrose and they tolerate low pH conditions (Tanzer *et al.*, 2001). These properties are called acidogenicity and acidity (Andre *et al.*, 2011). Extracellular polysaccharides are stored as nutrients when sucrose is unavailable in diet (Tanzer *et al.*, 2001).

The adhesion of *S. mutans* to the salivary components in the acquired enamel pellicle within dental plaque can be mediated in two ways: sucrose-independent and sucrose-dependent means. The sucrose-independent adhesion initiates the process of attachment while the sucrose dependent adhesion is responsible for starting colonization. The level of colonization is dependent on sucrose consumption. The efficiency of adhesion of *S. mutans* depends on the ability of *S. mutans* to synthesize glucans from sucrose and enhances the proportion of *S. mutans* within dental plaque (Banas, 2004).

The sucrose-dependent adhesion relies on the synthesis of glucans by the action of glucosyltransferases (GTFs). The mechanism by which GTFs splits sucrose into glucose and fructose is through the activity of sucrase. A polymer of glucan is then formed from a growing chain of glucose. The sucrose dependent colonization is the form and eventually caries develops. The hydrogen bonds of the glucan polymers (glucan binding proteins) facilitate the adhesion of *S. mutans* to the salivary pellicle and bacteria (Banas, 2004).

Acidogenicity and Aciduricity of *S. mutans*

Streptococcus mutans uses the glycolytic pathway to produce lactate, formate, acetate, and ethanol as fermentation products. The distribution of the fermentation products depends on the growth conditions. When glucose is abundant, lactate or lactic acid is the major product. Acidogenicity of isolates of *S. mutans* differ from one isolate to another. Changes in the ecology of the plaque flora are thought to be due to the acidogenicity of *S. mutans* and it leads to increase in proportions of *S. mutans* and other acid tolerant species. Upon ingestion of fermentable carbohydrates, pH levels are lowered in plaque by the cariogenic flora. Sustained plaque pH values below 5.5 favours the demineralization of enamel and the progression of dental caries (Banas, 2004).

Streptococcus mutans also exhibits aciduricity or acid-tolerance. This means that *S. mutans* has the ability to grow and retain glycolytic capabilities at a pH as low as pH 5.4. Another factor apart from acidogenicity that distinguishes *S. mutans* from the other oral *streptococci*. The F₁F₀-ATPase proton pump mediates the acid tolerance and adaptation with an accompanying change in gene and protein expression which leads to the acid-tolerance response (ATR). The organism is protected from sub-lethal pH challenge by the ATR. The ATR also protects the organism from acid shock and growth at pH (Banas, 2004).

In addition to the acidogenicity, aciduricity and the production of EPS, *S. mutans* form biofilm (dental plaque) which is responsible for dental caries. Biofilms are defined as groups of microorganisms that are attached to a surface and include of single microbial or several species. The environment is predominated mostly by mixed and single species and they occur in a different group of infections. The development of biofilm is initiated by bacteria in response to specific environmental signals, such as nutrient availability (O'Toole *et al.*, 2000). The provision of fresh nutrients leads to the continuation of the development of biofilms however, if nutrients are scarce, they detach from the surface and return to a planktonic mode of growth. When the environmental conditions change, bacteria sense the change and starts life on the surface. These environmental signals vary among organisms. Environmental signals that induce biofilm include the nutritional contents, pH, temperature, essential minerals such as iron and the concentration of solutes (O'Toole *et al.*, 2000).

Dental plaque (biofilm) is formed by attachment of early colonizers of bacteria to the acquired pellicle by adsorption to the tooth surface prior to tooth cleaning. These bacteria make the environment appropriate for early colonizing bacteria and fastidious bacteria

(obligate bacteria) to grow and modify. The attached bacteria start synthesising glucans forming biofilm matrix (Rani *et al.*, 2009).

1.2.2.2. *Lactobacillus* spp.

The mouth consists of *Lactobacilli* before the eruption of the teeth. However, *Lactobacilli* do not colonize the teeth, they colonize the dorsum of the tongue and are carried into saliva by the removal of the tongue's epithelium. They become established in the dental plaque. The number of *Lactobacilli* in saliva is reflected by the amount of simple carbohydrates that are consumed by the host. *Lactobacilli* exhibits characteristics of acidogenicity and acid tolerance. They are frequently cultivated from established caries lesions. Cariogenicity of some *Lactobacilli* is dependent upon intake of carbohydrate-rich diets and is observed in experimental animals (Tanzer *et al.*, 2001).

1.2.3. Diet

There is a synergistic relationship between diet, nutrition, oral health and disease. Oral health is affected by diet especially the integrity of tooth including the periodontium, the oral mucosa and the alveolar bone. It also affects the pH, and composition of the saliva and plaque. The integrity of teeth and surrounding tissues are affected by the changes in the intake of nutrients prior to alterations in diet, absorption, metabolism or excretion (Touger-Decker and Van Loveren, 2003). Dental caries has been referred to as a dietobacterial" disease. The disease occurs in the presence of dietary fermentable carbohydrates. Sucrose is the sole substrate for bacterial enzymes such as glucosyltransferases which are involved in the synthesis of glucan. The synthesis of extracellular glucan is a virulence factor of great importance (Zero *et al.*, 2009).

Dietary carbohydrates include sucrose, glucose maltose, lactose, fructose and starch. Sucrose is the most cariogenic carbohydrate. *S. mutans* rapidly metabolise sucrose and produce lactic acid which is responsible for the progression of dental caries. Furthermore, EPS can only be produced from the breakdown of sucrose into glucose and fructose (Touger-Decker and van Loveren, 2003).

1.2.4. Quantity and frequency of consumption

Diet is a contributor to the cariogenicity however, the frequency of consumption seems to be more significant. It was reported that the development of caries is related to the amount of sugars and the time that sugars are available in the mouth for the microorganisms rather than the ingestion of sugars. Frequency is important when caries is considered as the result of the change in demineralization and remineralization (Touger-Decker and Van Loveren, 2003). When the frequency of consumption increases, the more minerals diffuse from the teeth (demineralization), this means less remineralization. In this relation, the important confounder is the duration of the decrease in pH after consumption of cariogenic food. Many educational models have shown that the decrease in pH lasts about 30 minutes. However, when plaque is a few days old, pH telemetry measurements show that, the decrease in pH can last for numerous hours, this can be reversed by clearance of the site by removal of ingested food or stimulating saliva (Touger-Decker and Van Loveren, 2003).

The risk of caries is increased by the increase in snacking due to the increase in frequency of consumption of sugar. The exposure extends the duration of acid production tipping the scale towards the production of caries. These changes over time in response to acidogenic food are called Stephan responses or Stephan curve (Stephan and Miller, 1943). The pH of plaque is constant when nothing has been consumed (food or drink) that is, under normal or resting conditions. These conditions describe plaque that has not been predisposed to fermentable carbohydrates. Differences exist between individual and in different sites within an individual (Stephan and Miller, 1943). The pH rapidly decreases after dental plaque has been exposed to fermentable carbohydrates. The decrease can reach a minimum pH in 5-20 minutes due to the production of lactic acid. Following the decrease in pH, in over 30-60 minutes there is a gradual increase to the normal value which is influenced by several factors, although it differs with each individual. These factors include the fate of fermentable carbohydrates in the oral cavity, the pH value and buffering capacity of saliva (Stephan and Miller, 1943).

1.3. Prevention of dental caries

Dental caries can be prevented by correcting all the factors that are implicated in its development. Saliva flow can be improved, sucrose intake and frequency of intake can be reduced and oral hygiene improved.

The quantities of *S. mutans* can be reduced through oral hygiene. In the early years, a powerful proverb was stated by Leon Williams (1852-1931) that tooth decay does not occur in clean teeth however, this statement was not validated by scientific evidence. (Touger-Decker and van Loveren, 2003). The most reliable and considered measures of controlling plaque include tooth brushing and other mechanical cleaning however, the cleaning should be thorough and done regularly (Löe, 2000). Although many people exercise some degree of oral hygiene, tooth brushing appears to be the method of choice. However, wide variations exist in toothbrush design, brushing techniques, brushing time and frequency of brushing (Löe, 2000). Most individuals in the possession of a toothbrush, only brush the occlusal and facial tooth surfaces, and frequently only the labial surfaces of the anterior teeth which is not effective. Manual or powered tooth brushing is important for maintaining good oral hygiene. However, with tooth brushing alone, some areas are left untouched such as proximal and interdental areas. Pits and fissures are left out with unaided brushing as it is able to clean only the buccal, lingual and occlusal tooth surfaces (Löe, 2000).

The major focus of modern hygiene programmes aimed at preventing or reducing dental caries should be put on the interdental and proximal areas of the dentition. More interdental devices can be used such as dental floss, dental tape, wood sticks and interdental brushes. Other devices include single tufted brushes and electrical devices (Löe, 2000).

1.3.1 Saliva

Water and a mixture inorganic ions make up 99% of saliva. The inorganic ions include minor ions such as fluoride and other ions such as calcium, phosphate and potassium. Saliva neutralizes acids in the mouth through buffering capacity. Three buffer systems are used by the human saliva to regulate buffering capacity (Zabokova-Bilbilova *et al.*, 2007). The systems include the bicarbonate system, the phosphate system and the proteins. The inorganic phosphate concentration is high in non-stimulated saliva whereas the bicarbonate concentration is low. In stimulated saliva bicarbonate is in high concentration therefore, it is the most important buffer system (Zabokova-Bilbilova *et al.*, 2007). The phosphate buffer plays essential role when saliva flow is low (Puy, 2006).

There are four general ways in which saliva affect caries. Firstly, by mechanical cleaning, this will result in less build-up of plaque. Secondly, calcium, phosphate and fluoride reduce

the solubility of enamel. Thirdly, the acid produced by cariogenic bacteria or obtained in diet is buffered and neutralized. Lastly, by anti-bacterial activity (Zabokova-Bilbilova *et al.*, 2007). The concentrations of calcium and phosphate ions in saliva play a crucial role in demineralization and remineralization of tooth. These ions are essential components for the upkeep of strong and healthy teeth (Dodds *et al.*, 2005). Higher concentration of these ions in saliva have a protective effect against caries. They increase the driving forces of remineralization by reducing the solubility of enamel (Puy, 2006).

The elimination of sugars and other fermentable carbohydrates can be increased through saliva stimulated by sugar-free gums. Sorbitol, isomalt, xylitol and mannitol are examples of polyols that are tooth-friendly (Touger-Decker and van Loveren, 2003). Oral microflora is unable to metabolize xylitol, a 5-carbon sugar which has anti-cariogenic effects. These anti-cariogenic effects include stimulation of saliva resulting in increased buffer activity and an increase in pH, and improved remineralization. Sorbitol gums have shown to have equal effects as xylitol gum with the control of caries. Saliva is stimulated with no drop in critical pH (Touger-Decker and van Loveren, 2003).

1.3.2 Sucrose intake

An example of fermentable carbohydrates includes sugars. Most sugars are found in food such as dairy products, honey and fruits. Some sugars are added during the processing of food to change the flavour, taste or texture of food. Added sugars include dextrose, maple syrup, high fructose syrup and corn syrup. The digestion of fermentable carbohydrates begins in the oral cavity through the salivary amylase (Touger-Decker and van Loveren, 2003). *S. mutans* rapidly ferment sucrose and produce lactic acid which is responsible for the development of caries. In addition, EPS are also produced from sucrose. The colonization of *mutans streptococci* on teeth and their outgrowth is depended on sucrose. Therefore, the quantity and frequency of sucrose intake should be reduced. Sucrose can be replaced by other less cariogenic sugars. These include disaccharides particularly trehalose, threhalose and isomaltoses, sorbitol, xylitol, mannitol and erythritol (Touger-Decker and van Loveren, 2003).

1.3.3. Antimicrobial agents used in prevention of caries

Antimicrobial compounds work in different ways to slow the process of demineralization or improve the remineralization process. These are used in the oral cavity in combination with oral hygiene products for mechanical cleaning such as tooth brushing. Preventative studies were focussed mostly on fluoride and chlorhexidine, this was before the greater understanding on how plaque impacts caries process (Sim *et al.*, 2016). Many compounds have been explored, these include antimicrobial compounds such as quaternary ammonium which are used in many mouth-rinse that are sold in many countries over-the-counter. An example is cetyl pyridium chloride (CPC) which appears to have potency in preventing plaque. Most mouthwashes contain phenolic compounds, metal salts and plant extracts (Løe, 2000), calcium based remineralizing agents, nanohydroxyapatite, probiotics and xylitol (Sim *et al.*, 2016). They have shown some antibacterial activity and inherent side effects. Promising results have been seen in anti-adhesive compounds such as octopinol and delmopinol on gingivitis however, there is no evidence of effect on caries (Løe, 2000). Bacteria is beneficial at levels which are associated with good health therefore, the aim is to maintain bacteria at beneficial levels rather than killing bacteria (Sim *et al.*, 2016).

1.3.3.1. Fluoride

The remineralization of the tooth and enamel is due to minerals such as fluoride, calcium and phosphate. Fluoride reduces the dissolution of enamel and enhance enamel remineralization thereby protecting enamel from the development of caries through the regular brushing of the teeth with fluoride containing toothpaste. Incorporation of fluoride in the outer layers of enamel in adequate quantity has been proved as a means to decrease the incidence of caries development. The three mechanisms of action of fluoride include diffusion into bacterial membrane and inhibition of bacteria metabolism (Featherstone, 2000). It inhibits bacterial enzymes such as Enolase and reduce the production of intracellular and extracellular polysaccharides, however it has been described that bacteria can develop tolerance against fluoride (Nassar and Gregory, 2017).

Bacteria produces acid that convert topical fluoride to hydroxyapatite. Essential enzymes are inhibited by the diffusion of fluoride into the cells. Fluoride inhibits demineralization during

an acidic challenge (Featherstone, 2000). Demineralization is stopped or reversed when the components in saliva flows over plaque and raise the pH by neutralizing the acid. Minerals are driven back to the tooth when saliva is super saturated with phosphates and calcium ions (Featherstone, 2000). Remineralization is enhanced by fluoride through adsorption of calcium ions and phosphates on the crystal surface (Featherstone, 2000). Fluoride protects against acid erosion processes.

In some countries fluoride is incorporated into drinking water, table salts or milk to target general population. Otherwise fluoride containing toothpaste, mouth rinses and gels are also available (Pandit *et al.*, 2011).

1.3.3.2. Chlorhexidine gluconate

Chlorhexidine has been identified as the most effective antimicrobial compound tested for oral use. The most important property of chlorhexidine on oral tissue and teeth surface is the selective adsorption, absorption and slow release (substantivity). It has a prolonged antibacterial activity, which persists for more than 12 hours following to rinsing (Løe, 2000). Chlorhexidine has a broad spectrum of activity. It is effective against Gram-positive and Gram-negative bacteria, and yeasts. It has significant antimicrobial properties against bacteria that causes dental caries, it suppresses the growth of *mutans streptococci*. The bacterial membrane is damaged by chlorhexidine at higher concentrations, it causes lethal damage. Chlorhexidine interferes with oral bacterial metabolism at concentrations which are sub-lethal (Marsh and Martin 2003). A reduction in the number of bacteria has been observed in saliva when chlorhexidine is used daily. Plaque reduce by 55-97%. The daily use of chlorhexidine does not cause shifts in the composition of microflora and bacterial resistance (Løe, 2000).

Chlorhexidine varnishes, gels and mouthwashes have been used for the reduction of persistent *mutans streptococci*. Side effects such as staining of teeth to yellow-brown stain and changes in taste sensation has been observed with the use of chlorhexidine mouth rinse. Other side effects that have been reported in the soft tissues of oral cavity include burning sensations, dryness, soreness and ulcerations of gingival mucosa (Gold, 2008).

1.3.3.3. Triclosan

Triclosan is a broad-spectrum antimicrobial agent which can reduce inflammation and has been used in numerous oral care products. Triclosan at sub-lethal concentrations, has the ability to inhibit acid production and protease activity at by *streptococci* and *P. gingivalis* respectively. Reports on the combination of triclosan with microbial agents such as zinc has shown additive anti-plaque and anti-gingivitis effects. The clearance of triclosan is 20 minutes (Marsh and Martin, 2003).

1.4 Treatment of dental caries

The restoration of tooth has been thought as a cure for dental caries by dentists over a long period from the turn of the 20th century (Helwitz, 2007). The focus of caries management has shifted from surgical methods and restoration of tooth to the use and development of dental materials for the prevention of caries. Minimally invasive treatments have been employed for regions that are difficult to access and materials with which initial lesions can be infused to avoid further development (Helwitz, 2007). The restoration procedure includes fluoride treatment, fillings, crowns and root canal treatment.

1.5. Pharmacologic effects of plants

Literature based on the use of traditional medicine is growing; numerous studies have documented the treatment of oral diseases from the use of indigenous medicinal plants. Plant products have been trusted for the management of diseases across the world. Journals on this topic are found in many countries including Africa (Tapsoba and Deschamps, 2006). Plants are receiving attention due to their pharmacological effects such as anti-microbial, anti-carcinogenic and anti-oxidant properties (Song *et al.*, 2007). Most medicinal plants have now been documented as sources of natural anti-oxidant phenolic compounds. Sixty-two plants have been recognized in Bukina Faso as species belonging to 29 families that are used in the treatment of oral diseases (Henly-Smith, 2013). Many plant products have been successfully incorporated into dentifrice or mouthwash in many countries (Limsong *et al.*, 2004). Plants such as *Propolis*, *Mikania* species (Duarte *et al.*, 2003) and *Nidus vespa* have anti-plaque

properties (Xiao *et al.*, 2007), *Theobroma cacao* L. (chocolate), *Coffea arabica* L., *C. canephora* Pierre (coffee) and *Camellia sinensis* (L.) O. Kuntze (tea), are also effective against adhesion of *Streptococcus mutans* and *S. sanguinis* to the surfaces of the tooth (Ferrazzano, 2009). *Dodonaea viscosa* also has medicinal effects against oral pathogens; it inhibits biofilm formation by *S. mutans* and reduces the virulence of *Candida albicans* (Naidoo *et al.*, 2012).

1.6. *Dodonaea viscosa* var. *angustifolia* (DVA)

Dodonaea viscosa var. *angustifolia* (DVA) a woody perennial herb is also called a hop bush or sand olive. It belongs to the Sapindaceae family (a member of the soap family), subclass: Dicotyledonae (Getie *et al.*, 2003). The species is categorised by green narrow leaves which are pale and shiny with the length of up to 8cm long and the stem diameter of 20 cm (Anbg, 2006). DVA is found worldwide, it is found in tropical and subtropical areas. It is found in Africa, America and Australia. In South Africa, DVA is found in all the provinces (Zonyane *et al.*, 2013). DVA was named after a Flemish botanist of the 16th century, Professor Rembert Dodoens. *Viscosa* is from the Latin origin meaning sticky and refers to the texture of the leaves (Umamaheswaril *et al.*, 2015). *Dodonaea viscosa* is traditionally used worldwide and has been used by native people for medicinal purposes. It has been administered orally or as poultice for treatment of various ailments. Skin infections and swelling due to rheumatism have been treated using *D. viscosa*. Other ailments include inflammation, pain and chest complains (Teffo *et al.*, 2010). Stems or leaves infusions are used to treat sore throat, fever and the roots are used to treat colds. Itching and swelling has been relieved by use of the plant's leaves. The plant can also be used as an anti-spasmodic agent. Unspecified parts of the plants have been used to treat toothaches, headaches and sprains (Rani *et al.*, 2009 and Khan *et al.*, 2012). Decoctions of leaves of traditional medicine which have been administered orally have been used for the treatment of digestive disorders, constipation and ulcers (Zonyane *et al.*, 2013).

1.6.1. Chemical constituents of DVA

Previous reports on this plant resulted in separation and classification of numerous flavonoids, diterpenoid acids, biologically active Saponins, novel P-coumarin acid ester, Essential oils, Sterols and Tannins from aerial parts of the plants. Over 23 flavones have been characterized from bark, leaves and flowers (Rani *et al.*, 2009).

Flavonoids are known as polyphenols which are a major class of natural compounds which are naturally occurring in plants. They are secondary metabolites which are found in beverages and fruits, vegetables, cereals, tea, coffee and red wine (Seleem *et al.*, 2017). Flavonoids play a crucial part in numerous biological processes. The physiology of plants is dependent on the flavonoids, they are involved in the development and growth. Flavonoids are defence mechanisms in plants, and they influence the appearance of the flowers and fruits. The phenolic compounds are the most studied flavonoids due to their contribution to human health (Tuberoso *et al.*, 2009). The properties of the flavonoids are advantageous for human health in the body through interactions associated with critical cell signalling mechanisms and cellular targets (Seleem *et al.*, 2017).

1.6.2 Structure of a flavonoid

The structure of a flavonoid consists of a basic chemical structure, a diphenyl skeleton of propane, containing rings of benzene (ring A and B) linked by a linear chain of carbons (C6-C3-C6). A ring of pyran is formed from three carbons (heterocyclic ring containing oxygen, C ring) with one of the benzene rings, making a structure with 15 atoms of carbon arranged in three rings (Figure 1.3). Flavonoids are made up of seven subclasses according to the variations of the heterocyclic C-ring; the subclasses are: Flavonoids, Flavones, Flavonols, Flavonones, Flavononols, Isoflavones, Anthocyanins and Anthocyniadins (Leonarduzzi *et al.*, 2010).

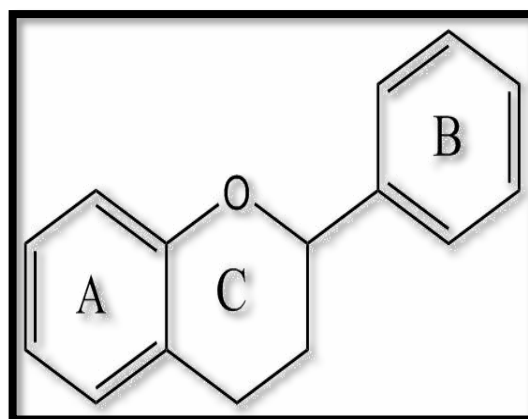


Figure 1.3: The basic structure of a flavonoid (Chem draw software)

1.6.3. Classification of Flavonoids

Flavonoids are classified into the following groups: Flavonols, Flavonones, Flavonoligans, Flavans, Isoflavones, Aurones, Neoflavonoids, Leucoanthocyanidins and Chalcones. Flavonols are known to provide health benefits and examples include Quercetin, Kaempferol, Myricetin and Fisetin. Flavones are defense mechanisms in plants. Examples of flavones include Luteolin and Apigenin. Flavonones have anti-oxidant, anti-allergic and anti-inflammatory properties examples include Hesperetin, Naringenin. Examples of flavonoid Glycosides are Astragalin and Rutin. Flavonoligans include Silibinin. Flavans such as catechin are natural anti-oxidants. (Figure 1.4). A variety of biological activities has been exhibited by all classes of flavonoids however, the flavones have been significantly explored (Singh *et al.*, 2014).

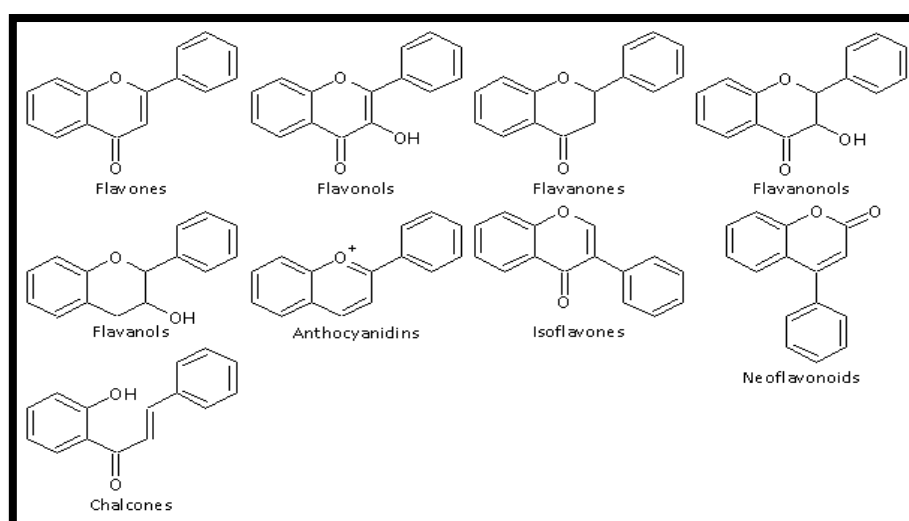


Figure 1.4: The classification of flavonoids (Panche *et al.*, 2016)

The structures of flavonoids differ by the position of functional groups on the three different rings. Flavonols are characterised by a hydroxyl group which is found in position 3 of the C ring. The flavonols are the most common and largest group which are mainly found in vegetables and fruits (Panche *et al.*, 2016). Flavones are characterised by a ketone and double bond in position 4 of the C ring and between position 2 and 3 respectively. Hydroxyl group is found in flavones derived from fruits and vegetables in position 5 of the A ring. Hydroxylation positions of certain fruits and vegetables differ based on the taxonomic classification. These positions can be found in position 7 of the A ring or 3' and 4' of the B ring (Panche *et al.*, 2016).

Isoflavones have structural similarities to estrogens. The B ring is attached to positions 3 of the C ring. Flavonoids with open structures are called chalcones and dihydrochalcones, they are categorized as flavonoids since they have similar pathways. All the other flavonoids are colourless except for anthocyanidins which give colour to the plants. (Panche *et al.*, 2016).

Flavones have been manufactured and assessed for numerous therapeutic actions such as anti-inflammatory, anti-oestrogenic, anti-microbial, anti-allergic, anti-oxidant, anti-tumor and cytotoxic activities. Flavones have the ability to undergo reactions such as reduction, degradation in the presence of a base, oxidation, rearrangement, substitution, addition, condensation and they also react with organometallic reagents (Singh *et al.*, 2014). Flavonoids are the most diverse and largest group in the family of polyphenols, there are more than 4000 flavonoids that have been documented from plants (Table 1.2). Various flavones have been identified from seeds, bark, flowers and leaves of *D.viscosa* (Rani *et al.*, 2009).

Table 1.2: Flavonoids of *Dodonaea viscosa* (Rani *et al.*, 2009)

Name	Chemical name	Reference
Aliarin	5,7,4'-trihydroxy-3'- (3hydroxymethylbutanol) 3,6- dimethoxyflavone	Sachdev & Kulshreshtha 1983
Pinocebrin	5,7-dihydroxyflavanone	Sachdev & Kulshreshtha 1983
Penduletin	5,4'-Dihydroxy-3,6,7- Trimethoxy flavone	Sachdev & Kulshreshtha 1983
Viscosol	3'-(γ,γ -dimethylallyl)-5,7- dihydroxy- 3,6,4'-trimethoxy flavone	Sachdev and Kulshreshtha, 1986
Sakuranetin	(S)-5,4'-dihydroxy-7- methoxyflavone	Mata <i>et al.</i> , 1991
Ermanin (Kaempferol 3,4'dimethylether	3,5,7,4'-Tetrahydroxyl-3,4'- dimethoxyflavone	Wollenweber, 1993
	3,5,7,4'-Tetrahydroxy-7- methoxyflavone	Wollenweber, 1993
Cirsimaritin (Scutellarein 6,7-Dimethoxy flavone)	5, 4'-Dihydroxy-6,7- dimethoxyflavone	Wollenweber, 1993
Pectolinarigenin(Scutellarein 6,4'- Dimethoxy flavone)	5, 7 -Dihydroxy-6, 4'- dimethoxyflavone	Wollenweber, 1993
Kaempferol 7,4'- dimethylether	3,5-Dihydroxy-7,4'- dimethoxyflavone	Harborne, 1999
Kaempferol 3,7,4'- trimethylether	5-Hydroxy-3,7,4'- trimethoxyflavone	Harborne & Baxter 1999
Santin	5,7-dihydroxy-3,6,4'3' tetramethoxyflavone(trimethoxy flavone)	Sachdev & Kulshreshtha 1983 Harborne & Baxter 1999
Acacetin 7- methyl ether	5 hydroxy -7,4'- dimethoxyflavone	Abdel-Mogis <i>et al.</i> , 2001
6 Hydroxy kaempferol – trimethyl ether (Penduletin)	6Hydroxy–3,6,7trimethoxy flavone	Wollenweber & Roitman 2007
Kaempferol 3 – methyl ether	5,7,4'Trihydroxy-3methoxyflavone	Wollenweber & Roitman 2007

1.6.4. Study flavonoid- Flavone

In this study the focus will be on a flavone which was recently identified as 5, 6, 8-Trihydroxy-7-methoxy-2-(4-methoxyphenyl)-4-H-chromen-4-one derived from *D. viscosa* var. *angustifolia*. This compound has been found to have anticariogenic properties against dental caries forming bacteria (Ngabaza *et al.*, 2017).

There are many phytochemical agents available for the treatment of oral infections. However, these agents are associated with side effects including nausea, diarrhoea and tooth staining and bacteria have ability to develop resistance. Bacterial resistance has been observed in some antibiotics used in oral treatment such as with Penicillin, Cephalosporins, Tetracycline and Erythromycin (Palombo, 2011). Since human pathogens are increasingly becoming resistant to antibacterial agents, it is necessary to provide other efficient measures of therapeutic interventions. The development of stealth nanoparticles drug delivery has been of great attention for centuries. These nanoparticles are prepared by modification of the surface of the nanoparticles with hydrophilic polymers (Palombo, 2011). The properties of stealth nanoparticles include better shelf stability of the coated plant compounds and controlled release. (Li *et al.*, 2001 and Rani *et al.*, 2009). Drugs that are used in combination with nanoparticles (NPs) show an increase in solubility and ability to adhere to biological surfaces thereby improving bioavailability and therapeutic activity because of the small size of the nanoparticles. The benefits of controlled release systems include protection from degradation, prolonged duration of the beneficial compounds, targeted delivery and controlled release rate (Wang *et al.*, 2016).

1.7. Nanotechnology and delivery systems

The application of science that controls materials at a molecular level and deals with dimensions of less than 100 nanometres is referred to as nanotechnology.

This application is attaining importance in many fields including medicine, biomedical sciences, drug or gene delivery, optics and chemical industry. Nanoparticles differ from bulk material chemically and physically due to properties such as large surface volume ratio and size are of great importance (Iravani, 2011). The characteristics of delivery systems affect their absorption, delivery, metabolism and elimination, these are crucial in controlling the in

in vivo activity of the distributed beneficial compound. Nanoparticles properties of importance in *in vivo* interactions are size, surface charge, hydrophobicity and targeting properties. The most important property is size, smaller size is essential for the entry into the cells, particle clearance and cell stimulation (Borel and Sabliov, 2014).

1.7.1. Nanomaterials

1.7.1.1. Metallic nanoparticles

Metal salts have been widely explored for the synthesis of nanoparticles for the delivery of drugs. The characteristics such as surface area, size and low volume ratio of metallic nanoparticles has been shown to have biocidal efficiency. Besides the release of these metal ions, the characteristics of the nanoparticles permit them to interrelate closely with the membranes of microbial organisms. The combination of metals salts and nanoparticles which have antimicrobial activity are now coated onto the matrix of the polymers for use within the oral cavity (Allaker, 2010). Silver and Gold have been used for years as antimicrobial agents. Other metal salts such as Copper, Zinc and Titanium have been used (Savithamma *et al.*, 2011).

The biological synthesis of metal nanoparticles using plants has received more attention as a suitable alternative to chemical and physical procedures and is currently under exploitation (Iravani, 2011 and Savithamma *et al.*, 2011). The nanoparticles preparation is very cost effective, rapid, clean, non-toxic and environmentally friendly (Harshiny *et al.*, 2015). These nano-scaled particles are important in Medicine and Pharmacy applications (Iravani, 2011).

1.7.1.2. Polymeric Nanoparticles

Many polymers have received considerable attention including synthesized polymers and natural occurring polymers. These polymers are stable and their surfaces are easily modifiable (Singh and Lillard, 2009). The nanoparticles sizes range from 10-1000 nm. The drug is attached to the PLGA nanoparticles in a number of ways, the drug can be dissolved, encapsulated or entrapped in the core of the membrane of the nanoparticles. The polymers should be biocompatible with the body in terms of adaptability (nontoxicity) and non-

antigenicity and should be biodegradable and biocompatible. The most commonly used polymers are: Poly lactic acid, Poly (D, L-glycolide), Poly D, L-lactide-co-glycolide) and Poly (cyanoacrylate) (Nagavarma *et al.*, 2012), Chitosan, Gelatin, Poly caprolactone and Poly-alkyl-cyanoacrylates (Kumari *et al.*, 2010).

1.7.2. Study polymers:

1.7.2.1. Poly (lactic-co-glycolic acid) polymers

Ratios with different monomers are used in the preparation of a linear structure of PLGA (Poly lactic-co-glycolic acid) through polymerization. The monomers include glycolic acid (GA) and lactic acid (LA) as shown in Figure 1.5. (Gentile *et al.*, 2014). These monomers are the end product when PLGA is hydrolyzed (Danhier, 2012).

The ratios of the monomers are used to identify PLGA polymer. The ratio PLGA 85:15 describes the composition of copolymer with 85% LA and 15% GA. The use PLGA polymers for drug delivery or biomaterial applications have negligible systemic toxicity as the monomers of PLGA are metabolized easily by the body (Danhier, 2012). Copolymers of Lactide and Glycolide have been the most studied in the search for appropriate polymers for delivery of drugs due to their biocompatibility and hydrolytic degradation to lactic and glycolic acids respectively which are subsequently eliminated as water (H₂O) and carbon dioxide (CO₂) through the Krebs cycle (Engineer *et al.*, 2011). Nanoparticles made from PLGA polymers have surfaces that are modifiable. These nanoparticles also show a degree of biocompatibility and biodegradability. The nanoparticles are efficient and safe to use as potential carriers of drugs due to their capabilities to encapsulate the drugs and release the drug in controlled manner (Wang *et al.*, 2016).

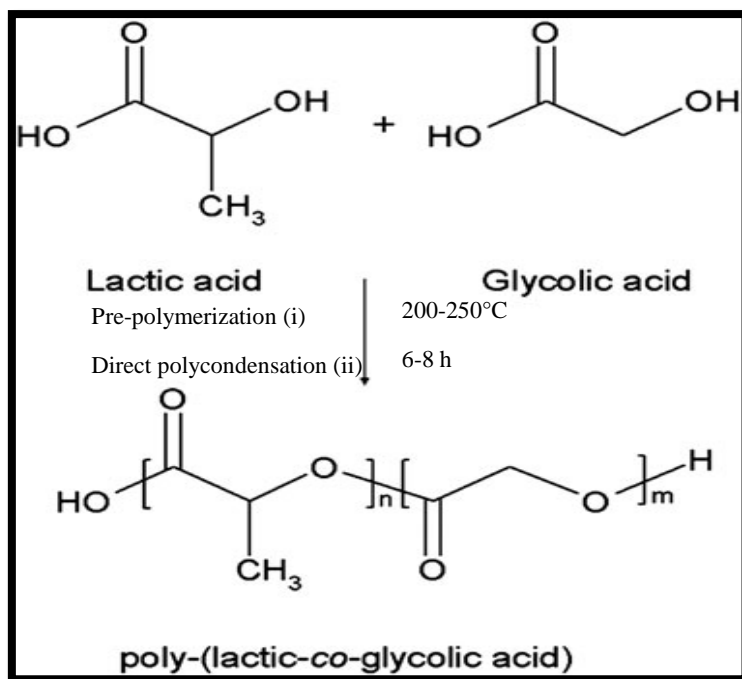


Figure 1.5: The structure of PLGA and its monomers (Gentile *et al.*, 2014)

The solubility of PLGA has been observed in a variety of solvents. These include solvents like Tetrahydrofuran (THF), Ethyl acetate, Acetone and Chlorinated solvents (Dichloromethane). The advantage of using PLGA co-polymer is that they can easily encapsulate any size of biomolecules and they can be formed to any shape. Various factors including weight of the monomers (initial), lactic and glycolic acid ratio, the exposure time to water and storage temperature affects the polymer's physical properties. The position of the alpha carbon on the methyl group determines the two enantiomeric isomers of lactide. PLGA has two isomers of lactide. Glycolic acid is highly crystalline with absence of side methyl side (Gentile *et al.*, 2014).

These polymers are an interesting class of material that can degrade to non-toxic products and have interesting medical and pharmaceutical applications such as use for matrices in delivery of drugs, scaffold for manufacturing of tissues and degradable implants in Orthopedic surgery. The degradation of PLGA is through the hydrolysis of its ester linkages (Gentile *et al.*, 2014).

1.7.2.2. Poly (ethylene) glycol polymers (PEG)

The monomers of ethylene glycol have been successfully polymerized by a process of linking the repeating units to form the polymer PEG (poly ethylene glycol), the shapes of the polymer can be linear or branched. PEG is a polyether with hydrophilic properties which can be found in a variety of molecular weights (Locatelli and Franchini, 2012). Other properties of PEG include biocompatibility, water solubility and non-toxicity. Due to the amphipathic nature of PEG, it has been widely used. Some of its uses include pharmaceutical applications and it has also been used in chemical modifications of natural and artificial polymers. Coating colloidal particles with PEG has been reported to evade recognition of the particles as foreign objects thereby avoiding elimination by the phagocytes through phagocytosis. (Wang *et al.*, 2016). The food and drug administration (FDA) have approved the use of PEG as a base in foods and in cosmetics. The use of PEG has also been approved in pharmaceuticals which include formulations of the nasal and rectal topical and injectable applications. PEG can easily be removed from the body by kidneys as urine or in the faeces. The kidneys are able to eliminate PEG with sizes of < 30 kDa and the sizes > 20 kDa) are removed in the faeces. PEG polymer has minimal toxicity and lacks immunogenicity under clinical administration (pegylated proteins do not generate antibodies) (Harris and Chess, 2003).

A process called pegylation is used to attach the drug of choice to the PEG structures. Studies reveal that when PEG is immersed in a solution the ethylene glycol subunits are linked to two or three molecules of water. The pegylated compounds are able to function five to ten times larger when they are bound to water molecules as compared to the corresponding soluble proteins with the same molecular mass. The size and mass of the PEG polymers can easily be confirmed by using gel electrophoresis and size exclusion chromatography. The drug that is attached is protected from degradation by enzymes and rapid clearance by the renal system by the PEG polymer and associated molecules of water. This limits the hostile immunologic effects and interactions with proteins. The stability of pegylated drugs has also been observed in a wide range of temperatures changes and pH (Harris and Chess, 2003).

1.7.2.3. PEG-PLGA copolymers

The physicochemical characteristics of PEG and other hydrophilic properties is enhanced in the conjugation of PLGA and PEG. Several drug formulations making use of nanoparticles have been attained by incorporating PLGA to PEG with PEG that contains different end terminals such as methoxy and carboxyl terminals (Wang *et al.*, 2016). PLGA-PEG copolymers are used in the application of microparticles, nanoparticles, micelles and hydrogels. One of the advantages of using PEG is that some properties can be tailored. The properties of PLGA-PEG copolymers such as morphology, particles size changes and enhanced efficacy provide them with a greater potential. In aqueous phase the micelles have a stabilizer in the shell surrounding the core of the PEG. The core also serves as protection *in vivo* for proteins and cellular adhesion (Zhang *et al.*, 2014). The degradation kinetics of the block copolymers as well as their solubility in water is dependent on the composition of the copolymers as well as their molecular weight. The solubility of polymers in water is high for polymers with composition of lower molecular weight and shorter hydrophobic chains. The solubility is low (insoluble) in polymers with longer hydrophobic chains and higher molecular weight, these polymers swell in water. The degradation time is also dependent on the composition of the polymers, for polymers with low molecular weight, shorter chains and more hydrophilic blocks with a high content of glycolide, the degradation time is shorter, and the degradation time is longer for polymers with longer chains and high molecular weight. Under the same conditions, homopolymers such as PLA and PGA with higher molecular weight will degrade relatively slowly whereas copolymers of lactide and glycolide with low molecular weight will degrade rapidly (Harris and Chess, 2003).

PLGA has been used in many ways in the dental field. The common applications include developing screws for bone fixation, treating periodontal pathogens and producing buccal mucosa or indirect pulp capping procedures. In periodontal treatment, PLGA is used for better local administration of antibiotics and to decrease systemic side effects of general antibiotic delivery. This is done in the form of PLGA implants, disks and dental films (Virilan *et al.*, 2015).

1.8. Cytotoxicity of nanoparticles

There are many biomedical applications that are emerging for the use of nanoparticles. These applications include the use of nanoparticles in drug delivery of bioactive compounds and imaging contrast agents which involves direct body injection or ingestion of the nanoparticle compounds by use of consumer products. The toxicity profile is a critical factor when the use of nanoparticles and their potential is evaluated *in vivo* for biomedical applications (Lewinski *et al.*, 2008). Many molecules have been used as coating bioconjugates for nanoparticles drug delivery and imaging. The bioconjugates include monoclonal antibodies for targeting of specific cells, proteins and DNA. It is of great importance to ensure that the nanoparticles do not cause hostile effects because these nanoparticles are deliberately engineered for the interaction with cells (Lewinski *et al.*, 2008).

There is a considerable concern over the effect of nanoparticles that are coated and nanoparticles that are not coated in terms of biodegradation of the nanoparticles in the cellular environment and the type of response the nanoparticles will induce once they are degraded. For instance, there might be accumulation of the biodegraded nanoparticles in the cellular environment which can cause alterations in genes or disruption of the integrity of organelles (Lewinski *et al.*, 2008). However, polymeric nanoparticles have monomers that are easily metabolized by the body. These materials degrade into non-toxic products. Certain characteristics have been observed in nanoparticles such as stability in blood, they are not toxic, they do not have the ability to activate neutrophils as they are non-immunogenic, they avoid the reticuloendothelial system and they are biodegradable (Kumari *et al.*, 2010). Therefore, negligible systemic toxicity has been observed when these nanoparticles are used in drug delivery and in biomaterial applications especially PLGA nanoparticles (Danhier, 2012).

Flavone (identified as 5, 6, 8-Trihydroxy-7-methoxy-2-(4-methoxyphenyl)-4-H-chromen-4-one) has been shown to have positive effects over the prevention of virulence factors of *S. mutans* such as anti-*S. mutans* activity, anti-acidogenic and anti-biofilm properties. However, should this flavone (5, 6, 8-Trihydroxy-7-methoxy-2-(4-methoxyphenyl)-4-H-chromen-4-one) be used in the oral cavity to prevent dental caries, it would be difficult to maintain the beneficial concentrations due to continual saliva flow. Improved substantivity can provide sustained release and prolong the activity of the beneficial concentrations. This can be achieved by using polymeric nanoparticles made up of PLGA-PEG copolymers which are

biocompatible and biodegradable. Therefore, the aim of this study was to investigate the anti-cariogenic and release properties of *Dodonaea viscosa var. angustifolia* derived flavone stabilized nanoparticles.

1.9 Aim

The aim of this study was to investigate the anti-cariogenic and release properties of *Dodonaea viscosa var. angustifolia* derived flavone stabilized nanoparticles.

1.10 Objectives

- To analyse crude leaf extracts using thin layer chromatography to separate the chemical constituents present in DVA.
- To further separate chemical constituents using column chromatography and collect the subfractions.
- To screen the subfractions for their anti-*streptococcus mutans*, anti-acidogenic and anti-biofilm properties and identify the beneficial subfraction using GC-MS, and Fourier transform infrared spectroscopy.
- To prepare beneficial subfraction encapsulated and stabilized PLGA-PEG nanoparticles and to characterize them using appropriate techniques.
- To determine the anti-cariogenic efficiency of the identified beneficial subfraction F 5.1 and the drug release profiles from the different nanoparticles prepared
- To determine the cytotoxicity of subfraction F 5.1 and prepared nanoparticles.

1.11. Dissertation plan

A schematic diagram of plan of dissertation is shown in Figure 1.6 to highlight the action of plan for the final dissertation.

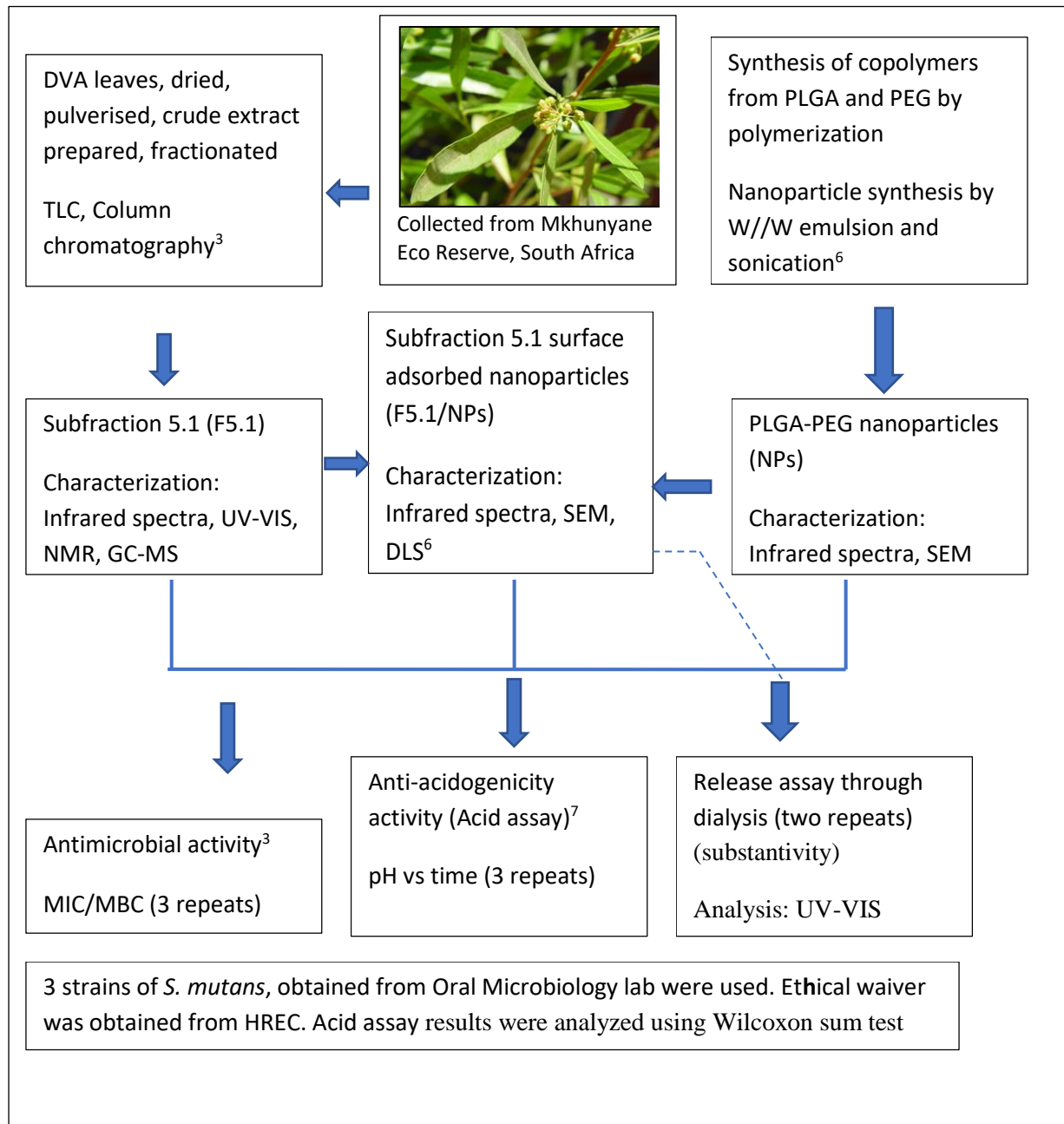


Figure 1.6: Flow diagram -Plan of dissertation

CHAPTER 2

2.1. Materials and methods

2.1.1 Test Cultures and inocula

Laboratory stock cultures of *Streptococcus mutans* from a previous study (ethical clearance number M10205) were used in this study. Three strains of *S. mutans*, two clinical isolates and one ATCC 10923 were grown on blood agar and incubated under CO₂ for 24 hours at 37°C. The cultures were then stored at -4°C. Ethical waiver was obtained from The Research Committee of the University of Witwatersrand (Appendix II). Fresh inocula was prepared for each experiment, the optical density of 0.2 (405 nm) was obtained with approximately 10⁵ - 10⁶ organisms per milliliter. The inocula was prepared in Tryptone Soy broth and used throughout the study.

2.1.2. Plant material

The plant *Dodonaea viscosa var. angustifolia* was collected in Mpumalanga province of South Africa from an Eco-Reserve in Pypeklipberg, Mkhunyane. The plant was identified as *Dodonaea viscosa var. angustifolia* Benth belonging to the Sapindaceaea family by a Taxonomist from the Herbarium at University of The Witwatersrand. Voucher specimens number J 94882 was previously deposited at this herbarium (Patel and Coogan, 2008)

2.2. Extraction and purification

The leaves of the plant *Dodonaea viscosa var. angustifolia* were dried and grounded to fine powder. The extracts were prepared according to a method described by Eloff (1999). The milled leaves (60 g) were mixed with methanol (600 ml) in an erlenmeyer flask and agitated for three days. The mixture was then carefully poured into a 1000 ml beaker leaving the leaves powder behind. The mixture was transferred into eppendorf tubes and centrifuged for 20 minutes at 2500 rpm. The supernatant was collected in a pre-weighed 1000 ml beaker. This procedure was repeated three times using the same powder. The constituted mixture was left to dry for two weeks under a fume hood. The beaker was weighed again. The dried crude extract yield was calculated.

2.2.1. Column chromatography

The dried crude extract was used to run column chromatography. A ratio of 50% v/v of hexane and ethyl acetate was used to dissolve crude extract overnight. Two phases were used, the stationary phase (slurry) and a mobile phase (ratio of hexane and ethyl acetate). A medium column with a width of 2.7 cm and length of 35 cm was used. The slurry was made using 50 grams of silica gel (70-230 mesh) and 50 ml of 100% hexane. The slurry was poured in the column and the crude was then loaded on the silica. The elution process was started using 100% hexane and the polarity was gradually increased with ethyl acetate from 100% hexane, to 90:10 hexane to ethyl acetate, 80:20, 70:30 and so on. Only the solvent mixture ratios that yielded fractions are listed in Table 2.1.

Table 2.1: Ratios of the solvents used in the elution process of crude extract

Ratios	Fraction
1. 100% Hexane: 0% Ethyl acetate	1
2. 70% Hexane: 30% Ethyl acetate	2
3. 60% Hexane: 40% Ethyl acetate	3
4. 40% Hexane: 60% Ethyl acetate	4
5. 0% Hexane: 100% Ethyl acetate	5

Flavones have been shown to have positive effects over the prevention of the virulence factors of *S. mutans* that lead to the development of dental caries. Fraction 5 was shown to have anti- *S. mutans* activity, anti-acidogenic and anti-biofilm properties, (Patel *et al.*, 2009; Naidoo *et al.*, 2012 and Ngabaza *et al.*, 2017) due to the presence of flavones therefore fraction 5 was chosen. Fraction 5 was then collected in a pre-weighed beaker and concentrated through drying. The dry fraction was weighed and reconstituted using ethyl acetate. The fraction was then fractioned further using column chromatography. A smaller column was used. The width of the column was 2 cm and the length 26 cm. The slurry was prepared using 12.8 g of silica and 30 ml of hexane. Further purification of fraction 5 produced two subfractions (F 5.1 and F 5.2) which were yellow and green in colour

respectively. The yellow subfraction was collected in a pre-weighed bottle and TLC chromatography was run for subfraction F 5.1. Chromatography was re-run using subfraction F 5.1 to purify the compound. F 5.1 was shown to have the highest anti-bacterial activity, highest anti-acidogenic properties and anti-biofilm when tested against *S. mutans* (Ngabaza *et al.*, 2017). F 5.1 was chosen for further analysis. F 5.1 was dissolved in DCM for rapid drying to powder under the fume hood. The resultant powder was then weighed.

2.2.2. Thin layer chromatography

Thin layer chromatography was used to group the fractions according to their TLC profiles using TLC plates lined with silica and three solvents that differ in polarity: Toulene/ Ethanol/ Ammonium hydroxide (18:2:0.2) which is non-polar, Dichloromethane/ Ethyl acetate/ Formic acid (10:8:2) with intermediate polarity and Ethyl acetate/ Methanol/ water (40:5:4.5) which is polar. A square shape silica plate was cut using a pair of scissors and used as a stationary phase. A ruler was used to draw a line across the silica gel plate and a pencil was used to make a spotting dot on the line. Capillary tubes were used to make a spot on the silica gel plate using the obtained fractions from column chromatography. The spotted silica gel plate was then transferred into a beaker containing the mobile phase and a lid was placed to cover the beaker. After a few minutes the plate was removed from the beaker and the silica plate was dried under a fume hood. Once dry, the plate was sprayed with 30 % v/v sulphuric acid and dried in the oven. The colours were then viewed under UV light at a wavelength of 356 nm.

2.2.3. Purification of F 5.1

Several re-runs of column chromatography were used to purify subfraction F 5.1 further. After purifying with silica gel, two more stationary phases were used to purify F 5.1 further. The stationary phases used were Sephadex and Biobeads. Firstly, subfraction F 5.1 was run on Biobeads as stationary phase and mixture of hexane and ethyl acetate as a mobile phase using a smaller column. The ratios of hexane and ethyl acetate used were of 40:60, 50:50 and so on until it reached a ratio of 0:100 which was able to separate the polar subfraction. There after the obtained solution was concentrated and then run on Sephadex with DCM as the solvent for elution on a small column.

2.4. Identification of subfraction F 5.1

2.4.1. Ultra violet visible spectroscopy (UV-vis)

The spectra of subfraction F 5.1 were analysed using Shimadzu 1800 UV spectrophotometer with double beam optics photometric system, monochromator (Czerny turner mounting), with wavelength range of 190-1100 nm and a silicon photodiode detector. UV-vis spectrum was obtained for subfraction F 5.1. Subfraction F 5.1 was dissolved in Ethanol. The data obtained were used to draw scatter plots.

2.4.2. Fourier Transform Infrared spectroscopy analysis (FTIR)

The Perkin Elmer FT-IR 100 spectrometer was used for infrared spectroscopy analysis. Ten milligrams per milliliter of subfraction F 5.1 was dissolved in ethyl acetate. A small pipette tube was used to draw up the sample from which one drop was placed on the diamond surface plate for analysis.

2.4.3 Gas Chromatography-Mass Spectroscopy

Gas chromatography-Mass spectroscopy was analysed using the Agilent Technologies mass spectrometer. The model used was the 5190-2293 gas chromatography which has inert column interface (HP-5ms ultra) coupled with a mass spectrometer (Agilent technologies 1909IS-433UI). Varied temperatures were used with the temperature being increased every minute with 5°C. The set starting temperature was 50°C and the gas carrier that was used was helium with split ratio of 1:50. The ion source and the auxiliary port was set at 230°C and 280°C respectively with 3 minutes set for solvent delay. Mass spectra and different retention times were used to identify the compounds through comparison with a catalogue in the Wiley 275 library of compounds.

2.5. Synthesis of beneficial nanoparticles

2.5.1 Synthesis of copolymers

Poly lactide glycolide acid with ratio of 85:15 and 50:50 lactide to glycolide, Poly ethylene glycol with acetic acid terminals, Stannous 2-ethylhexanoate, Poly Vinyl Alcohol (PVA), Sepharose beads, Silica gel (70-230 mesh) were purchased from sigma Aldrich. Liquid chemicals (Hexane, Ethyl acetate, Dichloromethane, Toluene) were purchased from Laboratory co. supplies, South Africa.

Copolymers were synthesized following an adaption from the method described by Li *et al.*, (2001) and Hosseininasab *et al.*, (2014). Different measurements of PLGA and PEG with different ratios and molecular weights and different terminal chains were dissolved in 50 ml of distilled Toulene in a round bottom flask (Table 2.2). The flask was equipped with a stirrer, condenser and Argon gas inlet. The beaker was placed on a hotplate and the starting temperature was set at 50°C. The flask was left to heat overnight. The temperature of the reaction was then increased to 130-145°C for 30 minutes before the addition of 10 µl of stannous-2-ethylhexanoate which served as a catalyst for the reaction. After addition of the catalyst, the temperature of the reaction was raised from 145°C to 170°C and left stirring for 8 hours. Polymerization was carried out under vacuum. Toluene was removed from the mixture under a reduced pressure using a Rotary evaporator. The residue was dissolved in 50 ml of dichloromethane. The DCM mixture was then transferred into a separating funnel and washed three times with water vigorously stirred at 60°C. A thick viscous mixture was collected into pre-weighed vials. Figure 2.1 shows a schematic reaction of the copolymer synthesis. DCM was evaporated in the fume hood and the copolymers were dried in a vacuum oven for 30 minutes. The ratio of PLGA to PEG was 70:30. The samples were then frozen overnight at -40°C in preparation for freeze drying. The samples were then loaded on the Benchtop Pro 8L ZL-105 freeze drying machine equipped with the lowest condenser temperature of -102/-105, maximum condenser capacity of 8L and the lowest system vacuum of ≤ 20 mTorr. The samples were left for 5 days to dry at a temperature of -102°C and at a pressure of 20 mTorr. After drying, the copolymers were transferred into a pre-weighed vial and stored under room temperature. Table 2.2 gives an outline of the masses used in preparation of nanoparticles.

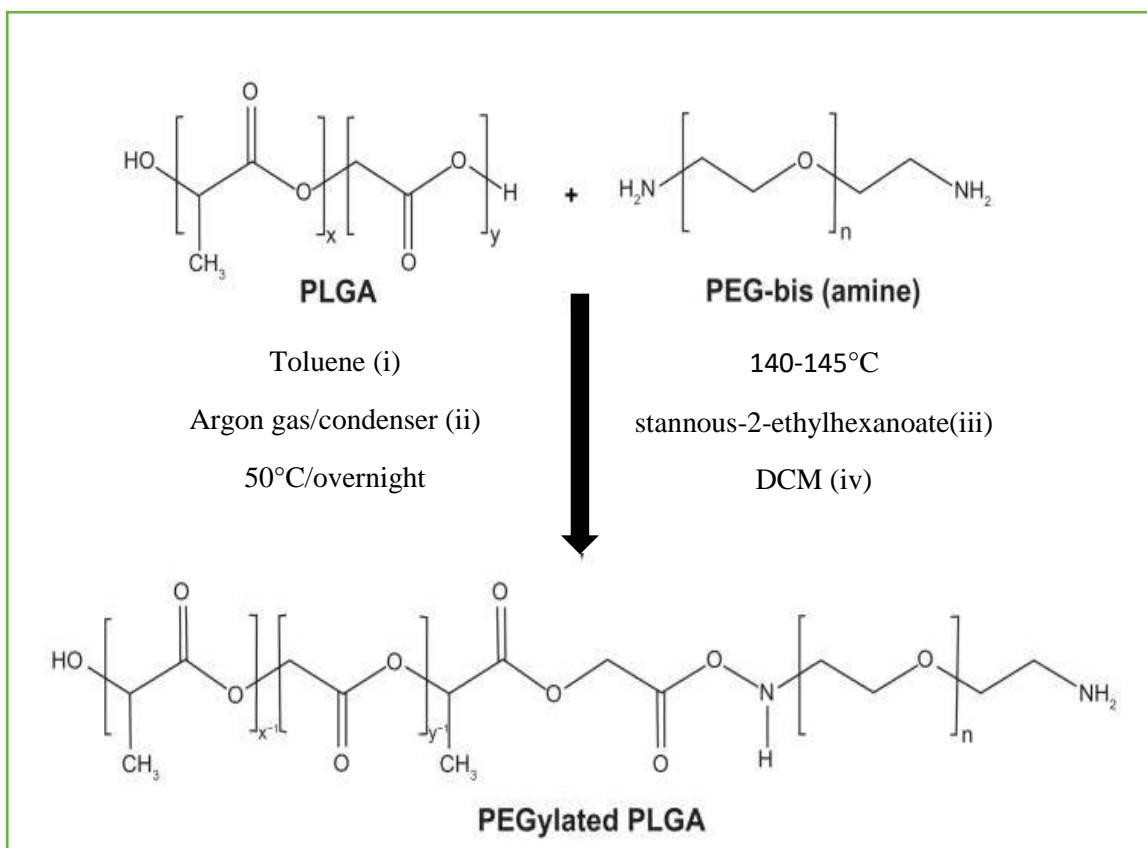


Figure 2.1: Reaction scheme for copolymers

Table 2.2: The mass and molecular weights of polymers used to synthesise copolymers

Polymer	Molecular weight	First batch	Second batch
		Mass used (g)	Mass used (g)
PLGA _{85:15}	50 000 – 75 000	0.56	1.62
PLGA _{50:50}	-	1.80	3.40
PEG _{METHOXY}	5 000	0.24	0.72
PEG _{ACETIC}	5 000	0.24	0.72

2.5.2. Synthesis of nanoparticles

Nanoparticles were prepared using w/o/w emulsion by adaptation of the method described by Li *et al.*, (2001). Briefly 120 mg of crude extract/ F5.1 was emulsified in 20 ml DCM containing 300mg of PLGA-PEG copolymers by homogenisation using sonication method for 30 seconds. Thereafter the first emulsion was poured into 20ml PVA solution (0.5% w/v) and homogenized using sonication method for 60 seconds. To prepare surface adsorbed nanoparticles the nanoparticles were prepared using 300mg of copolymers to form blank nanoparticles. Thereafter, 120mg of flavone was measured and added to 300mg of blank nanoparticles. The flavone was adsorbed to the surface of nanoparticle at 4°C under stirring using PVA as a surfactant. The mixture was then centrifuged at 5000 rpm for 5 minutes. The supernatant was discarded, and the nanoparticles were then transferred to 50 ml PVA solution (0.1% w/v) and stirred for 5 minutes to eliminate DCM. The nanoparticles were then centrifuged at 5 000 rpm for 25 minutes and washed twice with water before lyophilisation. Blank nanoparticles were prepared by the same method without adding crude or F 5.1 at any stage of the preparation, distilled water (dH₂O) was added to the first emulsion.

A total of 10 beneficial nanoparticles were prepared from plant extracts and polymers with antimicrobial activity. Figure 2.1 outlines the summary of the procedure for synthesis of the different nanoparticles. A total of 10 nanoparticles were prepared using crude and subfraction F 5.1. Nanoparticles were made from 300 mg of 50:50 PLGA-PEG ratio copolymer and attached to 120 mg of crude to make surface adsorbed nanoparticles and both surface and encapsulated nanoparticles. The same procedure was done for 85:15 PLGA-PEG copolymers. Another batch of nanoparticles was made from 300 mg of 50:50 PLGA-PEG copolymer and attached to 120 mg of subfraction F 5.1 to make surface adsorbed nanoparticles and both surface and encapsulated nanoparticles. The same procedure was carried out for 85:15 PLGA-PEG copolymers. Blank nanoparticles were made from 300 mg of 50:50 PLGA-PEG copolymers and 85:15 PLGA-PEG copolymers. Blank nanoparticles were not attached or encapsulated with crude extract or subfraction F 5.1, water was used instead.

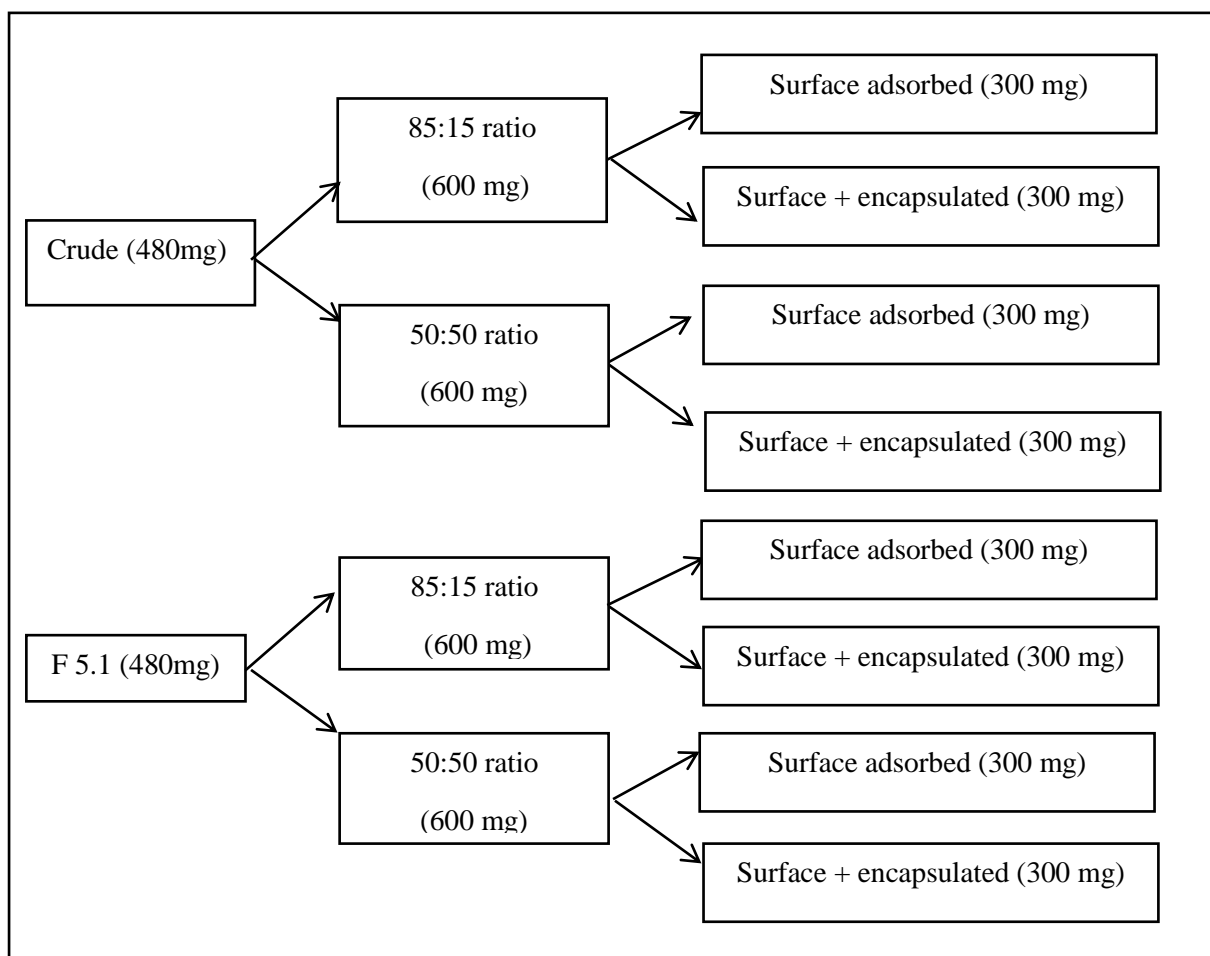


Figure 2.2 : Summary of the synthesis of nanoparticles

2.5.3. Purification of nanoparticles

The prepared nanoparticles were collected and purified by centrifugation at 5000 rpm for 5 min and washed with water three times before lyophilisation (freeze drying). Lyophilisation was done overnight using Bench top pro freeze-drying machine at a temperature of -102°C and pressure of 20 mTorr. The nanoparticles were then collected in powder form and stored at room temperature.

2.6. Characterization of nanoparticles

2.6.1. UV-vis spectroscopy of nanoparticles

Spectra for all the synthesised nanoparticles were determined using UV-vis spectrometer Shimadzu 1800 UV spectrophotometer with double beam optics photometric system,

monochromator (Czerny turner mounting), with wavelength range of 190-1100 nm and a silicon photodiode detector. The nanoparticles were dissolved in ethanol. The data obtained were used to draw plots and the peaks were analysed in comparison to those available in literature.

2.6.2 Fourier Transform Infrared spectroscopy analysis (FTIR) - Nanoparticles

The infrared spectroscopy analysis of the nanoparticles was done using the Perkin Elmer FT-IR 100 spectrometer. Ten milligrams per milliliter of the nanoparticles were dissolved in ethyl acetate. A small pipette tube was used to draw up the sample from which one drop was placed on the diamond surface plate for analysis.

2.6.3. Transmission Electron Microscopy and Scanning Electron Microscopy

The morphology of the nanoparticles was observed using Transmission electron microscopy (TEM) and the topology was determined using Scanning electron microscopy (SEM). SEM analysis was carried out using FEI Nova Nanolab FIB/SEM while for TEM the FEI spirit 120 kV TEM was used. For TEM analysis, nanoparticles were reconstituted in DCM and ultrasonicated. A few drops of the dissolved subfraction F5.1 loaded nanoparticles were transferred to a carbon film coated copper grid and dried. Observation was done at 80kV.

2.6.4. Dynamic Light Scattering (Zeta sizer)

The particle sizes and Zeta potentials were determined using Malvern Zeta sizer Nano ZS which is a dynamic light scattering instrument. This was done to determine the stability and hydrodynamic sizes of the nanoparticles. The nanoparticles and copolymers were suspended in water with different pH values. The pH values ranged from pH 2- pH 12.

2.6.5. Determination of drug loading and drug entrapment efficiency

Percentage drug loading efficiency was determined gravimetrically to assess the capacity of the nanoparticles with regards to the amount of drug (plant extract) in nanoparticles. The

percentage drug loading was calculated based on the weights of the incorporated drug and the nanoparticles using the following equation 2.1:

$$\text{Drug loading (\%)} = \frac{\text{Total amount F5.1} - \text{free F5.1}}{\text{Nanoparticles weight}} \times 100$$

The drug entrapment efficiency was determined by dispersing the PLGA/PEG nanoparticles in a buffer and the amount of the drug in the medium was assessed using UV-vis spectroscopy to obtain the amount of drug in PLGA/PEG nanoparticles with respect to the amount of drug used in the fabrication as determined by equation 2.2.

$$\text{Encapsulation efficiency(\%)} = \frac{\text{Total amount F5.1} - \text{free F5.1}}{\text{Total amount F5.1}} \times 100$$

2.7. *In vitro* drug release study

This study was done by modification of the methods described by Li *et al.*, (2001) and Ngwuluka *et al.*, (2011). Ten milligrams of surface stabilized nanoparticles were suspended in a dialysis tubing membrane containing 2 ml phosphate buffered saline (pH 7.4 and pH 5.5). The membrane was dispersed in 100 ml PBS (pH 7.4 and pH 5.5 respectively) and incubated at 37°C under gentle stirring. At predetermined intervals, 5ml samples were withdrawn. The 5 ml was replaced with fresh medium to maintain sink conditions. The study was done in duplicate. The amount of subfraction F 5.1 released was quantified using the UV spectrophotometer (Shimadzu UV-vis 1800 spectrophotometer).

2.8. Minimum inhibitory concentrations and Minimal bactericidal concentrations

Minimum inhibitory concentrations (MIC) refers to the lowest concentration that inhibits visible microbial growth and minimum bactericidal concentrations is the lowest concentration that is required to kill a microorganism. MIC was obtained using the micro-dilution assay described by Eloff (1998). A 96 well microtitre plate (Thermo fisher scientific) was used for the micro-dilutions. Crude plant extract, subfraction F 5.1, nanoparticles and subfraction loaded nanoparticles were reconstituted in dimethyl sulfoxide (25%, DMSO) to obtain a

concentration of 50 mg/ml. A hundred microliters of tryptic soy broth were added into each well of the 96 well plates and serial two-fold dilutions of the samples were prepared to obtain concentrations of 25 mg/ml in the first well to the 0.19 mg/ml in the last well. Then 100 μ l of culture inoculum was added to each well. Positive and negative controls were also used. Chlorhexidine gluconate was used as a positive control and distilled water was used as a negative control. DMSO was also used as negative control to show that it had no effect on bacteria. More controls for the culture and broth media were included to show that the culture was viable and that the broth was able to support growth and it was not contaminated with other bacteria. The plates were then incubated for 24 hours at 37°C. Lowest dilution with no visible growth was recorded as MIC. Three repeats were performed for all the samples using the three different strains of *S. mutans* generating 9 readings per sample. To determine minimum bactericidal concentration (MBC) after incubation from each well, 10 μ l of the mixture was subcultured onto blood agar plates to determine viable organisms. The lowest concentration that showed no growth was recorded as MBC. Based on the MIC results, for each sample 3 sub-inhibitory concentrations were selected for the subsequent Biofilm and acid assays. For further assays, subfraction F 5.1 loaded on the surface of PLGA/PEG copolymer was chosen due to its noteworthy antimicrobial activity.

2.9. Effect of chemical constituents on acid formation by *S. mutans*

The effects of subfraction F 5.1, subfraction loaded nanoparticles and blank nanoparticles on the acid production by cells of *S. mutans* were studied using a technique described by Nalina and Rahim, (2007) with modifications. Tryptone broth (2 ml) containing sub-inhibitory concentration of test samples was inoculated with 50 μ l of culture containing 10⁷ CFU/ml of *S. mutans* (optical density to 0.2 at 405 nm). Negative controls with water and positive control with chlorhexidine gluconate (0.2%) were included. Cultures were then incubated at 37°C under CO₂ and allowed to grow for a period of 10 hours. The pH was read at 0 hours, 10 hours and every 2 hours thereafter for 16 hours. The bacterial count was done at 0 hours, 12 hours and 16 hours using serial dilution techniques. These experiments were repeated three times for all the three strains of the *S. mutans*. The pH values of the control and tests were compared using the Wilcoxon rank-sum test (Mann-Whitney).

2.10. Effect of chemical constituents on biofilm formation by *S. mutans*

The effects of subfraction F 5.1, subfraction loaded nanoparticles and blank nanoparticles on *S. mutans* biofilm formation were tested using a technique described by Limsong *et al*, (2004) with modification. This technique was performed using glass slide. In the presence of test samples in bijou bottles, biofilms were grown on glass slides for 6 and 24 hours. Briefly, two ml of TSB containing test samples as well as 5% sucrose was added to bijou bottles. Thereafter, freshly grown culture of *S. mutans* (100 μ L) suspended in phosphate saline buffer (PBS) with OD of 0.2 was added to these bijou bottles. Lastly two glass slides coated with filter sterilized saliva were placed at 90° and incubated at 37° C under CO₂. Slides were removed at 6 hours and 24 hours and washed with PBS to remove unattached cells. The remaining attached cells (biofilm) were aseptically removed by scrapping off the biofilm using sterile slides. The cells were re-suspended and vortexed in 1 ml PBS. Ten-fold serial dilutions from 1:10 to 1:10 000 were prepared in a micro-titre plate using PBS. From each dilution 20 μ L was spread onto blood agar plates. Plates were incubated for 48 hours under CO₂ and the number of colonies on each plate was quantified to determine viable bacterial counts. Negative controls with water and positive control with chlorhexidine gluconate (0.2%) were included. Three repeats were done for this assay using three strains of *S. mutans*. The bacterial counts of the tests and negative controls were compared using student T-test and a percentage reduction of the colony forming units per ml for each test sample was calculated.

2.11. Cytotoxicity assay

Biocompatibility should always be investigated when designing new drug delivery biomaterials. More especially when the drugs are intended for long term administration. In this study normal human oral epithelial cells were used as *in vitro* model for studying cytotoxicity of the samples.

2.11.1. Cell culturing

Cell culture media was prepared by adding 50 ml of Dulbecco modified eagle medium (DMEM), 5 ml of fetal bovine serum (FBS) and 50 μ l of pen-strep (penicillin and streptomycin) antibiotics together. The mixture was then filter sterilised.

Human epithelial cells were taken out of the freezer (-80°C) and thawed at room temperature by rubbing the tube between hands. The cells were then transferred to 15 ml tubes. A suspension was made by adding 2 ml of FBS into T25 tissue culture flask containing the cells. The suspension was mixed gently using a pipette. After mixing the suspension the cells were centrifuged for 5 minutes at 1500 rpm. The supernatant was discarded, and the pellet was re-suspended in 1ml fresh media. The newly suspended cells were then transferred into a new 25 cm T25 tissue culture flask. Fresh media was added to the flask to provide nutrients for the cells. The flask was then incubated in 5% CO₂ incubator and left for two days to grow and attach to the flask walls undisturbed.

After two days of growth the cells were examined under the microscope for the adherence and growth of the cells. The media was discarded from the culture flask; thereafter 2ml of PBS was added in the flasks to remove excess media in the flask. To detach the cells from the surface of the flask, Trypsin was added to the flask and incubated for 3 to 5 minutes. Thereafter 5 ml of media was added to the flask containing trypsin and mixed gently using a pipette. The mixture was then transferred into 15 ml tubes and centrifuged for 5 minutes at 1500 rpm. The supernatant was discarded from the tubes leaving the pellet. The pellet was mixed with 5 ml of fresh media using a pipette and transferred into new culture flasks and labelled. More media was added to supplement the cells. The flasks were incubated again.

2.11.2. Determination of cell count and viability

The viability and numbers of cells were determined using the trypan blue method. Oral epithelial cells (20 µl) in medium were mixed with 20 µl of trypan blue. This mixture was placed in a vial, from this mixture 20 µl was removed, placed on a hemocytometer and spread with a cover slip. The viable cells were counted from the quadrants of the hemocytometer. This was done using a light microscope with a magnification of X1000.

The number of viable cells needed to get the desired concentration of 111000 cells per ml was then calculated using the following equation 2.3:

$$\text{No. of cells} = \frac{\# \text{ of cells in 4 grids}}{4} \times 2 \times 10000$$

The cell number was then multiplied by the amount of cell suspension needed to fill the applicable wells of a 96 well microtitre plate (McCauley *et al.*, 2013).

2.11.3. Seeding of cells into the microtitre plate and exposures

A 96 well microtitre plate was used for the cytotoxicity test. Media was added to the microtitre plates to form blank test control wells. Triton X was used as a positive control. The subfraction F 5.1 and subfraction F 5.1 nanoparticles were dissolved in DMSO. Therefore, DMSO control was also included. The cell suspension solution was then added to the wells. Hundred microliters of each was added to well, while with Triton X only 2% solution was added. The plates were then incubated at 37°C for 24 hours under 5% carbon dioxide. The concentrations of subfraction F 5.1 and subfraction F 5.1 stabilized nanoparticles in the test wells ranged from 25 mg/ml to 0.0125 mg/ml. After incubation, the media with the test samples and controls was removed and replaced with 100 µl of the MTT reagent (3-(4,5-Dimethylthiazol-2-yl)-2,5-diphenyltetrazolium bromide). The plates were further incubated for 3 hours at 37°C and 5% carbon dioxide. The MTT reagent was pipetted out and replaced with 100% DMSO to dissolve the formazan crystals. After 30 minutes of incubation, the plates were read with a spectrophotometer at 450 nm.

CHAPTER 3

RESULTS

3.1. Extraction and purification

3.1.1. Extraction

The methanolic extract prepared from *Dodonaea* leaves was dried under a fume hood and weighed to calculate the yield per given mass of dried leaves shown in Table 3.1.

Table 3.1: The percentage yield of dried methanolic crude extract

No. of methanolic extractions	Mass of DVA leaves (g)	Yield (g)	Yield (%)
1	60	6.2	10.3
2	60	4.8	8.0
3	60	5.4	9.0
4	60	3.9	6.5
5	60	4.1	6.8
Total	300	24.4	40.6

3.1.2. Column chromatography

The dried crude extract was fractionated using silica gel column chromatography and showed six fractions (F1-F6). These fractions were eluted based on polarity and they exhibited different colours. Fraction 1 showed a yellow colour, fraction 2 showed a green colour, fraction 3 showed a yellow colour slightly different from fraction 1, fraction 4 had a yellow green colour and fraction 5 had a deep yellow colour. Flavones are known to be yellow in colour therefore, a yellow fraction 5 (F 5) was selected from the column. Fraction 5 was further subfractionated to obtain subfractions (F 5.1 and F 5.2). Subfraction F5.1 was chosen as the main agent due to its antimicrobial activities. Subfraction F5.1 was found to have anti-*streptococcus mutans* activity, anti-acidogenic and anti-aciduric properties (Patel *et al.*, 2009;

Naidoo *et al.*, 2012 and Ngabaza *et al.*, 2017). The fraction of interest subfraction F 5.1 was purified by several re-runs of column chromatography. Subfraction F 5.1 was selected dried and weighed. The amount of F 5.1 that was extracted from all the crude extracts was 1.8g. This was then used for attachment to the surface of polymeric nanoparticles and anticariogenic tests.

3.1.3. Thin layer chromatography

Thin layer chromatography was used to group the fractions according to their TLC profiles using TLC plates lined with silica and three solvents that differ in polarity: Toulene/ Ethanol/ Ammonium hydroxide (TEA), Dichloromethane/ Ethyl acetate/ Formic acid (DEF), Ethyl acetate/ Methanol/ water (EMW). The TEA solvent combination was able to separate non-polar fractions, 1 and 2. DEF with an intermediate polar solvent combination was able to separate fractions 3 and 4. EMW was able to separate polar Fractions 5. Fraction 5 was spotted on a TLC plate and submerged into the solvent mixtures. A yellow distinct band was observed on the TLC plate after spraying with vanillin. This conforms to the yellow colour that is observed in elution which is typical of flavones.

3.2. Characterisation of subfraction F 5.1

3.2.1. UV-vis spectroscopy analysis of subfraction F 5.1

The obtained subfraction F 5.1 was characterized using UV-vis spectroscopy. The spectrum showed two major peaks (Figure 3.1). Band A was positioned at a wavelength of 334nm and Band B at 270nm. These peaks appeared in regions that were cited as identified in literature, where band A was expected in the range of 310nm-350nm and band B in the range of 250nm-290nm (Tsimogiannis *et al.*, 2007 and Ngabaza *et al.*, 2017).

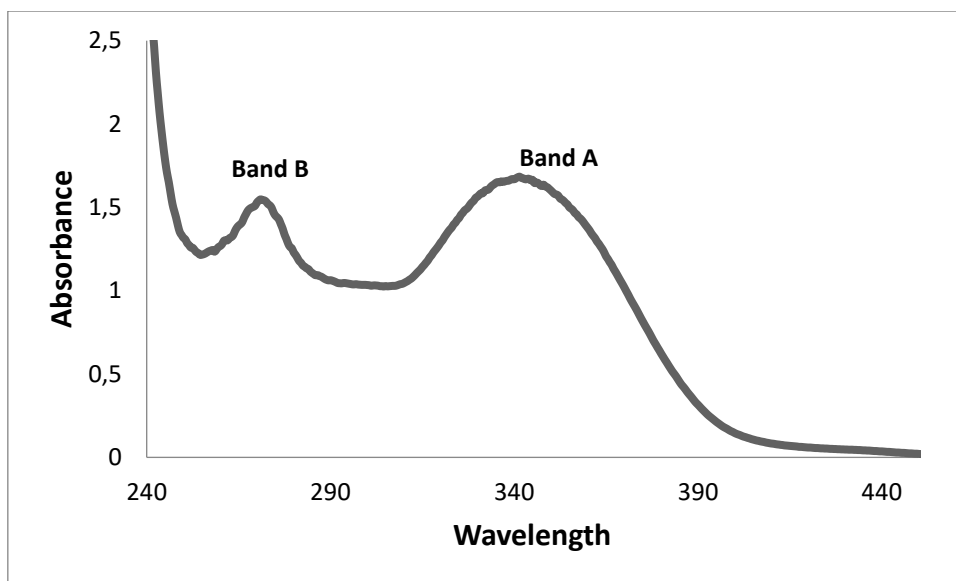


Figure 3.1: Spectrum bands of subfraction F 5.1 observed using UV-vis spectroscopy

3.2.2 Fourier transform infrared spectroscopy (FTIR) analysis of Subfraction F 5.1

The results obtained from Fourier transform infrared spectroscopy (FTIR) analysis of subfraction F 5.1 are shown in Figure 3.2 and Table 3.2 gives a summary of the absorption bands of subfraction F 5.1 as observed in literature.

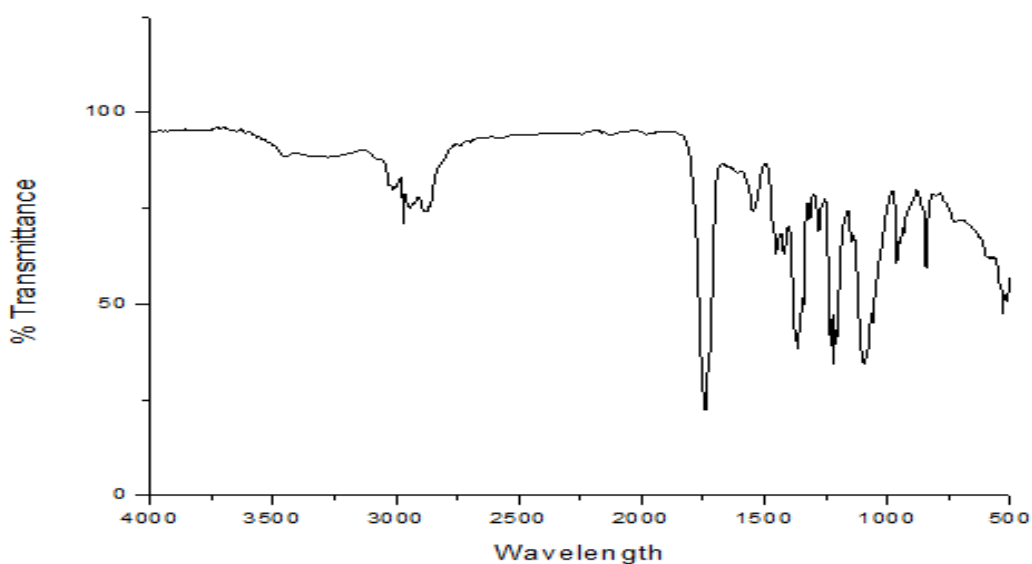


Figure 3.2: Fourier Transform Infrared spectroscopy analysis of subfraction F 5.1

The infrared spectrum was consistent with the structure of the expected flavone as cited in literature (Table 3.2). It shows that absorption band at 3455.3 cm^{-1} was assigned to hydroxyl groups. The absorption bands at 2880-2998 cm^{-1} was assigned to C-H, the absorption at 1454.6-1650.3 cm^{-1} was assigned to C=C and the band at 1739.6 cm^{-1} was assigned to C=O. A band at 1365.4 cm^{-1} was assigned to C-O, band 1278.7-1365.4 cm^{-1} was assigned to C-O-C, band 1059.8-1092.8 cm^{-1} was assigned to C-C and band 801.3 cm^{-1} was assigned to C-OH.

Table 3.2: Absorption vibration bands observed for subfraction F 5.1

Vibrations and wavelength (cm^{-1}) (Clark, 2000)		Vibrations and wavelength (cm^{-1}) (In this study)	
Stretches	C-H (2880-2998)	Stretches	C-H (2944.2-2969.2)
	O-H (3230-3550)		O-H (3455.3)
	C=O (1744)		C=O (1739.6)
	C=C (1469-1651)		C=C (1454.6-1650.3)
	C-O (1358)		C-O (1365.4)
	C-O-C (1282-1358)		C-O-C (1278.7-1365.4)
	C-C (1000-1168)		C-C (1059.8-1092.8)
Bends	C-OH (806)	Bends	C-OH (801.3)
	C-H (1450-1470)		C-H (1454)

3.2.3 Gas Chromatography-Mass Spectrometry analysis of subfraction F 5.1

Gas chromatography-mass spectroscopy and liquid chromatography-mass spectroscopy were used to identify subfraction F 5.1. The mass charge ratio observed in Figure 3.3 was $[M+H]$ with molecular mass of 331.08g/mol. Further elucidation by another technique (NMR) was not carried out in this work because the same flavone obtained was carried out in a previous study by Ngabaza *et al.*, 2017. The three preceding techniques (Chromatography, UV-vis spectroscopy and Infrared spectroscopy analyses) including GC-MS confirmed that the flavone was present in subfraction F 5.1. The results in Figure 3.3 show that the subfraction still contained a mixture of compounds. The lack of availability of flash chromatography equipment hindered true isolation of the pure compound which could have been elucidated further.

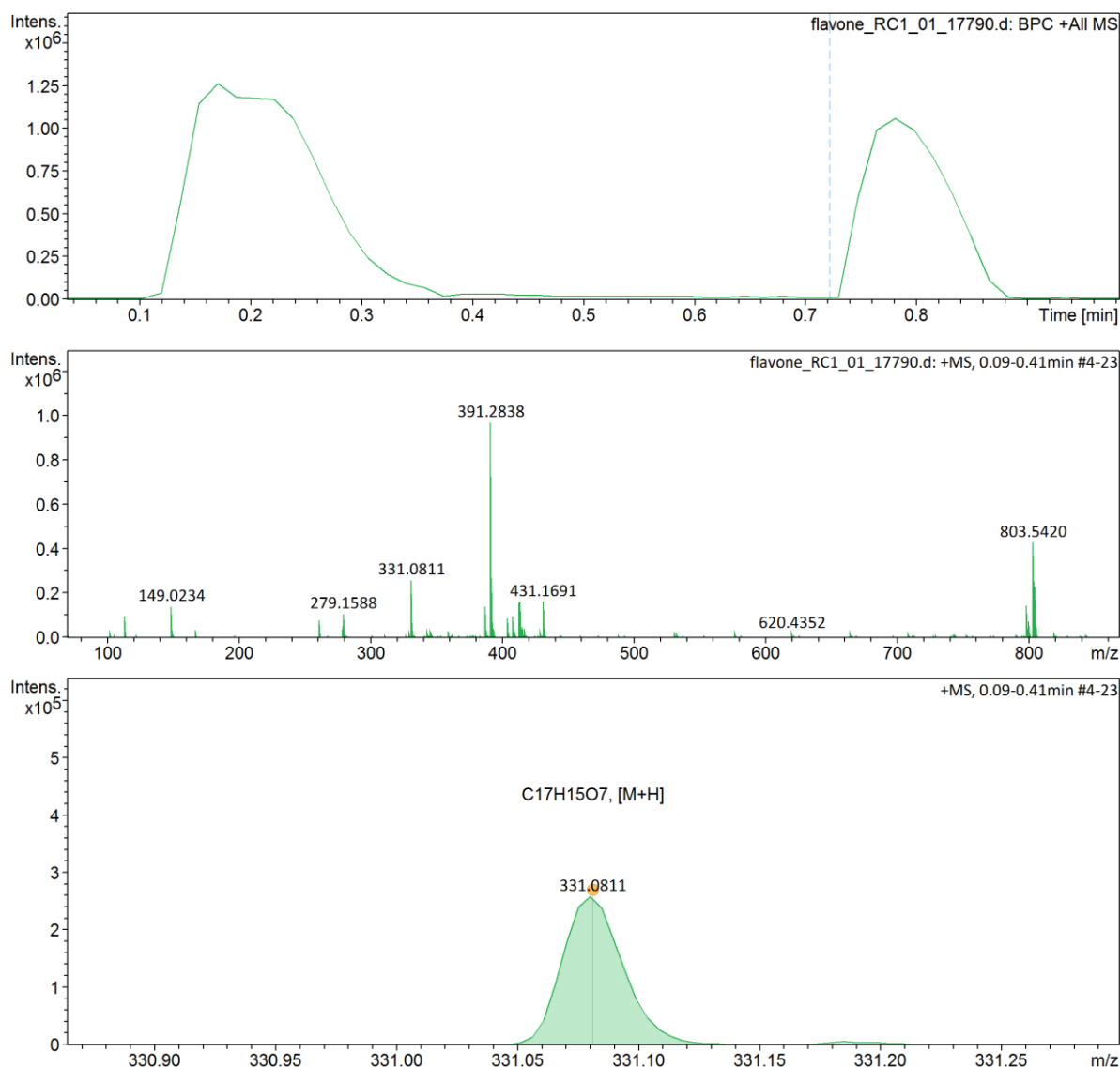


Figure 3.3: Gas chromatography-mass spectroscopy chromatogram of subfraction F 5.1

3.3. Synthesis of nanoparticles

Two polymers of PLGA with different ratios have been used to synthesise copolymers with PEG with acetic acid terminal. The ratios for PLGA are 50:50 and 85:15 of poly lactide to glycolide. A total of 10 different nanoparticles were prepared. The nanoparticles were loaded with subfraction F 5.1 and crude extract. The nanoparticles were prepared by adding 300 mg of copolymers and 120 mg of crude extract or subfraction F 5.1 for preparation of crude extract and subfraction containing nanoparticles containing nanoparticles respectively. The synthesized nanoparticles were lyophilized, and the respective weighting carried out as shown in Table 3.3.

Table 3.3: Prepared nanoparticles and their measurements

Compound	Prepared nanoparticles (mg)	
	50:50 PLGA/PEG acetic	85:15 PLGA/ PEG acetic
1. Blank	230	230
2. F5.1 surface adsorbed	210	320
3. F5.1 surface + encapsulated	270	290
4. Crude surface adsorbed	100	170
5. Crude surface + encapsulated	250	280

The nanoparticles prepared as shown in Table 3.3 were used to perform MIC/MBC as a preliminary screening to select the most active nanoparticles. Subfraction F 5.1 surface adsorbed nanoparticles were chosen and synthesised in large quantities along with the blank nanoparticles as a control. F 5.1 nanoparticles were prepared by combining F 5.1 and copolymers in the nanoparticle synthesis matrix and blank nanoparticles contained only the copolymers. F 5.1 was not added at any stage of synthesis for the blank nanoparticles. The following yields were obtained for both the blank and F 5.1 stabilized nanoparticles selected for continued investigation (Table 3.4).

Table 3.4: Yields obtained from synthesis of subfraction F 5.1 surface adsorbed nanoparticles

Nanoparticles 50:50 PLGA/PEG	Final yield of nanoparticles	Final amount of subfraction F 5.1 loaded in 10mg of NPs
1. Blank	860mg	0 mg
2. F5.1 surface adsorbed	960mg	4.4mg

3.4. Characterisation of synthesized nanoparticles

3.4.1 UV-vis spectroscopy analysis of synthesized nanoparticles

The synthesized nanoparticles were characterized using UV-vis spectroscopy. The spectrum of blank nanoparticles shows a minor peak at a wavelength of 278 nm, which confirms the

synthesis of nanoparticles was a success. The nanoparticles loaded with beneficial subfraction shows the major peaks at wavelength 275 nm and 333 nm from the subfraction as shown in Figure 3.4. The bands of the subfraction observed confirm the presence of flavone and successful loading of the subfraction onto the matrix of the polymeric nanoparticles.

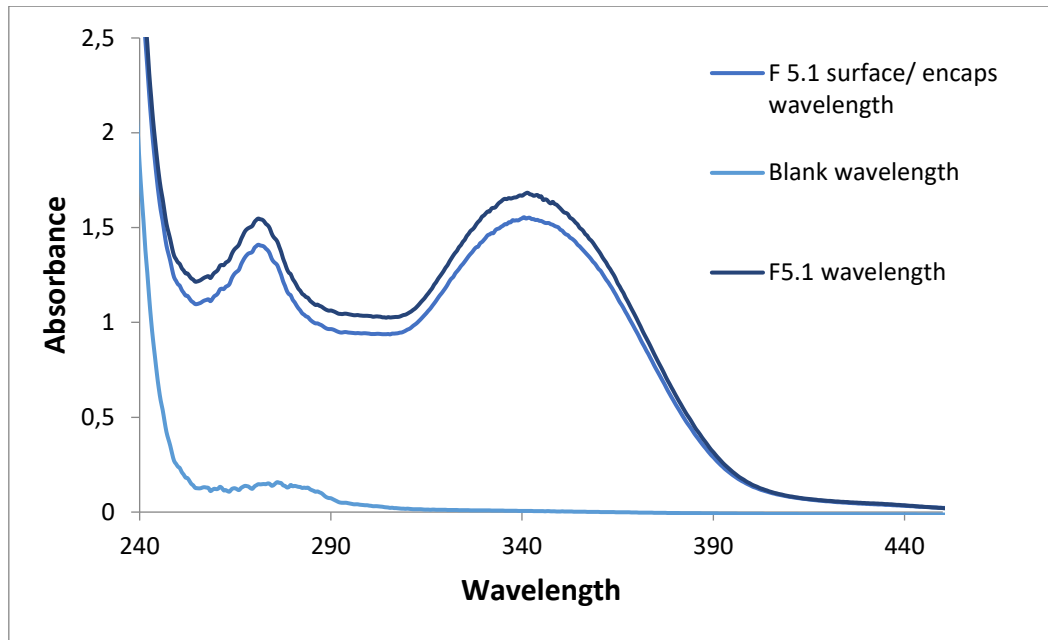


Figure 3.4: Spectrum bands of 50:50 PLGA-PEG nanoparticles load with subfraction F 5.1

3.4.2. Fourier Transform Infrared spectroscopy analysis of nanoparticles

The results obtained from infrared spectroscopy analysis are shown in Figure 3.5 and Table 3.5 for PLGA-PEG copolymers.

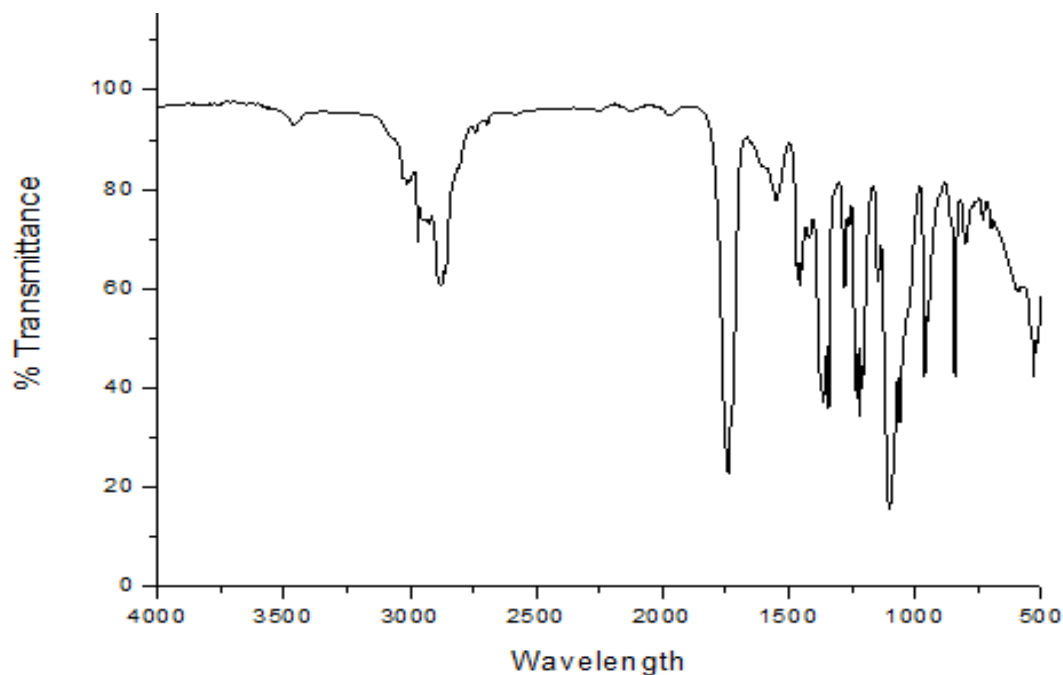


Figure 3.5: Fourier Transform Infrared spectroscopy analysis of PLGA-PEG copolymers

The infrared spectrum was consistent with the structure of the expected copolymers. From the FTIR spectrum presented in Figure 3.5, the absorption spectra at 3456.3 cm^{-1} was assigned to terminal hydroxyl groups in the copolymer from which PEG homopolymer has been removed. The bands at 2969.8 cm^{-1} and 3025.3 cm^{-1} were due to C-H stretch of CH_3 and those at 2945.9 cm^{-1} were due to C-H stretch of CH_2 . The band at 1739.1 cm^{-1} was assigned to the C=O stretch while absorption at $1059.7\text{--}1100\text{ cm}^{-1}$ was due to the C-O stretch. The absorption bands at 1365.2 and 799.8 cm^{-1} were due to bends of CH_3 and CH_2 respectively. The absorption spectra are shown in Table 3.5.

Table 3.5: Fourier Transform Infrared spectroscopy analysis of PLGA-PEG copolymers

Vibrations and wavelength (cm ⁻¹) (Li <i>et al.</i> , 2001)		Vibrations and wavelength (cm ⁻¹) (In this study)	
Stretches	C-OH (3509.9)	Stretches	C-OH (3456.3)
	C-H stretch of CH ₃ (2955-3010)		C-H stretch of CH ₃ (2969.8-3025.3)
	C-H stretch of CH ₂ (2885)		C-H stretch of CH ₂ (2945.9)
	C=O (1762.6)		C=O (1739.1)
	C-O (1089.6-1186)		C-O (1059.7-1100)
Bends	CH ₂ (715-725)	Bends	CH ₂ (799.8)
	CH ₃ (1370-1390)		CH ₃ (1365.2)

Figure 3.6 shows the infrared vibration spectrum observed for flavone stabilized nanoparticles. The vibrational stretches and bends observed were similar to those seen in PLGA-PEG copolymers and nanoparticles as well as those observed in subfraction F 5.1. This suggests that the loading of F 5.1 onto nanoparticles was successful. Table 3.6 shows the bends and stretches observed in PLGA-PEG nanoparticles in literature as well as stretches and bends observed in this study.

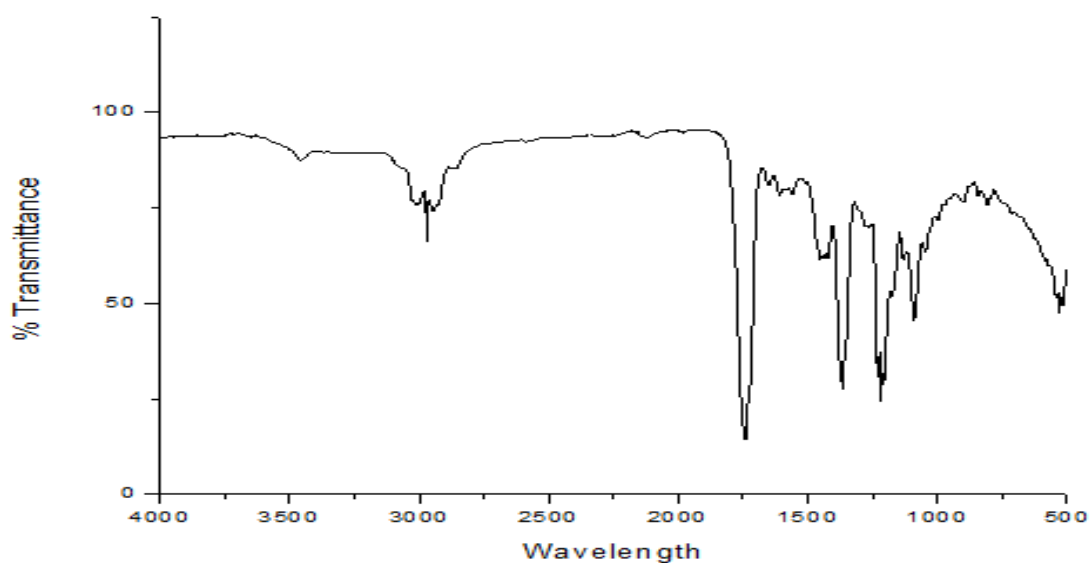


Figure 3.6: Fourier Transform Infrared spectroscopic analysis of F 5.1 nanoparticles

Table 3.6: Fourier Transform Infrared spectroscopy analysis of subfraction F 5.1 nanoparticles

Vibrations and wavelength (cm⁻¹) PLGA-PEG NPs in literature (Alimohammadi <i>et al.</i>, 2012)		Vibrations and wavelength (cm⁻¹) Blank NPs in this study	Vibrations and wavelength (cm⁻¹) F 5.1 NPs in this study
Stretches	C-H (2950)	C-H (2944.4)	C-H (2969.9-3025.3)
	C=O (1750-1765)	C=O (1739.1)	C=O (1740.1)
	C=C (1469-1651)	C=C (1455.0-1650.3)	C=C (1448.2-1649.9)
	C-O (1358)	C-O (1356.4)	C-O (1365.5)
	C-O-C (1085-1190)	C-O-C (1059)	C-O-C (1276.7-1365.5)
	C-C (1000-1168)	C-C (1100)	C-C (1045.1-1173.9)
	O-H (3400)	O-H (3456.3)	O-H (3455.9)
Bends	C-OH (806)	C-OH (799)	C-OH (805.8)

3.4.3. Particle size and morphology

3.4.3.1. Transmission electron microscopy

Figure 3.7, 3.8 and 3.9 shows the TEM images of the PLGA-PEG copolymers, blank nanoparticles and subfraction F 5.1 stabilized nanoparticles respectively. The images confirm the formation of blank nanoparticles and F 5.1 loaded nanoparticles.

The size of the nanoparticles was calculated from a TEM image using ImageJ software (ImageJ 1.45). Some images were not clear enough to use in ascertaining the nanoparticle size due to aggregation effects, however most of the visible nanoparticles in subfraction F 5.1 stabilized nanoparticles were analysed using ImageJ. The results from ImageJ analysis are shown in Table 3.7 and a distribution curve is shown in Figure 3.10. The results were shown in the form of area and radius. The nanoparticles were lying in the range of 6.8-12.3 nm. The mean diameter of the nanoparticles was 9.2 ± 5.7 .

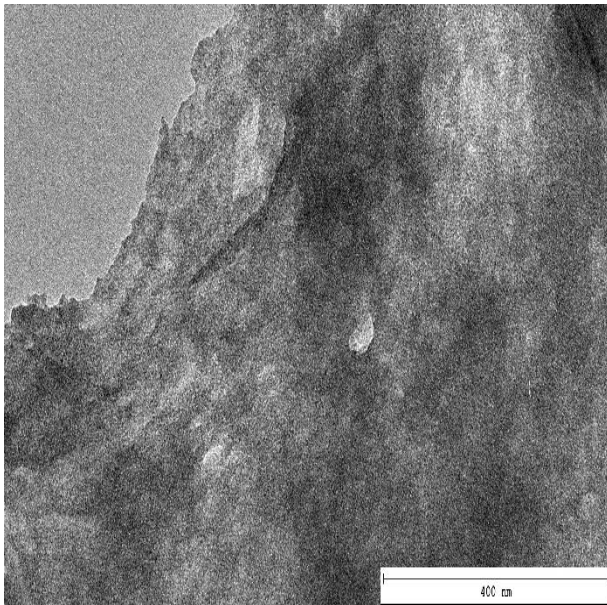


Figure 3.7: Transmission electron micrograph of PLGA-PEG copolymers

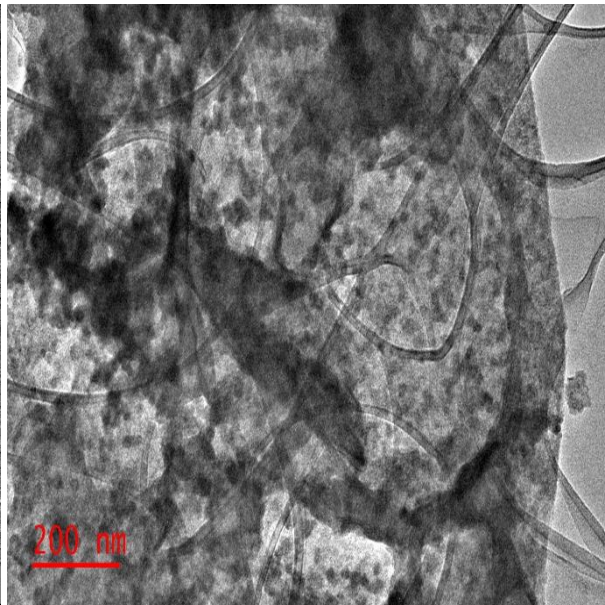


Figure 3.8: Transmission electron micrograph of PLGA-PEG blank nanoparticles

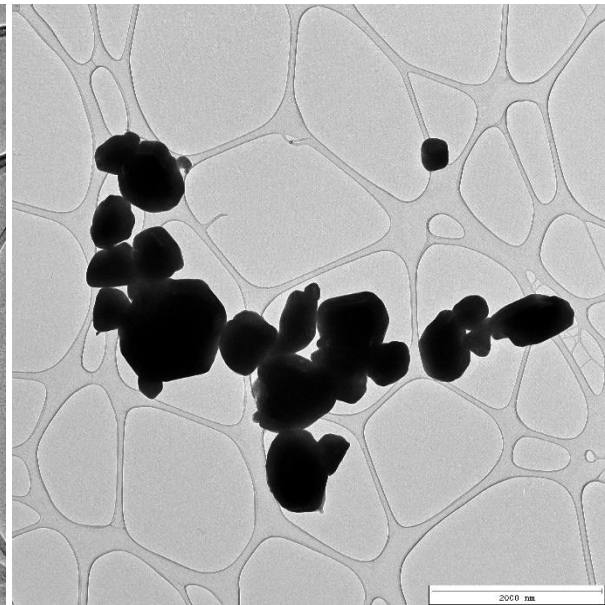


Figure 3.9: Transmission electron micrograph of PLGA-PEG subfraction F 5.1 nanoparticles

Table 3.7: Summary of the measurements obtained from Image J analysis of subfraction F 5.1 stabilized nanoparticles (using Image: Figure 3.10)

No.	Area (nm ²)	R ²	R	Diameter (nm)
1	36.0	11.5	3.4	6.8
2	49.0	15.6	3.9	7.9
3	57.0	18.1	4.3	8.5
4	56.0	17.8	4.2	8.4
5	57.0	18.1	4.3	8.5
6	42.0	13.4	3.6	7.3
7	49.0	15.6	3.9	7.9
8	108.0	34.4	5.8	11.7
9	65.0	20.7	4.6	9.1
10	65.0	20.7	4.6	9.1
11	119.0	37.9	6.2	12.3
12	93.0	29.6	5.4	10.9
Mean	66.3	21.1	4.6	9.2
±SD	26.3	8.0	2.8	5.7

R=Radius

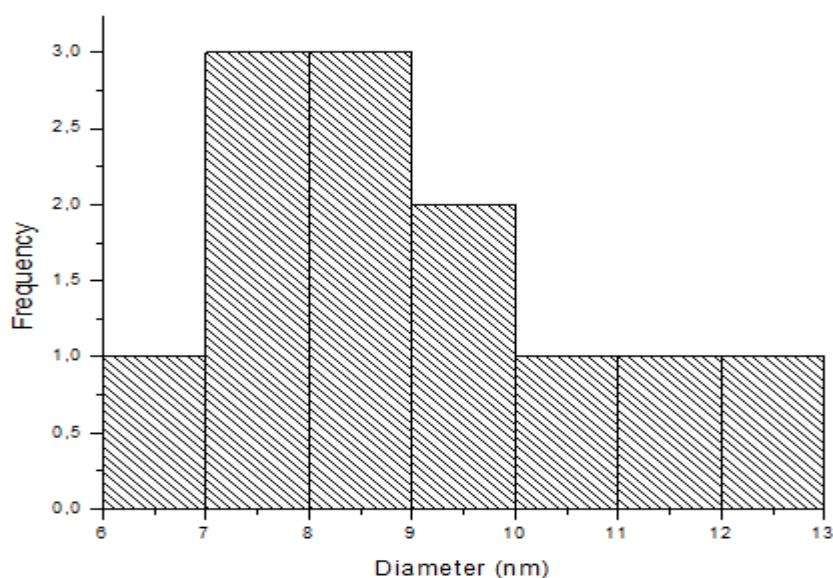


Figure 3.10: Histogram of the distribution of nanoparticles (using image 3.7)

3.4.3.2. Scanning electron microscopy

The morphology of the copolymers and nanoparticles was determined using scanning electron microscopy. Figure 3.11, 3.12 and 3.13 show the SEM images of PLGA-PEG copolymers, blank nanoparticles and subfraction F 5.1 stabilized nanoparticles obtained from scanning electron microscopy respectively. The PLGA-PEG copolymers show a distinct layer on the surface (Figure 3.11). Blank nanoparticle SEM image shows many layers this may be due to polymers protruding from the nanoparticle surface (Figure 3.12). The shape of subfraction F 5.1 stabilized nanoparticles appears to be of a flower structure (Figure 3.13).

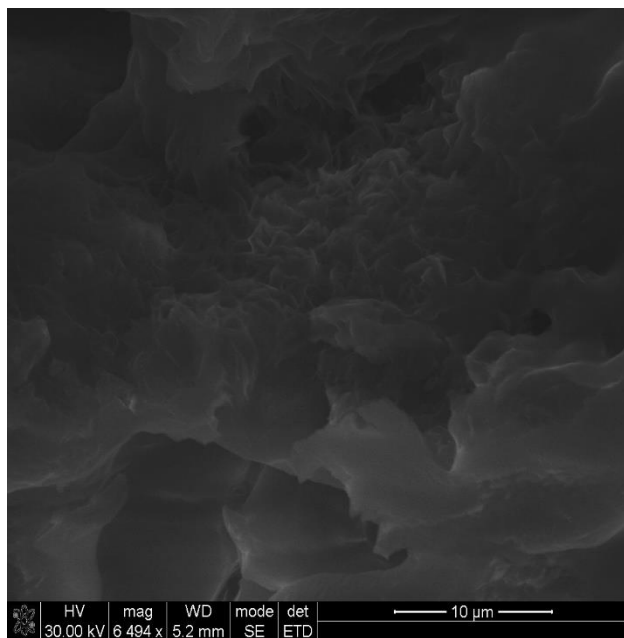


Figure 3.11: Scanning electron micrograph of PLGA-PEG copolymers

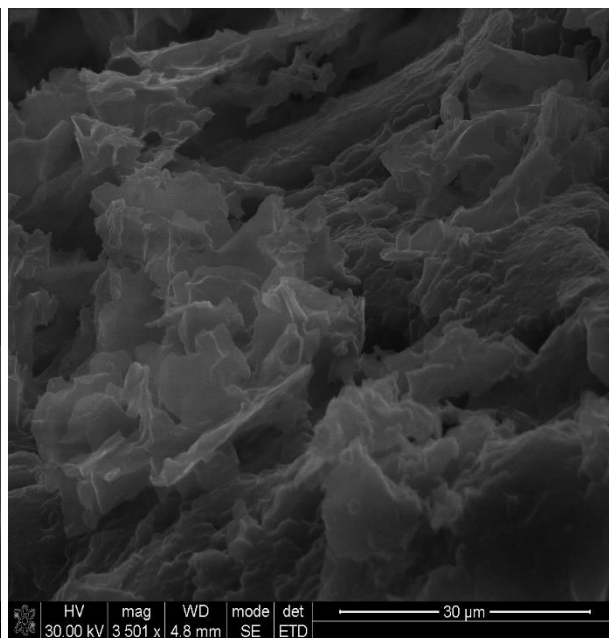


Figure 3.12: Scanning electron micrograph of PLGA-PEG blank nanoparticles

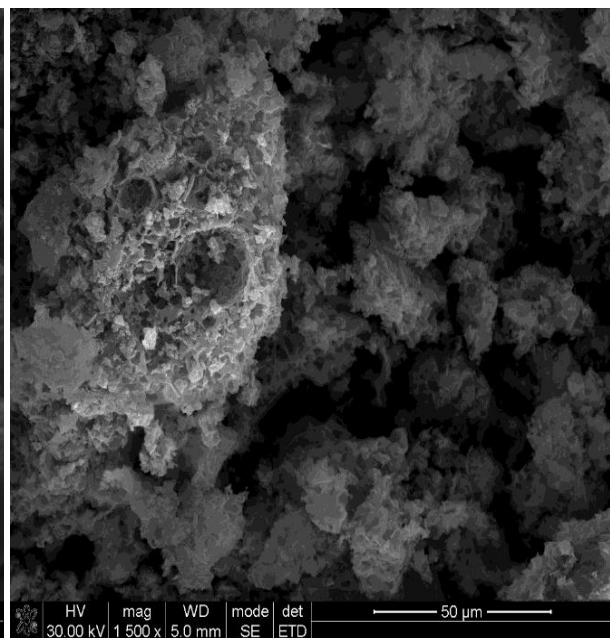


Figure 3.13: Scanning electron micrograph of PLGA-PEG subfraction F 5.1 stabilized nanoparticles

3.4.4. The influence of pH on Zeta size and Zeta potential

3.4.4.1. The influence of pH Zeta size and Zeta potential of PLGA-PEG blank nanoparticles.

Table 3.8 shows the sizes of the nanoparticles as well as the Zeta potential values in different pH media of PLGA-PEG blank nanoparticles. PLGA-PEG blank nanoparticles showed a smaller size at pH 11 (169.8 nm) and pH 12 (143.6 nm). Figure 3.14 shows the size distribution and poly dispersity index of blank nanoparticles in medium at different pH values.

The poly dispersity index (PDI) is a parameter that defines the particle size distribution of the nanoparticles (in particular, the magnitude of the distribution). Poly dispersity index values range between 0 and 1, where a PDI value of 0.1 represents monodispersity. Values greater than 0.1 indicate polydispersity in the sample while values between 0.1 and 0.25 indicate a narrow size particle distribution (Tantra *et al.*, 2010).

Table 3.8: The influence of pH on Zeta size and Zeta potential of PLGA-PEG blank nanoparticles

PH	Zeta size average (nm)	Poly dispersity index (PDI)	Zeta Potential (mV)
2	191.4	0.9	0.7
3	235.1	0.3	22.5
4	365.0	0.9	19.1
5	570.1	0.4	21.8
6	645.9	0.8	17.2
7	983.0	0.7	7.5
8	2360.8	0.4	9.0
9	2580.3	0.6	6.4
10	2141.7	0.4	-10.9
11	85.3	0.4	-16.6
12	116.2	0.2	-50.3
Mean	934.1	0.5	3.3

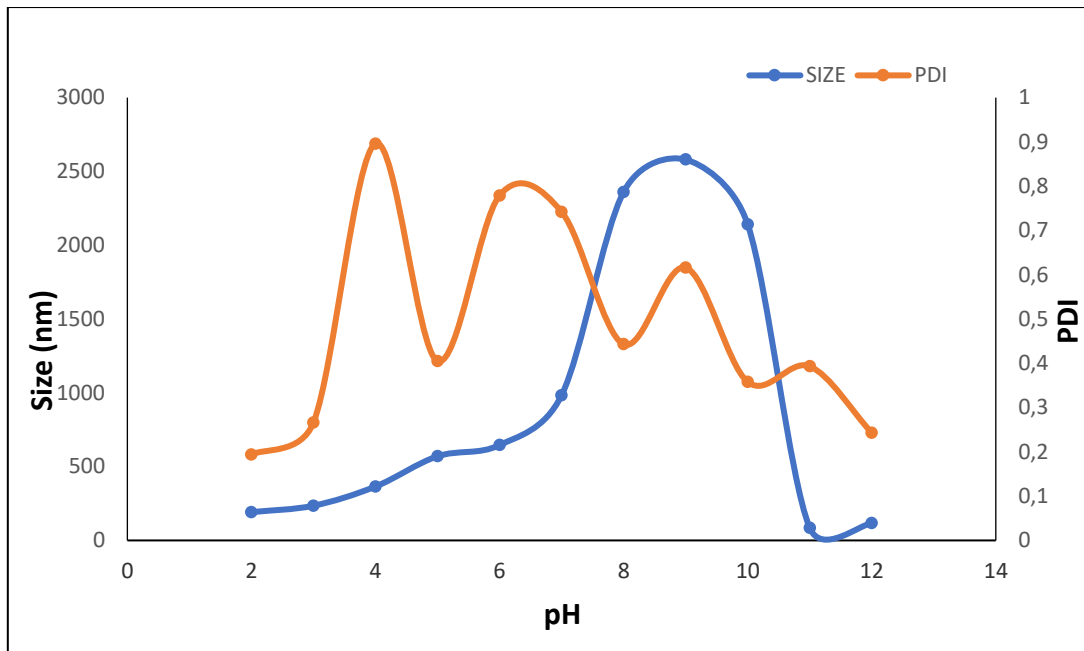


Figure 3.14: The effect of pH on particle size and PDI of PLGA-PEG blank nanoparticles

3.4.4.2. The influence of pH on Zeta size and Zeta potential of PLGA-PEG F 5.1 nanoparticles

The results on the influence of pH on Zeta size and Zeta potential are shown in Table 3.9. PLGA-PEG subfraction stabilized nanoparticles showed a smaller size at pH 11 (169.8 nm) and pH 12 (143.6 nm). Figure 3.15 shows the size distribution and poly dispersity index of PLGA-PEG subfraction stabilized nanoparticles in medium at different pH values.

Table 3.9: The influence of pH on Zeta size and Zeta potential of PLGA-PEG F 5.1 nanoparticles

PH	Zeta size average (nm)	Poly dispersity index (PDI)	Zeta Potential (mV)
2	232.9	0.4	12.7
3	536.5	0.8	4.3
4	2639	0.5	-0.6
5	284.6	0.6	-3.6
6	262.8	0.5	-10.2
7	189.8	0.5	-11.1
8	672.3	0.6	-18.3
9	972.1	0.8	-21.2
10	832.3	0.7	-9.4
11	169.8	0.2	-25.9
12	143.6	0.4	-42.8
Mean	630.5	0.6	-11.5

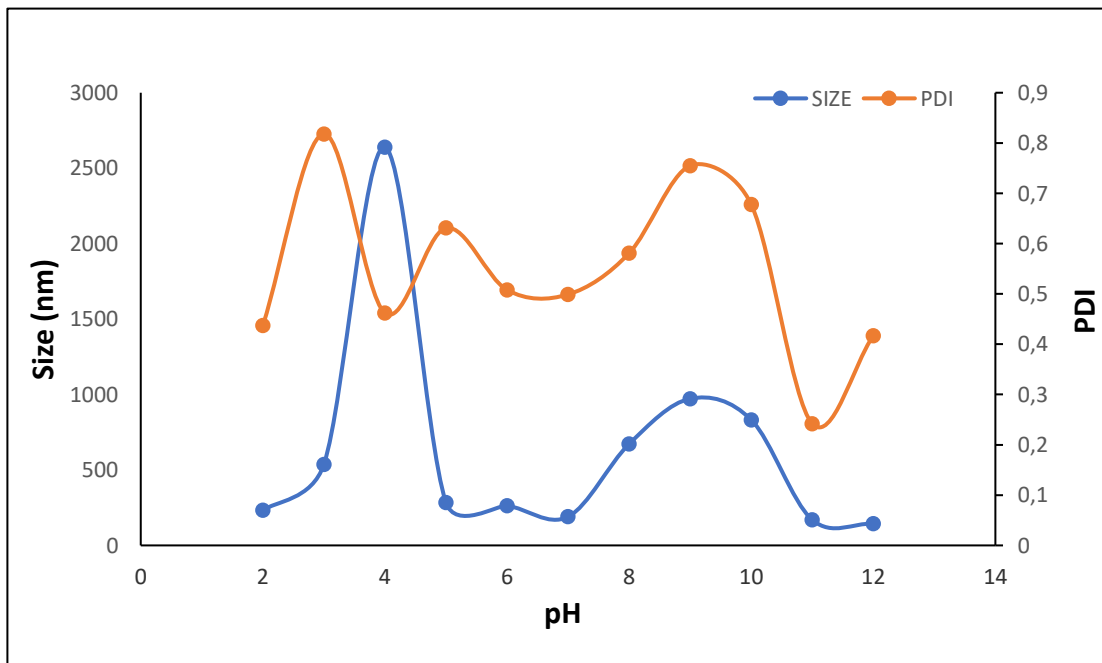


Figure 3.15: The effect of pH on particle size and PDI of subfraction F 5.1 nanoparticles

3.4.4.3. The influence of pH on Zeta potential of PLGA-PEG copolymers, PLGA-PEG blank nanoparticles and subfraction F 5.1 nanoparticles

Figure 3.16 shows a graph on the influence of pH on Zeta potential. Guidelines classify nanoparticle-dispersions with Zeta potential values of $\pm 0-10$ mV, $\pm 10-20$ mV and $\pm 20-30$ mV and $> \pm 30$ mV as highly unstable, relatively stable, moderately stable and highly stable respectively (Bhattacharjee, 2016). Copolymers were highly unstable at pH 2, pH 4-9, relatively stable at pH 10, moderately stable at pH 3 and highly stable at pH 11-12. Blank nanoparticles were highly unstable at pH 2, pH 7-10, relatively stable at pH 4, pH 6, pH 11, moderately stable at pH 3, pH 5 and highly stable at pH 12. Subfraction F 5.1 stabilized nanoparticles were highly unstable at pH 3-5, relatively stable at pH 2, pH 6-10, moderately stable at pH 9, pH 11 and highly stable at pH 12.

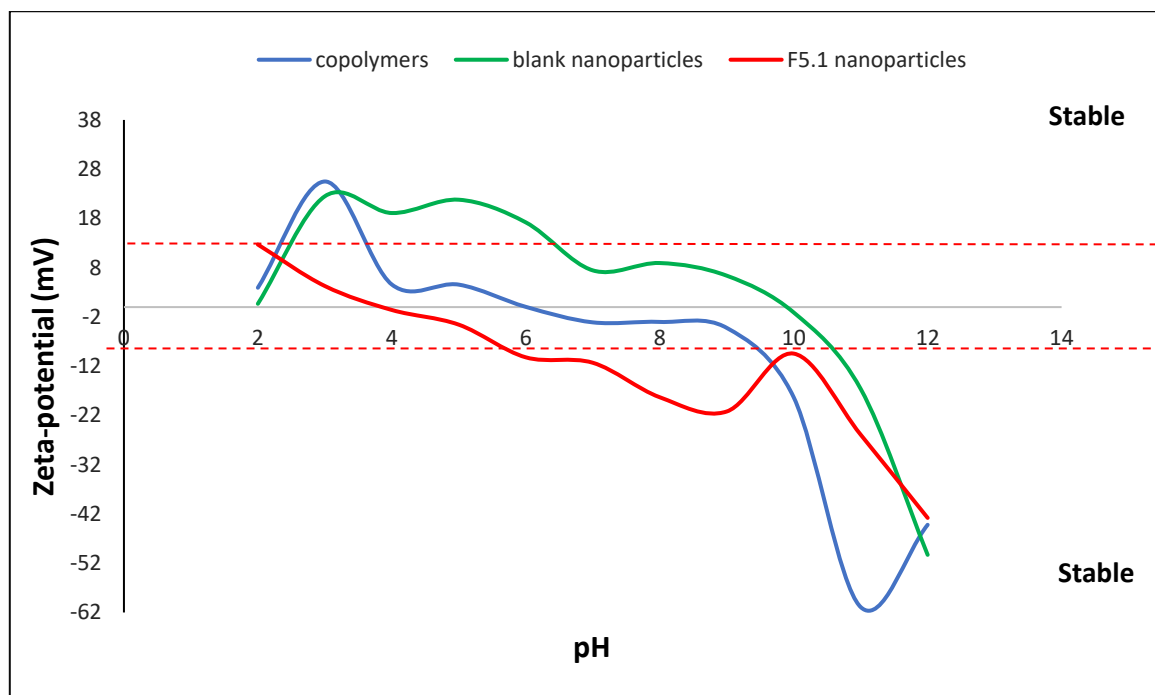


Figure 3.16: The influence of pH on Zeta potential of PLGA-PEG copolymers, blank nanoparticles and subfraction F 5.1 nanoparticles

Table 3.10 shows the summary of the hydrodynamic diameters, Zeta potential and poly dispersity index values of subfraction F 5.1 nanoparticles and blank nanoparticles.

Table 3.10: Summary of particle size and surface charge of PLGA-PEG copolymers, blank nanoparticles and subfraction F 5.1 stabilized nanoparticles (F5.1/NPs)

	Blank NPs	F5.1/NPs
Mean hydrodynamic diameter (nm)	934.1 ± 957.9	630.518 ± 725.2
Mean Zeta potential (mV)	3.3 ± 21.2	-11.483 ± 15.3
Mean poly dispersity index	0.5 ± 0.2	0.6 ± 0.2

3.5. Drug (Subfraction F 5.1) entrapment analyses

3.5.1. Determination of drug loading and drug entrapment

Percentage drug loading was determined gravimetrically to assess the capacity of nanoparticles towards the amount of drug loading (plant extract) in nanoparticles. The initial synthesis composed of 120mg of F5.1 and 300mg of nanoparticles. To produce nanoparticles in large quantity F5.1 was 120mg was then multiplied by 4 and 300mg nanoparticles were multiplied by 4. Therefore, 480mg F5.1 was loaded on 1.2g nanoparticles. The total yield of stabilized nanoparticles at the end of synthesis and after purification was 960mg.

$$\text{Drug loading (\%)} = \frac{\text{total amount of F5.1} - \text{free F5.1}}{\text{nanoparticles weight}} \times 100$$

$$\text{Drug loading (\%)} = \frac{480\text{mg} - 62\text{mg}}{960\text{mg}} \times 100$$

$$\text{Drug loading} = 43.5\%$$

The entrapment efficiency was calculated using the total amount of subfraction and free subfraction.

$$\text{entrapment efficiency (\%)} = \frac{\text{total amount of F5.1} - \text{free F5.1}}{\text{total amount of F5.1}} \times 100$$

$$\text{entrapment efficiency (\%)} = \frac{480\text{mg} - 62\text{mg}}{480\text{mg}} \times 100$$

$$\text{entrapment efficiency} = 87.1\%$$

The drug entrapment was determined by dispersing the PLGA/PEG nanoparticles in a phosphate buffered saline solution and the amount of the drug in the medium was assessed using UV-vis spectroscopy. This was done to obtain the amount of drug in PLGA/PEG nanoparticles with respect to the amount of drug used in the fabrication. In 10 mg of subfraction F 5.1 nanoparticles dissolved in 10 ml of solvent, it was found that 4.4 mg subfraction F 5.1 was entrapped in 10 mg of nanoparticles. This suggested that in 10 mg of nanoparticles, 4.4 mg of subfraction F 5.1 was loaded on the surface of PLGA-PEG copolymeric nanoparticles.

3.5.2. Drug release profile

Establishing a standard curve for the release of subfraction F 5.1 from nanoparticles

Ten milligrams of subfraction F 5.1 was dissolved in 10ml of ethanol. Several dilutions were prepared, and the sample was analysed using UV-vis spectroscopy. The absorption spectra were obtained from UV-vis spectroscopy (following the Beer Lambert law) and the concentrations were calculated (Table 3.11). A standard curve was plotted using the absorbance values and calculated concentrations (Figure 3.17).

Table 3.11: Quantities of subfraction F 5.1 release calculated from the absorption spectra

Absorbance	Concentration (mg/ml)
0.96	0.03
0.72	0.02
0.52	0.02
0.29	0.01
0.08	0.00

The values obtained were used to plot a standard curve (Figure 3.17). A formula was deduced from the standard plot and used to calculate the actual quantity of subfraction F 5.1 released from nanoparticles and thus the corresponding concentration to the absorption peaks.

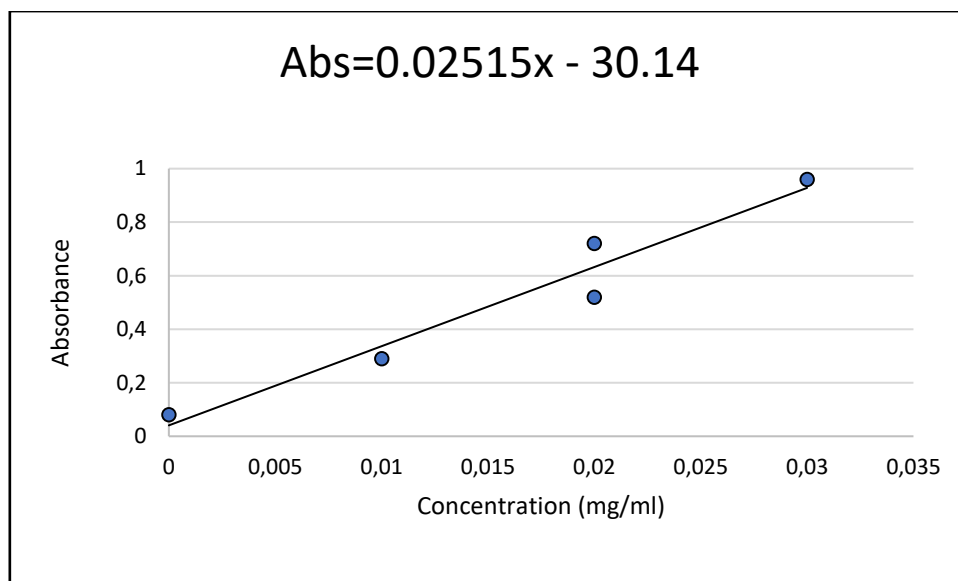


Figure 3.17: Standard curve for the concentrations of subfraction F 5.1

Release profiles

To determine the release profile of subfraction F 5.1 from polymeric nanoparticles, ten milligrams of the nanoparticles were suspended in a dialysis tubing membrane with size 2 (18/32"-14.3 mm). The release profile results are shown in Table 3.12. At pH 7.4 (physiological pH) there was a steady release of F 5.1 from the nanoparticles over a period of 12 hours. At cariogenic pH (5.5) the release of F 5.1 was higher compared to pH 7.4. At 5 hours of incubation, 0.10 mg/ml of F 5.1 was released at both pH values.

The values obtained show that the amount of subfraction F 5.1 was released steadily over time. The starting concentration was 4.4 mg of subfraction F 5.1 in 10 mg/ml of subfraction F 5.1 nanoparticles. Only 0.106 mg/ml was released at pH 7.4 after 12 hours of incubation. At pH 5.5 only 0.186 mg/ml was released after 12 hours. This implies that at both pH values, there was still some amount of subfraction F 5.1 left in the nanoparticles which will be released beyond 12 hours.

Table 3.12: The amount of F 5.1 released from nanoparticles over a period of 12 hours

Time (Hours)	Fraction released mg/ml	
	pH 7.4	pH 5.5
0	0.034	0.015
1	0.072	0.043
2	0.094	0.072
3	0.096	0.083
4	0.106	0.108
5	0.106	0.110
6	0.107	0.118
7	0.106	0.139
8	0.106	0.146
9	0.101	0.157
10	0.101	0.163
11	0.100	0.172
12	0.106	0.186
Mean	0.095	0.116
±SD	0.021	0.052

3.5.3. Release kinetics model of nanoparticles

In order to determine the release mechanism of subfraction F 5.1 from the polymeric matrix of the nanoparticles, mathematical release models were calculated from the nanoparticles using DDSolver software and Excel using the results obtained when percentage dissolution was calculated. The results are shown in Table 3.13.

According to the kinetic model values obtained in Table 3.13, the n-value describes the mode of release of the drug from the nanoparticles. Based on the n-fickian diffusion method, the release in pH 7.4 was through diffusion and the release of subfraction F 5.1 in pH 5.5 was through non-diffusion. The n-fickian mechanism states that for a fickian diffusion method the n-value is less or equal to 0.45 and for the non-fickian diffusion method, the n-value is greater than 0.45 (Dash *et al.*, 2010).

Table 3.13: Mathematical release model of F 5.1 from the nanoparticles

Kinetic model	pH 7.4	pH 5.5
Zero Order	0.91	0.99
First Order	0.94	0.99
Higuchi	0.99	0.98
n-value	0.28	0.71
Korsmeyer-Peppas	0.98	1.00
Hixson-Crowell	0.93	1.00

Figures 3.18 and 3.19 show the amount of subfraction F 5.1 released from the copolymeric nanoparticles over a period of 12 hours. DDSolver software and Excel were used to calculate the percentage of subfraction released with respect to the total amount of subfraction loaded within the nanoparticles. Only 40% of the drug was released from the nanoparticles at 12 hours at pH 7.4 which is a physiological pH of the oral cavity. At pH 5.5, only 60% of subfraction F 5.1 was released from the subfraction loaded nanoparticles.

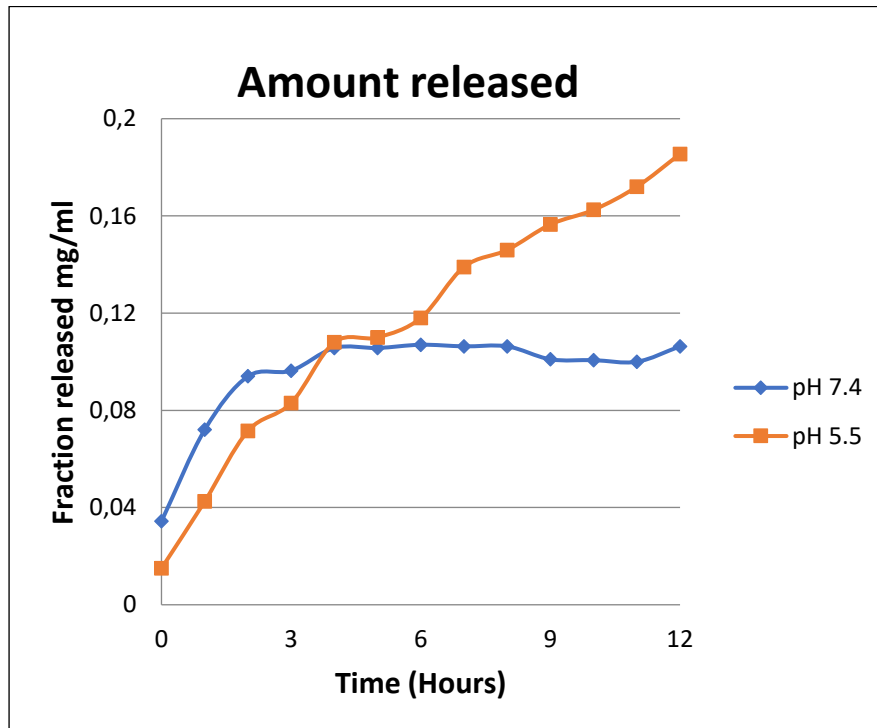


Figure 3.18: The amount of drug (F 5.1) released from nanoparticles over a period of 12 hours

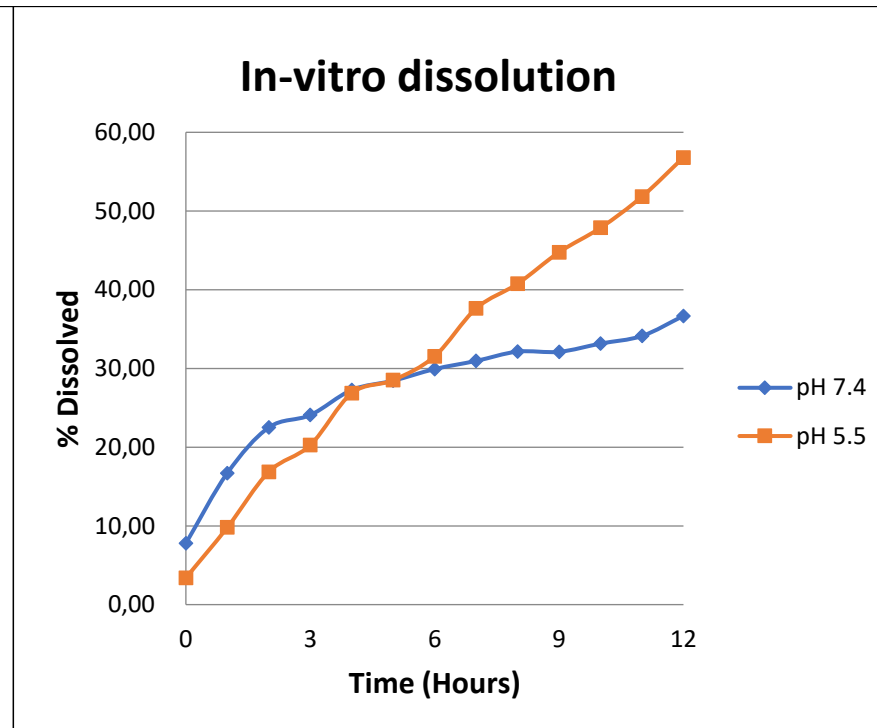


Figure 3.19: The percentage drug (F 5.1) dissolution from nanoparticles over a period of 12 hours

3.6. Antimicrobial study

3.6.1. Screening of subfraction F 5.1 and crude extract

The results of the minimum inhibitory concentrations and minimum bactericidal concentrations of the beneficial of subfraction F 5.1 and crude extract are shown in Table 3.14. The Crude extract and subfraction F 5.1 were screened to show that they have some degree of antibacterial activity. Three repeats were done for each strain of *S. mutans*. Subfraction F 5.1 had the lowest median MIC of 1.56 mg/ml and MBC of 3.125 mg/ml. The crude extract had median MIC of 3.125 mg/ml and MBC of 6.25 mg/ml.

Table 3.14: Antimicrobial screening of crude extract, subfraction F 5.1 against *Streptococcus mutans* strains

Organism:	Repeat	F 5.1 (mg/ml)		Crude (mg/ml)	
		MIC	MBC	MIC	MBC
<i>S. mutans</i> SM1	1	1.56	3.125	6.25	12.5
	2	0.78	1.56	6.25	12.5
	3	0.78	1.56	6.25	12.5
SM6	1	1.56	3.125	6.25	12.5
	2	1.56	3.125	3.125	6.25
	3	1.56	3.125	3.125	6.25
ATCC 10923	1	1.56	3.125	6.25	12.5
	2	1.56	3.125	6.25	12.5
	3	1.56	3.125	6.25	12.5
	Median	1.56	3.125	3.125	6.25

3.6.2. Screening of prepared nanoparticles

Depending on the ratios of lactide to glycolide (85:15 and 50:50), two subgroups of nanoparticles were prepared and screened for their antimicrobial activity. Nanoparticles in both ratios were made up of NPS alone (no flavone), crude extract and F 5.1 (surface

adsorbed and both surface/encapsulated). All the ten synthesised nanoparticles were screened and showed antimicrobial activity against all the three strains *S. mutans* used. The results obtained for these tests are shown in Table 3.15. The MIC's of these nanoparticles ranged from 1.56 mg/ml to 25 mg/ml. Negative and positive controls were used for this test. There was no growth observed in chlorhexidine gluconate which was used as a positive control. The negative controls which contained water and vehicle solvent DMSO both had growth. Among these nanoparticles 50:50 PLGA-PEG F 5.1 surface adsorbed showed better results compared to other nanoparticles. The lowest minimum inhibitory concentration (MIC) was recorded for F 5.1 surface attached nanoparticles with a value of 1.56 mg/ml and the minimum bactericidal concentration was 3.125 mg/ml. This was the same as the MIC value obtained with only F 5.1 which shows that it has retained its antimicrobial activity.

Table 3.15: Antimicrobial screening of 50:50 and 85:15 PLGA-PEG nanoparticles against *Streptococcus mutans* strains

<i>S. mutans</i>	Repeat	Minimum Inhibitory Concentration (MIC) and Minimum bactericidal concentration (MBC) in mg/ml 85:15 PLGA-PEG Nanoparticles									
		Blank NPS		F5.1 Surface/ Encaps NPS		F5.1 Surface NPS		Crude surface NPS		Crude surf/Encaps NPS	
		MIC	MBC	MIC	MBC	MIC	MBC	MIC	MBC	MIC	MBC
SM1	1	6.25	12.5	3.125	6.25	3.125	6.25	3.125	6.25	6.25	12.5
	2	6.25	12.5	3.125	6.25	3.125	6.25	6.25	12.5	6.25	12.5
	3	6.25	12.5	3.125	6.25	6.25	12.5	6.25	12.5	6.25	12.5
SM6	1	12.5	25	1.56	3.125	1.56	3.125	3.125	6.25	6.25	12.5
	2	12.5	25	3.125	6.25	3.125	6.25	3.125	6.25	6.25	12.5
	3	12.5	25	3.125	6.25	3.125	6.25	3.125	6.25	6.25	12.5
ATCC 10923	1	6.25	12.5	3.125	6.25	3.125	6.25	3.125	6.25	6.25	12.5
	2	6.25	12.5	3.125	6.25	3.125	6.25	3.125	6.25	6.25	12.5
	3	6.25	12.5	3.125	6.25	3.125	6.25	3.125	6.25	6.25	12.5
	Median	12.5	25	3.125	6.25	3.125	6.25	3.125	6.25	6.25	12.5
<i>S. mutans</i>	Repeat	Minimum Inhibitory Concentration (MIC) and Minimum bactericidal concentration (MBC) in mg/ml 50:50 PLGA-PEG Nanoparticles									
		Blank NPS		F5.1 Surface/ Encaps NPS		F 5.1 Surface NPS		Crude surface NPS		Crude surf/Encaps NPS	
		MIC	MBC	MIC	MBC	MIC	MBC	MIC	MBC	MIC	MBC
SM1	1	6.25	12.5	1.56	3.125	0.78	1.56	3.125	6.25	6.25	12.5
	2	3.125	6.25	1.56	3.125	1.56	3.125	6.25	12.5	6.25	12.5
	3	6.25	12.5	1.56	3.125	0.78	1.56	6.25	12.5	3.125	6.25
SM6	1	6.25	12.5	3.125	6.25	1.56	3.125	3.125	6.25	3.125	6.25
	2	6.25	12.5	3.125	6.25	1.56	3.125	3.125	6.25	3.125	6.25
	3	6.25	12.5	3.125	6.25	1.56	3.125	1.56	3.125	3.125	6.25
ATCC 10923	1	6.25	12.5	3.125	6.25	0.78	1.56	3.125	6.25	3.125	6.25
	2	6.25	12.5	3.125	6.25	0.78	1.56	3.125	6.25	3.125	6.25
	3	6.25	12.5	3.125	6.25	1.56	3.125	3.125	6.25	3.125	6.25
	Median	6.25	12.5	3.125	6.25	1.56	3.125	3.125	6.25	3.125	6.25

3.6.3. Screening of selected nanoparticles

Further studies were done using the best active compound. Three more sets of MIC/MBC tests were done for the chosen compound using the three strains of *Streptococcus mutans*. The chosen nanoparticle was subfraction F 5.1 surface adsorbed. The MIC/MBC results of F 5.1, F 5.1 NPs, and blank NPs are shown in Table 3.16. F 5.1 had the lowest MIC whereas blank NPs had a highest MIC value. The MIC value of F 5.1 surface stabilized nanoparticles was 1.56 mg/ml and the MBC value was 3.125 mg/ml.

The dose of subfraction F 5.1 stabilized nanoparticles was not adjusted to be the same amount as that of raw subfraction F 5.1. The dose of subfraction F 5.1 attached to the nanoparticles was 4.4 mg in 10 mg of the nanoparticles as shown previously in Table 3.4. This implies that in 50 mg/ml of nanoparticles 22 mg/ml of subfraction was loaded therefore, encapsulation with nanoparticles improved antimicrobial activity. The concentration of F 5.1 in the MIC obtained was 0.7 mg/ml.

Table 3.16: Antimicrobial activity of synthesised nanoparticles against *S. mutans*

<i>S. mutans</i>	Repeat	MIC/MBC (mg/ml) n=9					
		Subfraction F 5.1		Subfraction F 5.1 NPs		Blank NPs	
		MIC	MBC	MIC	MBC	MIC	MBC
SM1	1	1.56	3.125	0.78	1.56	6.25	12.5
	2	0.78	1.56	1.56	3.125	6.25	12.5
	3	0.78	1.56	1.56	3.125	6.25	12.5
SM6	1	1.56	3.125	1.56	3.125	12.5	25
	2	0.78	1.56	1.56	3.125	6.25	12.5
	3	0.78	1.56	1.56	3.125	12.5	25
ATCC 10923	1	1.56	3.125	1.56	3.125	6.25	12.5
	2	0.78	1.56	1.56	3.125	6.25	12.5
	3	0.78	1.56	0.78	1.56	6.25	12.5
	Median	0.78	1.56	1.56*	3.125	6.25	12.5

*10 mg of NPs contains 4.4 mg of F.5.1 therefore,

50 mg/ml (F5.1/NPs) = 22 mg/ml F5.1

1.56 mg/ml (F5.1/NPs) = 0.7 mg/ml F5.1

Based on the MIC/MBC (minimum inhibitory concentrations/ minimum bactericidal concentrations) results obtained, three sub-inhibitory concentrations were selected from subfraction F 5.1, subfraction F 5.1 surface stabilized nanoparticles as well as blank nanoparticles (no flavone). The three sub-inhibitory concentrations were used for acid assay and biofilm assay (Table 3.17).

The lowest concentration selected for subfraction 5.1 was 0.10 mg/ml and for subfraction F 5.1 surface stabilized nanoparticles was 0.20 mg/ml. For blank nanoparticles the lowest concentration was 0.78 mg/ml.

Table 3.17: Concentrations of the beneficial compounds used in acid assay and biofilm assay

Compound	Concentrations (mg/ml)					
	3.125	1.56	0.78	0.39	0.20	0.10
Subfraction F 5.1				X	X	X
F 5.1 nanoparticles			X	X	X	
Blank nanoparticles	X	X	X			

3.7. The effect of beneficial compounds on acid production by *S. mutans*

Three strains of *S. mutans* were incubated in the presence of sub-inhibitory concentrations outlined in Table 3.17. The pH and counts in all the tests were recorded over a time interval. For pH measurements, the readings were taken at the beginning of incubation (time 0), after 9 hours of incubation, and from there on the readings were done every two hours for 17 hours. The bacterial counts were also done at time 0 hours, 9 hours, 13 hours and 17 hours (4 hours gap from the 9 hours). The counts were done from each test tube to show that the difference in pH measurements were not due to differences in bacterial counts.

3.7.1. The effect of subfraction F 5.1 on acid production

The results showing the effect of subfraction F 5.1 on acid production against *S. mutans* are presented in Table 3.18. All the tests treated with subfraction F 5.1 had a higher pH compared to the control. The average control pH dropped to pH 5.2 after 14 hours of incubation which

was lower than the pH recorded for F 5.1 treated assay which dropped to pH 6.8 after 14 hours of incubation. All the three sub-inhibitory concentrations of subfraction F 5.1 never reached a critical pH of 5.5 over 17 hours of incubation whereas the control reached a critical pH of 5.5 after 14 hours of incubation. The lowest concentration of subfraction F 5.1 which inhibited acid production was 0.10 mg/ml.

The results of the bacterial counts between the tests cultures and control showed no difference (counts in tests similar to counts in control) (Table 3.19). Notable pH difference was observed after 8 hours of incubation. The difference in bacterial count showed that the inhibition was due to F 5.1 not the difference in bacterial counts. Bacterial counts were converted in to log values and the results of pH and log counts are depicted in Figure 3.21.

Statistical comparison between each of the three sub-inhibitory concentrations and controls indicated that all the sub-inhibitory concentrations significantly reduced acid production by *S. mutans* with P value of 0.02 (Figure 3.20) and that the bacterial counts observed were not significantly different with P value of 0.15 (Figure 3.21). This shows that the inhibition in acid production between the tests and controls is not related to the growth.

Table 3.18: The effect of subfraction F 5.1 on acid production by *S. mutans*

Compound (mg/ml)	Cultures <i>S. mutans</i>	Effect of subfraction 5.1 on acid production by <i>S. mutans</i> (pH)												
		Repeats	0 hours		9 hours		11 hours		13 hours		15 hours		17 hours	
			Control	F5.1	Control	F5.1	Control	F5.1	Control	F5.1	Control	F5.1	Control	F5.1
0.39	ATCC 10923	1	7.10	7.10	6.78	7.08	6.63	7.00	6.05	6.99	5.49	6.85	5.32	6.77
		2	7.10	7.10	6.77	7.09	6.08	6.98	5.20	6.87	4.70	6.80	4.51	6.74
		3	7.10	7.10	6.83	7.10	6.61	7.07	6.12	6.92	5.98	6.85	5.13	6.80
	SM1	1	7.10	7.10	6.60	7.04	6.04	7.01	5.68	6.99	5.30	6.72	4.29	6.56
		2	7.10	7.10	6.54	6.96	5.99	6.91	5.05	6.89	4.51	6.83	4.59	6.74
		3	7.10	7.10	6.62	7.03	6.08	7.00	5.42	6.90	5.01	6.84	4.32	6.73
	SM6	1	7.10	7.10	6.67	7.10	6.20	7.05	5.98	6.98	5.69	6.87	4.89	6.73
		2	7.10	7.10	6.25	7.09	6.01	7.05	5.62	6.96	5.18	6.80	4.73	6.71
		3	7.10	7.10	6.29	7.09	5.98	7.00	5.42	6.94	5.12	6.82	4.39	6.70
		Mean	7.10	7.10	6.59	7.06	6.18	7.01	5.62	6.94	5.00	6.82	4.69	6.72
0.20	ATCC 10923	1	7.10	7.10	6.60	7.02	6.04	7.01	5.68	6.84	5.30	6.59	4.29	6.52
		2	7.10	7.10	6.54	7.10	5.99	7.00	5.05	6.87	4.51	6.71	4.59	6.69
		3	7.10	7.10	6.62	7.04	6.08	7.01	5.42	6.90	5.01	6.82	4.32	6.71
	SM1	1	7.10	7.10	6.67	7.09	6.20	7.06	5.98	6.99	5.69	6.94	4.89	6.79
		2	7.10	7.10	6.25	7.09	6.01	7.04	5.62	7.01	5.18	6.97	4.73	6.82
		3	7.10	7.10	6.29	7.10	5.98	7.03	5.42	6.98	5.12	6.82	4.39	6.68
	SM6	1	7.10	7.10	6.67	7.09	6.20	7.06	5.98	6.99	5.69	6.94	4.89	6.79
		2	7.10	7.10	6.25	7.09	6.01	7.04	5.62	7.01	5.18	6.97	4.73	6.82
		3	7.10	7.10	6.29	7.10	5.98	7.03	5.42	6.98	5.12	6.82	4.39	6.68
		Mean	7.10	7.10	6.46	7.08	6.05	7.03	5.58	6.96	5.20	6.84	4.58	6.72
0.10	ATCC 10923	1	7.10	7.10	6.78	7.00	6.63	6.97	6.05	6.96	5.49	6.82	5.32	6.70
		2	7.10	7.10	6.77	7.00	6.08	6.98	5.20	6.90	4.70	6.81	4.51	6.73
		3	7.10	7.10	6.83	7.00	6.61	6.96	6.12	6.94	5.98	6.90	5.13	6.84
	SM1	1	7.10	7.10	6.60	7.01	6.04	6.84	5.68	6.82	5.30	6.63	4.29	6.60
		2	7.10	7.10	6.54	7.10	5.99	7.01	5.05	6.97	4.51	6.81	4.59	6.80
		3	7.10	7.10	6.62	7.08	6.08	7.05	5.42	7.03	5.01	6.85	4.32	6.80
	SM6	1	7.10	7.10	6.67	7.05	6.20	7.03	5.98	6.90	5.69	6.82	4.89	6.78
		2	7.10	7.10	6.25	7.10	6.01	7.06	5.62	6.97	5.18	6.88	4.73	6.77
		3	7.10	7.10	6.29	7.10	5.98	7.01	5.42	6.94	5.12	6.86	4.39	6.69
		Mean	7.10	7.10	6.59	7.06	6.18	6.99	5.62	6.94	5.22	6.82	4.69	6.75

Table 3.19: The effect of subfraction F 5.1 on the growth of *S. mutans* in acid assay

Culture	Repeat	Acid assay: Effect of subfraction F 5.1 on bacterial counts (cfu/ml)												
		0 hours	9 hours				13 hours				17 hours			
		ALL	Control	0.39	0.20	0.10	control	0.39	0.20	0.10	Control	0.39	0.20	0.10
ATCC 10923	1	3.0×10 ⁶	1.7×10 ⁸	2.4×10 ⁷	4.6×10 ⁷	7.5×10 ⁷	2.8×10 ⁸	2.9×10 ⁷	9.4×10 ⁷	3.8×10 ⁷	5.6×10 ⁷	1.8×10 ⁷	1.1×10 ⁷	1.6×10 ⁷
	2	6.3×10 ⁶	5.1×10 ⁸	8.3×10 ⁷	1.0×10 ⁸	8.9×10 ⁷	1.9×10 ⁹	4.7×10 ⁷	3.1×10 ⁸	1.7×10 ⁷	2.6×10 ⁸	2.2×10 ⁷	4.8×10 ⁸	1.5×10 ⁷
	3	5.3×10 ⁶	3.0×10 ⁸	8.4×10 ⁷	3.6×10 ⁷	7.7×10 ⁷	2.4×10 ⁸	9.7×10 ⁷	6.6×10 ⁷	7.0×10 ⁷	2.0×10 ⁸	2.0×10 ⁸	2.4×10 ⁷	1.0×10 ⁷
SM1	1	7.5×10 ⁶	4.8×10 ⁸	1.2×10 ⁷	4.8×10 ⁷	2.4×10 ⁸	8.7×10 ⁸	4.2×10 ⁷	6.7×10 ⁷	8.3×10 ⁸	2.6×10 ⁸	1.2×10 ⁷	2.8×10 ⁷	2.7×10 ⁸
	2	3.8×10 ⁶	3.4×10 ⁸	5.3×10 ⁶	2.1×10 ⁷	2.9×10 ⁷	2.9×10 ⁸	3.3×10 ⁶	3.5×10 ⁷	1.8×10 ⁷	1.4×10 ⁸	7.5×10 ⁵	4.1×10 ⁶	1.4×10 ⁶
	3	1.1×10 ⁶	3.5×10 ⁸	2.4×10 ⁷	6.1×10 ⁷	4.6×10 ⁷	2.6×10 ⁸	6.6×10 ⁶	4.8×10 ⁷	2.4×10 ⁷	3.4×10 ⁸	1.9×10 ⁶	2.3×10 ⁶	6.3×10 ⁶
SM6	1	1.1×10 ⁶	1.4×10 ⁸	2.1×10 ⁷	3.4×10 ⁷	6.7×10 ⁷	8.3×10 ⁸	2.4×10 ⁸	2.7×10 ⁸	2.1×10 ⁸	1.8×10 ⁸	6.3×10 ⁷	2.6×10 ⁷	3.6×10 ⁸
	2	3.5×10 ⁶	3.8×10 ⁸	1.7×10 ⁸	4.9×10 ⁸	1.8×10 ⁸	4.5×10 ⁸	2.2×10 ⁸	2.1×10 ⁷	1.5×10 ⁸	2.6×10 ⁸	5.5×10 ⁷	2.0×10 ⁷	4.1×10 ⁷
	3	1.2×10 ⁶	1.6×10 ⁸	4.7×10 ⁷	7.5×10 ⁷	7.5×10 ⁷	2.3×10 ⁸	1.3×10 ⁸	9.7×10 ⁸	9.7×10 ⁸	8.7×10 ⁸	1.7×10 ⁸	2.7×10 ⁸	2.7×10 ⁸
	Mean	3.2×10 ⁶	3.0×10 ⁸	5.3×10 ⁷	1.0×10 ⁸	1.0×10 ⁸	5.9×10 ⁸	9.2×10 ⁷	2.1×10 ⁸	2.6×10 ⁸	2.0×10 ⁸	6.0×10 ⁷	21.1×10 ⁸	1.1×10 ⁸
	±SD	2.5×10 ⁵	1.4×10 ⁸	5.3×10 ⁷	1.5×10 ⁸	6.8 ×10 ⁷	5.5×10 ⁸	8.9×10 ⁷	3.1×10 ⁸	3.7×10 ⁸	2.3×10 ⁸	7.2×10 ⁸	1.7×10 ⁸	1.5×10 ⁸

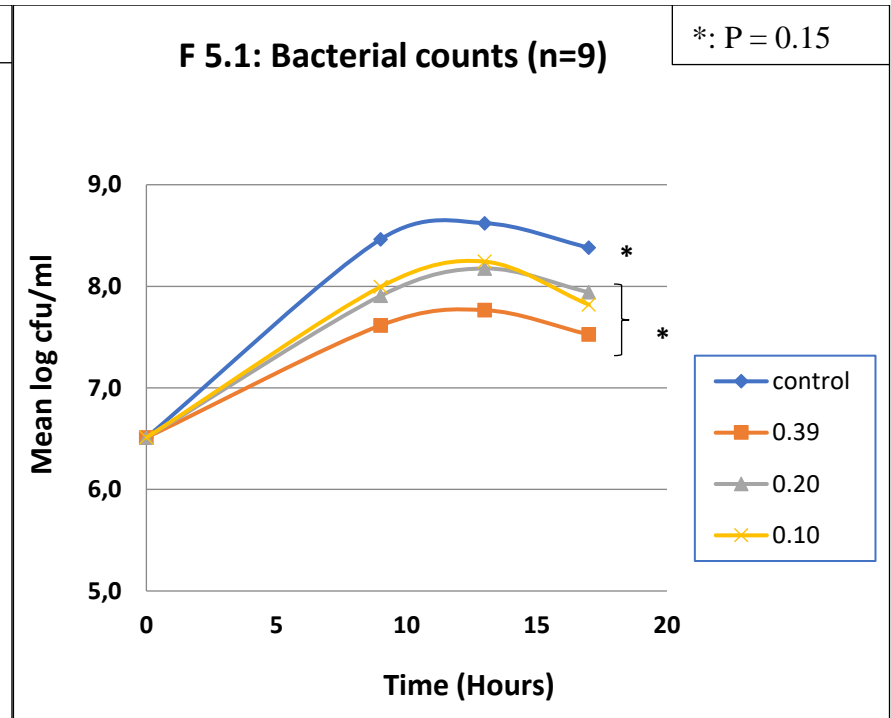
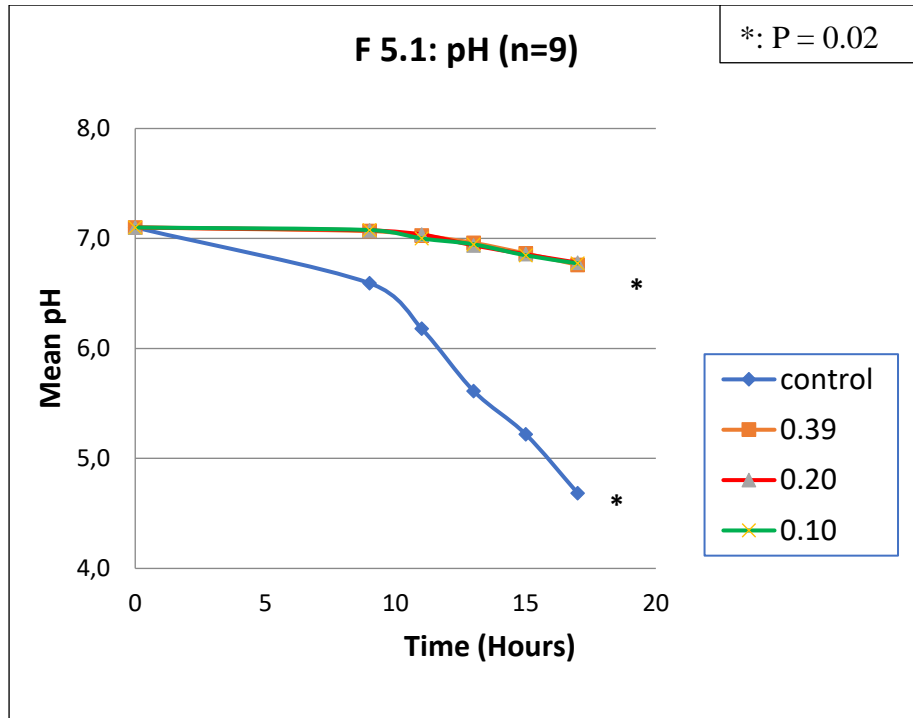


Figure 3.20: The effect of subfraction F 5.1 on acid production of *S. mutans* in acid assay. *: Comparison in acid production by *S. mutans* between control and test cultures over a period of 17 hours.

Figure 3.21: The effect of subfraction F 5.1 on the growth of *S. mutans* in acid production. *: Comparison of bacterial counts in *S. mutans* between control and test cultures over a period of 17 hours.

3.7.2. The effect of subfraction F 5.1 nanoparticles on acid production

Table 3.20 shows the results of effect of subfraction F 5.1 surface stabilized nanoparticles on acid production against *S. mutans*. All the tests treated with subfraction F 5.1 stabilized nanoparticles had a higher pH compared to the control. The average control pH dropped to pH 5.2 after 14 hours of incubation which was lower than the pH recorded with F 5.1 stabilized nanoparticles treated assay which dropped to pH 6.8 after 14 hours of incubation. Figure 3.22 highlights the effect of subfraction F 5.1 nanoparticles observed in the production of acid by *S. mutans*.

The results of the bacterial counts between the tests cultures and control showed no difference (counts in tests similar to counts in control) (Table 3.21). Notable pH difference was observed after 8 hours of incubation. The difference in bacterial count showed that the inhibition was due to F 5.1/NPs not the difference in bacterial counts. Bacterial counts were converted in to log values and the results log counts are depicted in Figure 3.23.

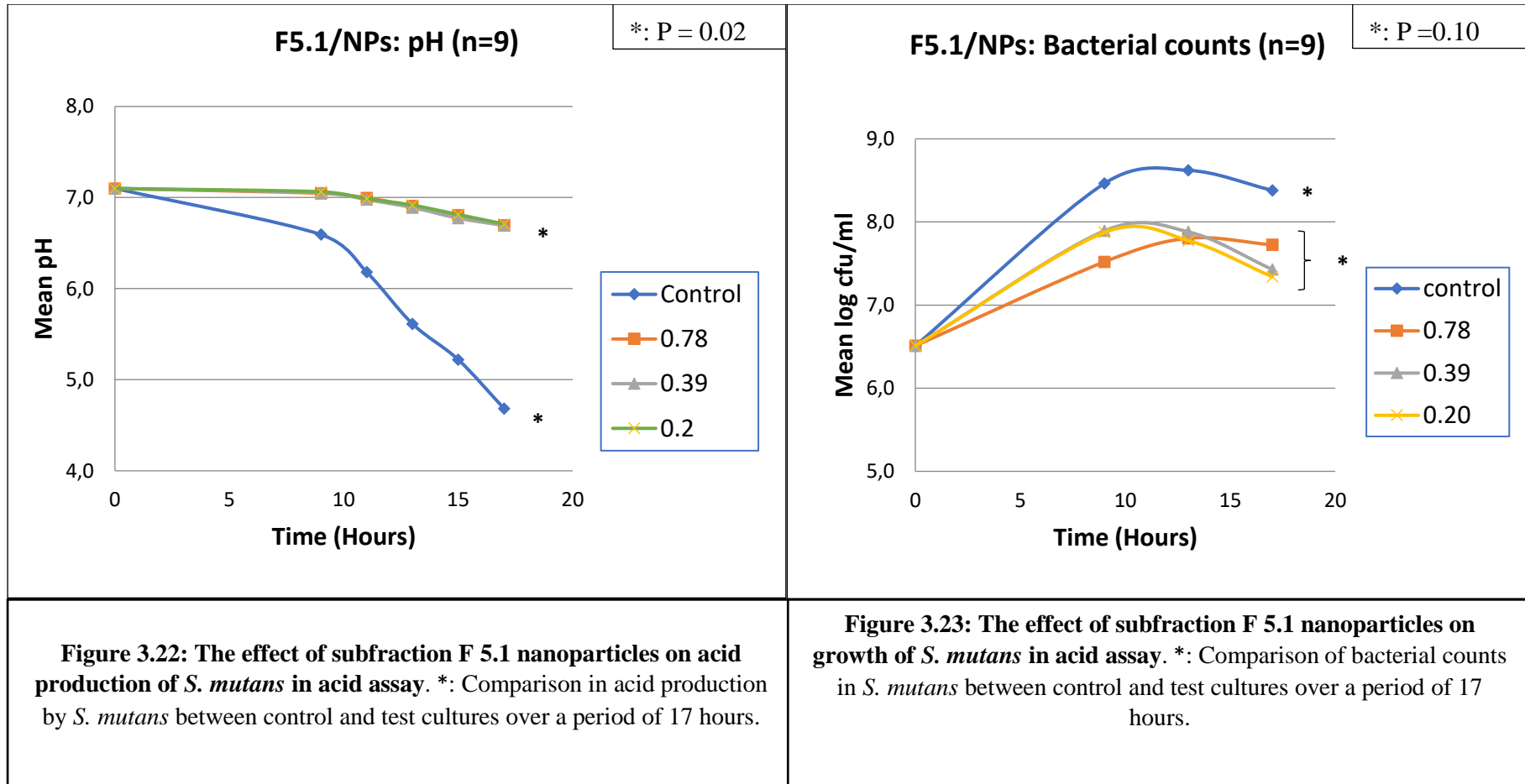
Statistical comparison (Figure 3.22) between each of the three sub-inhibitory concentrations of subfraction stabilized nanoparticles and controls also indicated that all the sub-inhibitory concentrations significantly reduced acid production by *S. mutans* with P value of 0.02. The bacterial counts between the control and tests were nonsignificant with P value of 0.10 (Figure 3.23). This shows that the inhibition of acid production between the tests and controls is not related to the growth.

Table 3.20: The effect of subfraction F 5.1 nanoparticles on acid production on *S. mutans*

Compound (mg/ml)	Cultures <i>S. mutans</i>	Effect of subfraction F 5.1 nanoparticles on acid production by <i>S. mutans</i> (pH)												
		Repeats	0 hours		9 hours		11 hours		13 hours		15 hours		17 hours	
			Control	F5.1/NPS	Control	F5.1/NPS	Control	F5.1/NPS	Control	F5.1/NPS	Control	F5.1/NPS	Control	F5.1/NPS
0.78	ATCC 10923	1	7.10	7.10	6.78	7.08	6.63	7.04	6.05	6.95	5.49	6.84	5.32	6.70
		2	7.10	7.10	6.77	7.01	6.08	7.00	5.20	6.84	4.70	6.78	4.51	6.66
		3	7.10	7.10	6.83	7.08	6.61	6.97	6.12	6.94	5.98	6.90	5.13	6.80
	SM1	1	7.10	7.10	6.60	7.03	6.04	7.00	5.68	6.94	5.30	6.78	4.29	6.66
		2	7.10	7.10	6.54	7.01	5.99	6.98	5.05	6.83	4.51	6.75	4.59	6.72
		3	7.10	7.10	6.62	7.07	6.08	7.05	5.42	6.98	5.01	6.81	4.32	6.72
	SM6	1	7.10	7.10	6.67	7.04	6.63	6.96	5.98	6.91	5.69	6.83	4.89	6.67
		2	7.10	7.10	6.25	7.03	6.08	6.99	5.62	6.93	5.18	6.81	4.73	6.72
		3	7.10	7.10	6.29	7.05	6.61	6.98	5.42	6.83	5.12	6.76	4.39	6.60
		Mean	7.10	7.10	6.59	7.04	6.31	6.89	5.62	6.91	5.22	6.81	4.69	6.69
0.39	ATCC 10923	1	7.10	7.10	6.78	7.09	6.63	7.01	6.05	6.92	5.49	6.85	5.32	6.75
		2	7.10	7.10	6.77	7.00	6.08	6.98	5.20	6.90	4.70	6.85	4.51	6.80
		3	7.10	7.10	6.83	7.07	6.61	6.99	6.12	6.82	5.98	6.78	5.13	6.73
	SM1	1	7.10	7.10	6.60	7.00	6.04	6.98	5.68	6.88	5.30	6.66	4.29	6.66
		2	7.10	7.10	6.54	7.02	5.99	6.97	5.05	6.86	4.51	6.72	4.59	6.69
		3	7.10	7.10	6.62	7.09	6.08	7.01	5.42	6.99	5.01	6.80	4.32	6.68
	SM6	1	7.10	7.10	6.67	7.05	6.63	6.88	5.98	6.78	5.69	6.72	4.89	6.60
		2	7.10	7.10	6.25	7.07	6.08	7.05	5.62	6.99	5.18	6.80	4.73	6.72
		3	7.10	7.10	6.29	7.08	6.61	6.93	5.42	6.86	5.12	6.79	4.39	6.60
		Mean	7.10	7.10	6.59	7.05	6.31	6.98	5.62	6.89	5.22	6.77	4.69	6.69
0.2	ATCC 10923	1	7.10	7.10	6.60	7.03	6.04	7.00	5.68	6.94	5.30	6.78	4.29	6.66
		2	7.10	7.10	6.54	7.01	5.99	6.98	5.05	6.83	4.51	6.75	4.59	6.72
		3	7.10	7.10	6.62	7.07	6.08	7.05	5.42	6.98	5.01	6.81	4.32	6.72
	SM1	1	7.10	7.10	6.60	7.06	6.04	6.99	5.68	6.97	5.30	6.70	4.29	6.61
		2	7.10	7.10	6.54	7.06	5.99	7.00	5.05	6.87	4.51	6.83	4.59	6.80
		3	7.10	7.10	6.62	7.09	6.08	7.05	5.42	7.01	5.01	6.95	4.32	6.83
	SM6	1	7.10	7.10	6.67	7.03	6.63	6.87	5.98	6.82	5.69	6.77	4.89	6.64
		2	7.10	7.10	6.25	7.05	6.08	7.00	5.62	6.95	5.18	6.80	4.73	6.68
		3	7.10	7.10	6.29	7.03	6.61	6.94	5.42	6.88	5.12	6.78	4.39	6.60
		Mean	7.10	7.10	6.53	7.05	6.17	6.99	5.48	6.92	4.85	6.80	4.49	6.70

Table 3.21: The effect of subfraction F 5.1 nanoparticles on the growth of *S. mutans* in Acid production

Culture	Repeat	Acid assay: Effect of subfraction F 5.1 nanoparticles on bacterial counts (cfu/ml)												
		0 hours	9 hours				13 hours				17 hours			
		ALL	Control	0.78	0.39	0.20	control	0.78	0.39	0.20	Control	0.78	0.39	0.20
ATCC 10923	1	3.0×10 ⁶	1.7×10 ⁸	3.5×10 ⁷	3.4×10 ⁷	2.9×10 ⁸	2.8×10 ⁸	2.9×10 ⁷	8.6×10 ⁷	4.2×10 ⁷	5.6×10 ⁷	1.2×10 ⁷	3.5×10 ⁷	2.8×10 ⁷
	2	6.3×10 ⁶	5.1×10 ⁸	2.4×10 ⁷	1.5×10 ⁸	7.0×10 ⁷	1.9×10 ⁹	4.2×10 ⁷	3.8×10 ⁷	4.8×10 ⁷	2.6×10 ⁸	3.5×10 ⁷	3.9×10 ⁷	1.4×10 ⁷
	3	5.3×10 ⁶	3.0×10 ⁸	2.4×10 ⁷	1.0×10 ⁸	1.5×10 ⁸	2.4×10 ⁸	2.1×10 ⁷	3.8×10 ⁷	1.8×10 ⁸	2.0×10 ⁸	7.5×10 ⁶	5.1×10 ⁷	3.2×10 ⁸
SM6	1	7.5×10 ⁶	4.8×10 ⁸	3.6×10 ⁷	2.9×10 ⁷	7.6×10 ⁷	8.7×10 ⁸	3.8×10 ⁷	4.2×10 ⁷	6.9×10 ⁷	2.6×10 ⁸	9.2×10 ⁷	3.0×10 ⁶	5.3×10 ⁷
	2	3.8×10 ⁶	3.4×10 ⁸	2.4×10 ⁶	3.9×10 ⁷	3.4×10 ⁷	2.9×10 ⁸	4.1×10 ⁶	3.8×10 ⁶	3.2×10 ⁷	1.4×10 ⁸	1.7×10 ⁶	1.1×10 ⁶	2.3×10 ⁶
	3	1.1×10 ⁶	3.5×10 ⁸	1.5×10 ⁷	2.3×10 ⁷	2.9×10 ⁷	2.6×10 ⁸	3.5×10 ⁷	1.9×10 ⁷	1.6×10 ⁷	3.4×10 ⁸	3.5×10 ⁶	2.2×10 ⁶	6.2×10 ⁶
SM6	1	1.1×10 ⁶	1.4×10 ⁸	2.3×10 ⁷	3.8×10 ⁸	1.2×10 ⁸	8.3×10 ⁸	7.2×10 ⁷	1.8×10 ⁸	3.1×10 ⁸	1.8×10 ⁸	1.1×10 ⁸	8.3×10 ⁷	8.8×10 ⁷
	2	3.5×10 ⁶	3.8×10 ⁸	6.4×10 ⁷	4.7×10 ⁷	9.4×10 ⁷	4.5×10 ⁸	4.0×10 ⁷	1.5×10 ⁷	9.6×10 ⁷	2.6×10 ⁸	2.2×10 ⁷	1.0×10 ⁷	1.7×10 ⁷
	3	1.2×10 ⁶	1.6×10 ⁸	1.3×10 ⁸	6.9×10 ⁷	3.5×10 ⁷	2.3×10 ⁸	8.4×10 ⁸	9.0×10 ⁸	9.9×10 ⁷	8.7×10 ⁸	6.5×10 ⁸	6.0×10 ⁸	4.8×10 ⁸
	Mean	3.3×10 ⁶	3.0×10 ⁸	7.2×10 ⁷	3.9×10 ⁷	1.0×10 ⁸	5.9×10 ⁸	1.3×10 ⁸	1.5×10 ⁸	1.0×10 ⁸	2.0×10 ⁸	1.0×10 ⁸	8.8×10 ⁷	8.2×10 ⁷
	±SD	2.3×10 ⁶	1.4×10 ⁸	3.8×10 ⁷	1.1×10 ⁷	8.2×10 ⁸	7.9×10 ⁸	2.7×10 ⁸	2.9×10 ⁷	9.3×10 ⁷	2.3×10 ⁸	2.1×10 ⁸	1.9×10 ⁸	1.7×10 ⁸



3.7.3. The effect of blank nanoparticles on acid production by *S. mutans*

Nanoparticles (no flavone) also showed reduction in acid production (Table 3.22). The average control pH dropped to pH 5.2 after 14 hours of incubation which was lower than the nanoparticles which dropped to pH 6.7 after 14 hours of incubation. Figure 3.24 highlights the effect of blank nanoparticles observed in the production of acid by *S. mutans*.

There was not much difference in bacterial counts between tests and control. The results of the bacterial counts between the tests cultures and control showed no difference (counts in tests similar to counts in control) (Table 3.23). Notable pH difference was observed after 8 hours of incubation. The difference in bacterial count showed that the inhibition was due to blank nanoparticles not the difference in bacterial counts. Bacterial counts were converted in to log values and the results log counts are depicted in Figure 3.25.

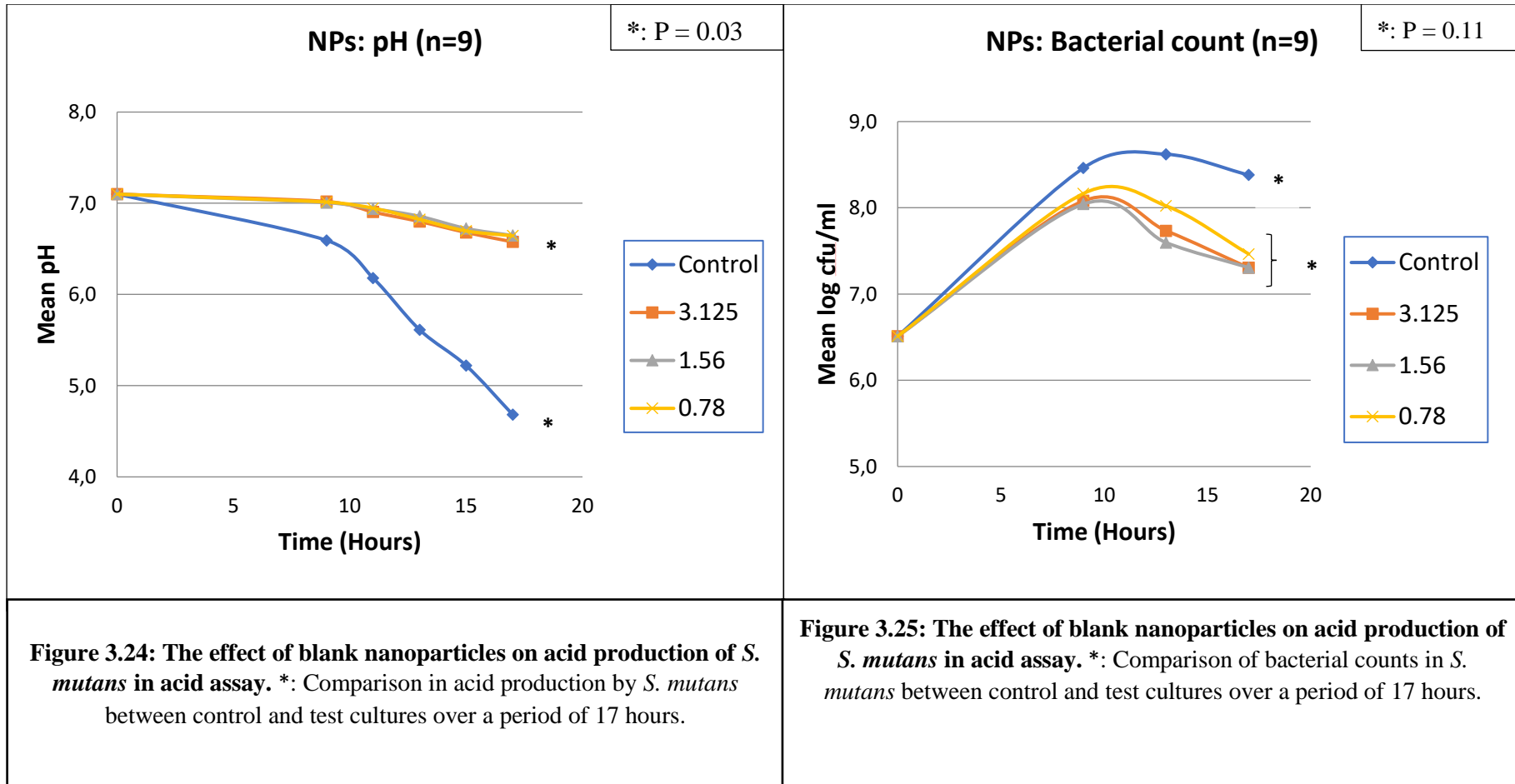
Statistical comparison between each of the three sub-inhibitory concentrations of blank nanoparticles and controls indicated that all the sub-inhibitory concentrations significantly reduced acid production by *S. mutans* with P value of 0.03 (Figure 3.24). The bacterial counts between the control and tests were nonsignificant with P value 0.11 (Figure 3.25). This shows that the inhibition of acid production between the tests and controls is not related to the growth.

Table 3.22: The effect of blank nanoparticles on acid production by *S. mutans*

Compound (mg/ml)	Cultures <i>S. mutans</i>	Effect of blank nanoparticles on acid production by <i>S. mutans</i> (pH)													
		Repeats	0 hours		9 hours		11 hours		13 hours		15 hours		17 hours		
3.125	ATCC 10923		Control	NPS	Control	NPS	Control	NPS	Control	NPS	Control	NPS	Control	NPS	
		1	7.10	7.10	6.60	7.03	6.63	6.99	6.05	6.90	5.49	6.79	5.32	6.60	
		2	7.10	7.10	6.54	6.98	6.08	6.85	5.20	6.80	4.70	6.73	4.51	6.64	
	SM1	1	7.10	7.10	6.60	6.95	6.04	6.61	5.68	6.56	5.30	6.36	4.29	6.30	
		2	7.10	7.10	6.54	7.06	5.99	6.99	5.05	6.82	4.51	6.80	4.59	6.71	
		3	7.10	7.10	6.62	7.04	6.08	6.98	5.42	6.91	5.01	6.87	4.32	6.79	
	SM6	1	7.10	7.10	7.04	7.02	6.63	6.88	5.98	6.84	5.69	6.70	4.89	6.60	
		2	7.10	7.10	7.03	7.00	6.08	6.91	5.62	6.78	5.18	6.64	4.73	6.48	
		3	7.10	7.10	7.05	7.00	6.61	6.96	5.42	6.80	5.12	6.61	4.39	6.47	
		Mean	7.10	7.10	6.74	7.02	6.31	6.91	5.62	6.80	5.22	6.68	5.20	6.55	
	1.56	ATCC 10923	1	7.10	7.10	6.60	7.04	6.63	6.98	6.05	6.80	5.49	6.71	5.32	6.60
			2	7.10	7.10	6.54	6.92	6.08	6.87	5.20	6.79	4.70	6.66	4.51	6.58
			3	7.10	7.10	6.62	7.05	6.61	6.96	6.12	6.85	5.98	6.65	5.13	6.49
SM1		1	7.10	7.10	6.60	7.01	6.04	6.98	5.68	6.92	5.30	6.84	4.29	6.76	
		2	7.10	7.10	6.54	7.08	5.99	7.03	5.05	6.99	4.51	6.79	4.59	6.61	
		3	7.10	7.10	6.62	7.07	6.08	6.99	5.42	6.94	5.01	6.83	4.32	6.81	
SM6		1	7.10	7.10	7.05	6.99	6.63	6.89	5.98	6.85	5.69	6.71	4.89	6.51	
		2	7.10	7.10	7.07	6.99	6.08	6.86	5.62	6.80	5.18	6.77	4.73	6.51	
		3	7.10	7.10	7.08	6.94	6.61	6.90	5.42	6.77	5.12	6.69	4.39	6.49	
		Mean	7.10	7.10	6.74	7.01	6.31	6.94	5.62	6.86	5.22	6.74	5.20	6.60	
0.78		ATCC 10923	1	7.10	7.10	6.60	7.04	6.63	6.97	6.05	6.86	5.49	6.70	5.32	6.62
			2	7.10	7.10	6.54	6.96	6.08	6.90	5.20	6.82	4.70	6.70	4.51	6.63
			3	7.10	7.10	6.62	7.07	6.61	6.99	6.12	6.88	5.98	6.77	5.13	6.67
	SM1	1	7.10	7.10	6.60	7.02	6.04	6.99	5.68	6.80	5.30	6.74	4.29	6.65	
		2	7.10	7.10	6.54	7.05	5.99	7.00	5.05	6.81	4.51	6.78	4.59	6.68	
		3	7.10	7.10	6.62	7.08	6.08	7.05	5.42	6.85	5.01	6.79	4.32	6.71	
	SM6	1	7.10	7.10	7.03	6.95	6.63	6.90	5.98	6.88	5.69	6.70	4.89	6.54	
		2	7.10	7.10	7.05	7.01	6.08	6.84	5.62	6.81	5.18	6.67	4.73	6.48	
		3	7.10	7.10	7.03	6.96	6.61	6.91	5.42	6.79	5.12	6.61	4.39	6.40	
		Mean	7.10	7.10	6.74	7.02	6.31	6.95	5.62	6.83	5.22	6.72	5.20	6.60	

Table 3.23: The effect of blank nanoparticles on the growth of *S. mutans* in Acid assay

	Acid assay: Effect of Blank nanoparticles on bacterial counts (cfu/ml)													
	Repeat	0 hours	9 hours				13 hours				17 hours			
Culture		ALL	Control	3.125	1.56	0.78	control	3.125	1.56	0.78	control	3.125	1.56	0.78
ATCC 10923	1	3.0×10 ⁶	1.7×10 ⁸	3.5×10 ⁷	1.7×10 ⁸	1.4×10 ⁸	2.8×10 ⁸	4.4×10 ⁷	7.8×10 ⁷	5.0×10 ⁷	5.6×10 ⁷	1.7×10 ⁷	8.5×10 ⁶	1.2×10 ⁷
	2	6.3×10 ⁶	5.1×10 ⁸	2.9×10 ⁸	9.9×10 ⁷	2.1×10 ⁸	1.9×10 ⁹	5.4×10 ⁷	4.5×10 ⁷	4.5×10 ⁷	2.6×10 ⁸	1.8×10 ⁷	4.1×10 ⁶	4.7×10 ⁷
	3	5.3×10 ⁶	3.0×10 ⁸	1.3×10 ⁸	8.6×10 ⁷	1.1×10 ⁸	2.4×10 ⁸	2.9×10 ⁷	1.1×10 ⁷	1.1×10 ⁸	2.0×10 ⁸	2.8×10 ⁷	2.1×10 ⁸	4.8×10 ⁶
SM1	1	7.5×10 ⁶	4.8×10 ⁸	3.9×10 ⁷	2.1×10 ⁸	4.0×10 ⁸	8.7×10 ⁸	1.6×10 ⁷	2.0×10 ⁸	1.0×10 ⁸	2.6×10 ⁸	1.2×10 ⁷	1.9×10 ⁷	6.6×10 ⁷
	2	3.8×10 ⁶	3.4×10 ⁸	5.6×10 ⁷	1.0×10 ⁷	1.6×10 ⁷	2.9×10 ⁸	1.3×10 ⁷	9.5×10 ⁷	3.1×10 ⁷	1.4×10 ⁸	2.6×10 ⁶	2.6×10 ⁶	3.1×10 ⁶
	3	1.1×10 ⁶	3.5×10 ⁸	3.4×10 ⁷	6.3×10 ⁷	3.5×10 ⁷	2.6×10 ⁸	2.6×10 ⁷	3.1×10 ⁷	6.1×10 ⁷	3.4×10 ⁸	5.0×10 ⁶	3.4×10 ⁶	2.5×10 ⁷
SM6	1	1.1×10 ⁶	1.4×10 ⁸	2.1×10 ⁷	3.1×10 ⁷	1.2×10 ⁸	8.3×10 ⁸	1.6×10 ⁸	4.0×10 ⁷	1.8×10 ⁸	1.8×10 ⁸	1.2×10 ⁸	2.3×10 ⁸	3.0×10 ⁷
	2	3.5×10 ⁶	3.8×10 ⁸	1.6×10 ⁸	1.6×10 ⁸	1.9×10 ⁸	4.5×10 ⁸	2.0×10 ⁸	2.6×10 ⁷	1.7×10 ⁸	2.6×10 ⁸	3.0×10 ⁷	2.0×10 ⁷	5.8×10 ⁷
	3	1.2×10 ⁶	1.6×10 ⁸	2.7×10 ⁸	1.6×10 ⁸	1.1×10 ⁸	2.3×10 ⁸	2.6×10 ⁸	2.5×10 ⁸	1.7×10 ⁸	8.7×10 ⁸	3.0×10 ⁷	2.2×10 ⁷	2.7×10 ⁷
	Mean	3.3×10⁶	3.7×10⁸	1.5×10⁸	1.1×10⁸	1.5×10⁸	5.9×10⁸	9.0×10⁷	1.1×10⁸	2.1×10⁸	2.1×10⁸	2.0×10⁸	2.9×10⁷	3.7×10⁷
±SD	2.3×10⁶	1.4×10⁸	1.1×10⁸	6.9×10⁷	1.1×10⁷	5.5×10⁸	9.3×10⁷	1.3×10⁸	5.9×10⁷	2.3×10⁸	3.6×10⁷	9.4×10⁷	2.3×10⁷	



3.7.4. Summary of the effects of compounds on the acid production assay

The three sub-inhibitory concentrations of F 5.1, F 5.1 NPs and blank NPs significantly inhibited acid production in *S. mutans*. However, the concentrations used to inhibit acid production were different, highest concentration of NPs were required whereas lowest concentration of F 5.1 was required (NPs > F 5.1/NPs > F 5.1). F 5.1 showed better activity followed by F 5.1 surface adsorbed nanoparticles. This is similar to what was observed in MIC/MBC results. The dose of subfraction F 5.1 in stabilized nanoparticles was not adjusted to be the same amount as the raw subfraction F 5.1. The dose of subfraction F 5.1 in stabilized nanoparticles contained 4.4 mg in 10 mg of nanoparticles. This implies that, the three sub-inhibitory concentrations of the nanoparticles used contained less subfraction F 5.1 as compared to raw subfraction F 5.1 used. Therefore, loading the subfraction onto the nanoparticles improved the activity and inhibited acid production.

Table 3.24 highlights the statistical comparison between pH and bacterial counts of the control and tests in the acid production assay. Tests with a significance level of $P < 0.05$ are highlighted.

Table 3.24: The statistical comparison between control and tests in acid assay

Compound	Test	Comparison	P value
F5.1	Ph	Control to all concentrations (Overall)	0.02
		Control to F5.1 0.39mg/ml	0.02
		Control to F5.1 0.20mg/ml	0.02
		Control to F5.1 0.10mg/ml	0.02
	Bacterial counts	Control to all concentrations (Overall)	0.15
		Control to 0.39mg/ml	0.08
		Control to 0.20mg/ml	0.22
		Control to 0.10mg/ml	0.22
F5.1 NPs	pH	control to all concentrations (Overall)	0.02
		control to 0.78mg/ml	0.02
		control to 0.39 mg/ml	0.02
		control to 0.20mg/ml	0.02
	Bacterial counts	Control to all concentrations (Overall)	0.10
		Control to 0.78mg/ml	0.09
		Control to 0.39mg/ml	0.11
		Control to 0.20mg/ml	0.09
Blank NPs	pH	Control to all concentrations (Overall)	0.03
		Control to 3.125mg/ml	0.03
		Control to 1.56mg/ml	0.03
		Control to 0.78mg/ml	0.03
	Bacterial counts	Control to all concentrations (Overall)	0.11
		Control to 3.125mg/ml	0.10
		Control to 1.56mg/ml	0.08
		Control to 0.78mg/ml	0.15

3.8. The effect of beneficial compounds on biofilm production by *S. mutans*

3.8.1 The effect of subfraction F 5.1 on biofilm production by *S. mutans*

The Table 3.25 shows the counts of *Streptococcus mutans* observed in biofilm developed in the presence of subfraction F 5.1. *Streptococcus mutans* was exposed to sub-inhibitory concentrations of subfraction F 5.1 for period of 6 hours and 24 hours. The bacterial counts of *S. mutans* exposed to the subfraction F 5.1 at three different sub-inhibitory concentrations were lower than the counts observed in the control both at 6 hours and 24 hours of exposure. The counts of *S. mutans* at 6 hours and 24 hours of incubation were all higher for the control, the counts increased with time.

The log conversion of the bacterial counts is shown in Table 3.26. The log values were used to plot a graph of the effect of subfraction F 5.1 on the formation of biofilm by *S. mutans* over a period of 6 hours and 24 hours (Figure 3.26).

Table 3.25: The effect of sub-inhibitory concentrations of subfraction F 5.1 on biofilm formation by *S. mutans*

Culture	Repeat	Bacterial counts (cfu/ml) in biofilm of <i>S. mutans</i> in the presence of Subfraction F 5.1												
		0hours	6hours (mg/ml)						24 hours (mg/ml)					
			0.39		0.20		0.10		0.39		0.20		0.10	
		ALL	Control	Test	Control	Test	Control	Test	Control	Test	Control	Test	Control	Test
ATCC	1	1.1×10 ⁵	3.5×10 ⁶	2.5×10 ⁴	3.5×10 ⁶	4.0×10 ⁴	3.5×10 ⁶	6.1×10 ⁴	1.8×10 ⁷	1.9×10 ⁵	1.8×10 ⁷	2.2×10 ⁵	1.8×10 ⁷	4.1×10 ⁵
	2	1.3×10 ⁵	3.6×10 ⁶	3.1×10 ⁴	3.6×10 ⁶	4.7×10 ⁴	3.6×10 ⁶	7.6×10 ⁴	1.1×10 ⁷	5.0×10 ⁵	1.1×10 ⁷	5.5×10 ⁵	1.1×10 ⁷	6.0×10 ⁵
	3	2.1×10 ⁵	4.8×10 ⁶	4.8×10 ⁴	4.8×10 ⁶	6.2×10 ⁴	4.8×10 ⁶	7.1×10 ⁴	2.2×10 ⁷	4.2×10 ⁵	2.2×10 ⁷	7.7×10 ⁵	2.2×10 ⁷	9.6×10 ⁵
SM1	1	2.1×10 ⁵	5.0×10 ⁶	2.2×10 ⁴	5.0×10 ⁶	2.3×10 ⁴	5.0×10 ⁶	3.0×10 ⁴	8.0×10 ⁷	2.6×10 ⁵	8.0×10 ⁷	3.6×10 ⁵	8.0×10 ⁷	4.0×10 ⁵
	2	2.0×10 ⁵	4.7×10 ⁶	1.2×10 ⁴	4.7×10 ⁶	1.4×10 ⁴	4.7×10 ⁶	1.7×10 ⁴	7.8×10 ⁷	3.5×10 ⁵	7.8×10 ⁷	4.3×10 ⁵	7.8×10 ⁷	5.4×10 ⁵
	3	4.8×10 ⁵	6.2×10 ⁶	1.8×10 ⁴	6.2×10 ⁶	2.0×10 ⁴	6.2×10 ⁶	2.7×10 ⁴	7.4×10 ⁷	4.0×10 ⁵	7.4×10 ⁷	4.4×10 ⁵	7.4×10 ⁷	5.7×10 ⁵
SM6	1	5.4×10 ⁵	2.1×10 ⁶	4.1×10 ⁴	2.1×10 ⁶	4.9×10 ⁴	2.1×10 ⁶	5.3×10 ⁴	9.6×10 ⁷	2.1×10 ⁵	9.6×10 ⁷	2.8×10 ⁵	9.6×10 ⁷	3.0×10 ⁵
	2	3.4×10 ⁵	5.7×10 ⁶	3.6×10 ⁴	5.7×10 ⁶	5.0×10 ⁴	5.7×10 ⁶	5.1×10 ⁴	2.1×10 ⁷	4.6×10 ⁵	2.1×10 ⁷	5.5×10 ⁵	2.1×10 ⁷	6.1×10 ⁵
	3	8.9×10 ⁴	2.5×10 ⁶	2.4×10 ⁴	2.5×10 ⁶	3.2×10 ⁴	2.5×10 ⁶	4.5×10 ⁴	3.2×10 ⁷	1.4×10 ⁵	3.2×10 ⁷	2.6×10 ⁵	3.2×10 ⁷	4.3×10 ⁵
	Mean ±SD	2.6×10 ⁵ 1.6×10 ⁵	4.2×10 ⁶ 1.4×10 ⁶	2.9×10 ⁴ 1.1×10 ⁴	4.2×10 ⁶ 1.4×10 ⁶	3.8×10 ⁴ 1.6×10 ⁴	4.2×10 ⁶ 1.4×10 ⁶	4.8×10 ⁴ 2.0×10 ⁴	4.8×10 ⁷ 3.3×10 ⁷	3.3×10 ⁵ 1.3×10 ⁵	4.8×10 ⁷ 3.3×10 ⁷	4.3×10 ⁵ 1.7×10 ⁵	4.8×10 ⁷ 3.3×10 ⁷	5.4×10 ⁵ 1.9×10 ⁵

Table 3.26: The log conversion of bacterial count of *S. mutans* in biofilm formation: subfraction F 5.1

Log conversion of Bacterial counts in biofilm formation by <i>S. mutans</i> : Subfraction F 5.1										
		0 hours	6 hours exposure at mg/ml				24 hours exposure at mg/ml			
Cultures	Repeat	ALL	control	0.39	0.20	0.10	control	0.39	0.20	0.10
ATCC 10923	1	5.0	6.5	4.4	4.6	4.4	7.3	5.3	5.3	5.6
	2	5.1	6.6	4.5	4.7	4.9	7.0	5.7	5.7	5.8
	3	5.3	6.7	4.7	4.8	4.9	7.3	5.6	5.9	6.0
SM1	1	5.3	6.7	4.3	4.4	4.5	7.9	5.4	5.6	5.6
	2	5.3	6.7	4.1	4.2	4.2	7.9	5.5	5.6	5.7
	3	5.7	6.8	4.3	4.3	4.4	7.9	5.6	5.6	5.8
SM6	1	5.7	6.3	4.6	4.7	4.7	8.0	5.3	5.5	5.5
	2	5.5	6.8	4.6	4.7	4.7	7.3	5.7	5.7	5.8
	3	5.0	6.4	4.4	4.5	4.7	7.5	5.2	5.4	5.6
	Mean ±SD	5.3 0.3	6.6 0.2	4.4 0.2	4.5 0.2	4.6 0.2	7.6 0.4	5.5 0.2	5.6 0.2	5.7 0.1

Table 3.27 shows the percentage reduction values obtained. The highest concentration of F 5.1 that reduced biofilm formation was 0.39 mg/ml. The reduction was 99.9 % at 6 hours and 98.9% at 24 hours. The lowest concentration of F 5.1 that reduced biofilm formation was 0.10 mg/ml and the reduction was 99.4% at 6 hours and 98.8% at 24 hours. The statistical analysis for the comparison between control and the sub-inhibitory concentrations of F 5.1 shows that the sub-inhibitory concentrations of F 5.1 significantly inhibited biofilm production by *S. mutans* at 6 hours and 24 hours with P value of <0.01 (Figure 3.26).

Table 3.27: The percentage reduction in biofilm production by *S. mutans*: F 5.1

Cultures <i>S. mutans</i>	Repeat	% Reduction in biofilm formation in the presence of Subfraction F 5.1					
		6 hours exposure at mg/ml			24 hours exposure at mg/ml		
		0.39	0.20	0.10	0.39	0.20	0.10
ATCC 10923	1	99.9	99.4	98.2	98.9	98.8	97.7
	2	99.1	98.7	97.9	95.6	95.0	94.6
	3	99.0	98.7	98.5	98.1	96.5	95.6
SM1	1	99.6	99.5	99.4	99.7	99.6	99.5
	2	99.7	99.7	99.6	99.6	99.5	99.3
	3	99.7	99.7	99.6	99.5	99.4	99.2
SM6	1	98.1	97.7	97.5	99.8	99.7	99.7
	2	99.4	99.1	99.1	97.8	97.4	97.0
	3	99.0	98.7	98.2	99.6	99.2	98.7
	Mean ±SD	99.3 0.56	99.0 0.65	98.7 0.79	98.7 1.38	98.3 1.67	97.9 1.84

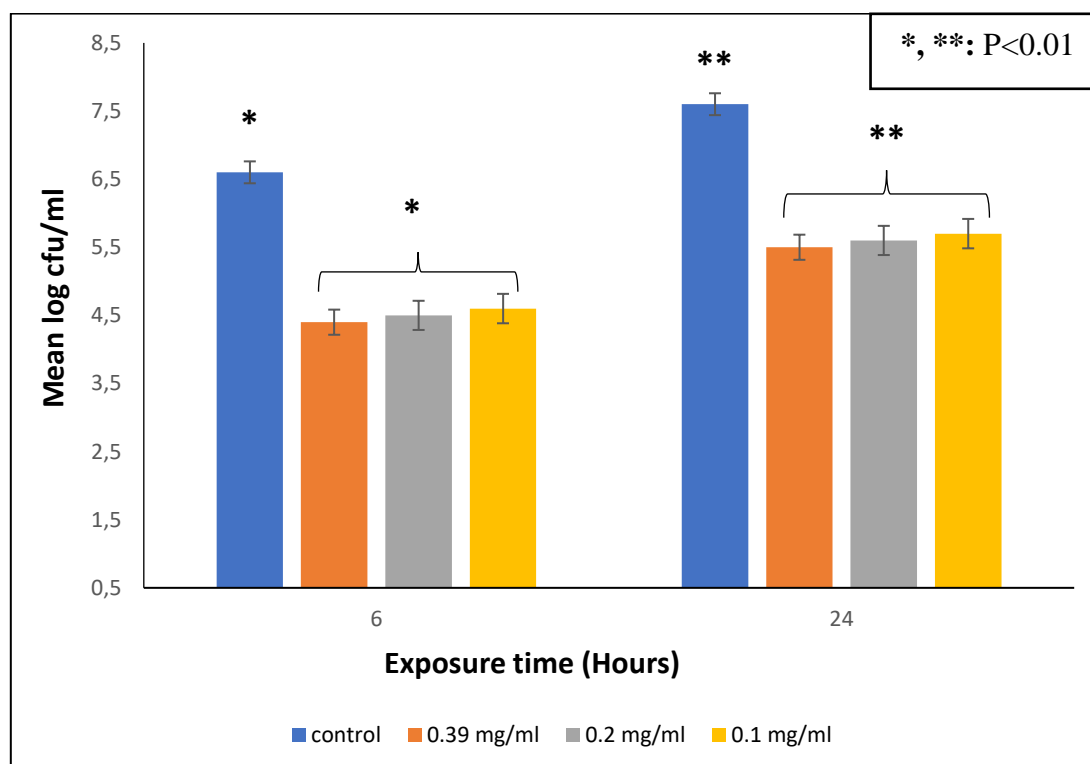


Figure 3.26: The effect of subfraction F 5.1 on biofilm formation *S. mutans* after 6 and 24 hours of exposure

3.8.2. The effect of subfraction F 5.1 surface stabilized nanoparticles on biofilm formation by *S. mutans*

The three sub-inhibitory concentrations of subfraction F 5.1 surface stabilized nanoparticles was also investigated using the glass slide technique. The slides were exposed to the nanoparticles for 6 hours and 24 hours. Table 3.28 shows the results of the effect of subfraction F 5.1 stabilized nanoparticles on the formation of biofilm by *S. mutans*. The bacterial counts in biofilm increased with increase in time. Control had a higher number of bacterial counts compared to subfraction F 5.1 surface stabilized nanoparticles.

Table 3.29 shows the log conversion values of the bacterial counts obtained. The log values were used to plot a graph of the effect of subfraction F 5.1 surface stabilized nanoparticles on the formation of biofilm by *S. mutans* over a period of 6 hours and 24 hours (Figure 3.27).

Table 3.28: The effect of sub-inhibitory concentrations of subfraction F 5.1 stabilized nanoparticles on biofilm formation by *S. mutans*

Culture	Repeat	Bacterial counts (cfu/ml) in biofilm of <i>S. mutans</i> in the presence of Subfraction F 5.1 Nanoparticles												
		0 hours ALL	6 hours exposure at mg/ml						24 hours exposure at mg/ml					
			0.78		0.39		0.20		0.78		0.39		0.20	
			Control	Test	Control	Test	Control	Test	Control	Test	Control	Test	Control	Test
ATCC	1	1.1×10 ⁵	3.5×10 ⁶	3.1×10 ⁵	3.5×10 ⁶	4.3×10 ⁵	3.5×10 ⁶	6.9×10 ⁵	1.8×10 ⁷	2.3×10 ⁶	1.8×10 ⁷	2.7×10 ⁶	1.8×10 ⁷	3.6×10 ⁶
	2	1.3×10 ⁵	3.6×10 ⁶	5.0×10 ⁵	3.6×10 ⁶	7.4×10 ⁵	3.6×10 ⁶	9.9×10 ⁵	1.1×10 ⁷	5.4×10 ⁵	1.1×10 ⁷	6.5×10 ⁵	1.1×10 ⁷	8.2×10 ⁶
	3	2.1×10 ⁵	4.8×10 ⁶	4.6×10 ⁵	4.8×10 ⁶	6.5×10 ⁵	4.8×10 ⁶	9.7×10 ⁵	2.2×10 ⁷	2.4×10 ⁶	2.2×10 ⁷	3.8×10 ⁶	2.2×10 ⁷	4.9×10 ⁶
SM1	1	2.1×10 ⁵	5.0×10 ⁶	2.5×10 ⁵	5.0×10 ⁶	2.7×10 ⁵	5.0×10 ⁶	4.0×10 ⁵	8.0×10 ⁷	5.6×10 ⁶	8.0×10 ⁷	8.9×10 ⁶	8.0×10 ⁷	9.7×10 ⁶
	2	2.0×10 ⁵	4.7×10 ⁶	2.6×10 ⁵	4.7×10 ⁶	2.9×10 ⁵	4.7×10 ⁶	3.6×10 ⁵	7.8×10 ⁷	3.2×10 ⁶	7.8×10 ⁷	4.9×10 ⁶	7.8×10 ⁷	5.6×10 ⁶
	3	4.8×10 ⁵	6.2×10 ⁶	2.0×10 ⁵	6.2×10 ⁶	2.3×10 ⁵	6.2×10 ⁶	3.9×10 ⁵	7.4×10 ⁷	4.3×10 ⁶	7.4×10 ⁷	6.2×10 ⁶	7.4×10 ⁷	7.1×10 ⁶
SM6	1	5.4×10 ⁵	2.1×10 ⁶	3.9×10 ⁵	2.1×10 ⁶	4.4×10 ⁵	2.1×10 ⁶	6.0×10 ⁵	9.6×10 ⁷	4.1×10 ⁶	9.6×10 ⁷	5.1×10 ⁶	9.6×10 ⁷	6.9×10 ⁶
	2	3.4×10 ⁵	5.7×10 ⁶	3.4×10 ⁵	5.7×10 ⁶	4.1×10 ⁵	5.7×10 ⁶	6.0×10 ⁵	2.1×10 ⁷	2.2×10 ⁶	2.1×10 ⁷	3.6×10 ⁶	2.1×10 ⁷	5.2×10 ⁶
	3	8.9×10 ⁴	2.5×10 ⁶	2.4×10 ⁵	2.5×10 ⁶	3.1×10 ⁵	2.5×10 ⁶	3.8×10 ⁵	3.2×10 ⁷	2.8×10 ⁶	3.2×10 ⁷	3.3×10 ⁶	3.2×10 ⁷	3.9×10 ⁶
	Mean	2.6×10 ⁵	4.2×10 ⁶	3.2×10 ⁵	4.2×10 ⁶	4.2×10 ⁵	4.2×10 ⁶	5.9×10 ⁵	4.8×10 ⁷	3.0×10 ⁶	4.8×10 ⁷	4.3×10 ⁶	4.8×10 ⁷	5.3×10 ⁶
	±SD	1.6×10 ⁵	1.4×10 ⁶	1.2×10 ⁵	1.4×10 ⁶	1.7×10 ⁵	1.4×10 ⁶	2.5×10 ⁵	3.3×10 ⁷	1.5×10 ⁶	3.3×10 ⁷	2.3×10 ⁶	3.3×10 ⁷	2.5×10 ⁶

Table 3.29: Log conversion of Bacterial counts in biofilm formation by *S. mutans*: Subfraction F 5.1 stabilized nanoparticles

Log conversion of Bacterial counts in biofilm formation by <i>S. mutans</i> : Subfraction F 5.1 nanoparticles										
Cultures	Repeat	0 hours	6 hours exposure at mg/ml				24 hours exposure at mg/ml			
		ALL	control	0.78	0.39	0.20	Contro l	0.78	0.39	0.20
ATCC 10923	1	5.0	6.5	5.5	5.6	5.8	7.3	6.6	6.4	6.6
	2	5.1	6.6	5.7	5.9	6.0	7.0	5.7	5.8	6.9
	3	5.3	6.7	5.7	5.8	6.0	7.3	6.4	6.6	6.7
SM1	1	5.3	6.7	5.4	5.4	5.6	7.9	6.8	7.0	7.0
	2	5.3	6.7	5.4	5.5	5.6	7.9	6.5	6.7	6.8
	3	5.7	6.8	5.3	5.4	5.6	7.9	6.6	6.8	6.9
SM6	1	5.7	6.3	5.7	5.6	5.8	8.0	6.6	6.7	6.8
	2	5.5	6.8	5.5	5.6	5.8	7.3	6.3	6.7	6.7
	3	5.0	6.4	5.4	5.6	5.8	7.5	6.4	6.5	6.6
	Mean ±SD	5.3 0.3	6.6 0.2	5.5 0.2	5.6 0.2	5.8 0.2	7.6 0.4	6.4 0.3	6.6 0.3	6.8 0.2

Table 3.30 shows the percentage reduction values obtained. The highest concentration of F 5.1 stabilized nanoparticles that reduced biofilm formation was 0.78 mg/ml. The reduction was 91.1% at 6 hours and 92.4% at 24 hours. The lowest concentration of F 5.1 surface stabilized nanoparticles that reduced biofilm formation was 0.20 mg/ml and the reduction was 84.0% at 6 hours and 85.8% at 24 hours. The statistical analysis for the comparison between control and the sub-inhibitory concentrations of F 5.1 surface stabilized nanoparticles show that the sub-inhibitory concentrations of F 5.1/NPs significantly inhibited biofilm production by *S. mutans* at 6 hours and 24 hours with P value of <0.01 (Figure 3.27).

Table 3.30: The percentage reduction in biofilm by *S. mutans*: subfraction F 5.1 stabilized nanoparticles

Cultures <i>S. mutans</i>	% Reduction in biofilm formation: Subfraction F 5.1 nanoparticles						
	Repeat	6 hours exposure at mg/ml			24 hours exposure at mg/ml		
		0.78	0.39	0.20	0.78	0.39	0.20
ATCC 10923	1	91.1	87.7	80.3	87.2	85.0	80.0
	2	86.1	79.4	72.5	95.1	94.1	92.6
	3	90.4	86.5	70.8	89.1	82.7	72.7
SM1	1	95.0	94.5	92.0	93.0	88.9	87.9
	2	99.5	93.8	92.3	95.9	93.7	92.8
	3	96.8	95.5	93.7	94.2	91.6	90.4
SM6	1	81.4	79.1	71.4	95.7	94.7	92.8
	2	94.0	92.8	89.5	89.5	82.9	75.2
	3	90.4	87.6	84.8	91.3	89.7	87.8
	Mean ±SD	91.1 4.8	88.5 6.2	84.0 8.5	92.4 3.2	89.3 4.7	85.8 7.8

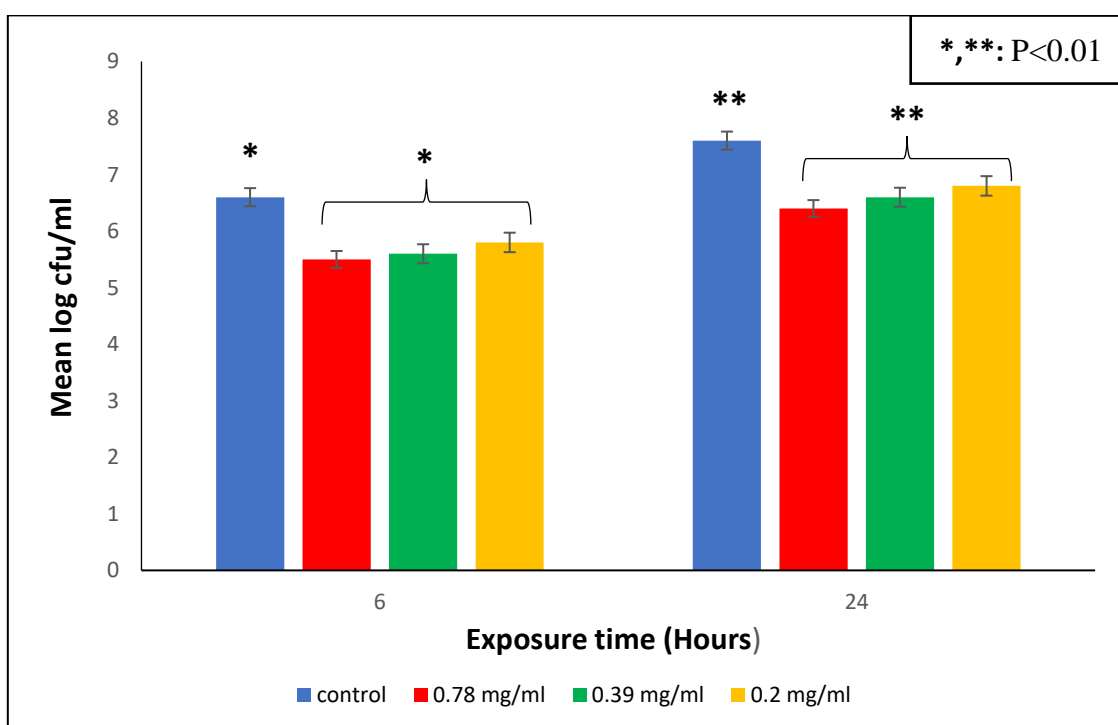


Figure 3.27: The effect of subfraction F 5.1 nanoparticles on biofilm formation by *S. mutans* after 6 and 24 hours of exposure

3.8.3. The effect of blank nanoparticles on biofilm formation by *S. mutans*

The three sub-inhibitory concentrations of blank nanoparticles were also investigated. Table 3.31 shows the results of the effect of blank nanoparticles on the formation of biofilm by *S. mutans*. The blank nanoparticles showed some inhibition, the reduction in bacterial counts in biofilm increased with increase in time. Control had a higher number of bacterial counts compared to nanoparticles.

Table 3.32 shows the log conversion values of the bacterial counts obtained. The log values were used to plot a graph of the effect of nanoparticles on the formation of biofilm by *S. mutans* over a period of 6 hours and 24 hours (Figure 3.28).

Table 3.31: The effect of sub-inhibitory concentrations of blank nanoparticles on biofilm formation by *S. mutans*

Culture	Repeat	Bacterial counts (cfu/ml) in biofilm of <i>S. mutans</i> in the presence of Blank nanoparticles												
		0 hours ALL	6 hours exposure at mg/ml						24 hours exposure at mg/ml					
			3.125		1.56		0.78		3.125		1.56		0.78	
			Control	Test	Control	Test	Control	Test	Control	Test	Control	Test	Control	Test
ATCC	1	1.1×10 ⁵	3.5×10 ⁶	1.6×10 ⁶	3.5×10 ⁶	2.0×10 ⁶	3.5×10 ⁶	2.2×10 ⁶	1.8×10 ⁷	7.4×10 ⁶	1.8×10 ⁷	8.5×10 ⁶	1.8×10 ⁷	9.9×10 ⁶
	2	1.3×10 ⁵	3.6×10 ⁶	1.5×10 ⁶	3.6×10 ⁶	2.2×10 ⁶	3.6×10 ⁶	2.8×10 ⁶	1.1×10 ⁷	4.6×10 ⁶	1.1×10 ⁷	7.8×10 ⁶	1.1×10 ⁷	8.7×10 ⁶
	3	2.1×10 ⁵	4.8×10 ⁶	2.0×10 ⁶	4.8×10 ⁶	2.6×10 ⁶	4.8×10 ⁶	3.3×10 ⁶	2.2×10 ⁷	5.2×10 ⁶	2.2×10 ⁷	6.9×10 ⁶	2.2×10 ⁷	7.4×10 ⁶
SM1	1	2.1×10 ⁵	5.0×10 ⁶	1.9×10 ⁶	5.0×10 ⁶	2.2×10 ⁶	5.0×10 ⁶	3.1×10 ⁶	8.0×10 ⁷	3.3×10 ⁷	8.0×10 ⁷	4.5×10 ⁷	8.0×10 ⁷	5.0×10 ⁷
	2	2.0×10 ⁵	4.7×10 ⁶	1.5×10 ⁶	4.7×10 ⁶	1.6×10 ⁶	4.7×10 ⁶	1.8×10 ⁶	7.8×10 ⁷	3.5×10 ⁷	7.8×10 ⁷	4.2×10 ⁷	7.8×10 ⁷	5.1×10 ⁷
	3	4.8×10 ⁵	6.2×10 ⁶	2.5×10 ⁶	6.2×10 ⁶	2.8×10 ⁶	6.2×10 ⁶	3.4×10 ⁶	7.4×10 ⁷	3.0×10 ⁷	7.4×10 ⁷	3.4×10 ⁷	7.4×10 ⁷	4.2×10 ⁷
SM6	1	5.4×10 ⁵	2.1×10 ⁶	1.0×10 ⁶	2.1×10 ⁶	1.2×10 ⁶	2.1×10 ⁶	1.5×10 ⁶	9.6×10 ⁷	4.6×10 ⁷	9.6×10 ⁷	5.5×10 ⁷	9.6×10 ⁷	6.1×10 ⁷
	2	3.4×10 ⁵	5.7×10 ⁶	1.9×10 ⁶	5.7×10 ⁶	2.3×10 ⁶	5.7×10 ⁶	3.4×10 ⁶	2.1×10 ⁷	1.0×10 ⁷	2.1×10 ⁷	1.2×10 ⁷	2.1×10 ⁷	1.6×10 ⁷
	3	8.9×10 ⁴	2.5×10 ⁶	1.1×10 ⁶	2.5×10 ⁶	1.6×10 ⁶	2.5×10 ⁶	2.0×10 ⁶	3.2×10 ⁷	2.2×10 ⁷	3.2×10 ⁷	3.5×10 ⁷	3.2×10 ⁷	3.7×10 ⁷
	Mean ±SD	2.5×10 ⁵ 1.6×10 ⁵	3.2×10 ⁵ 1.4×10 ⁶	1.7×10 ⁶ 4.7×10 ⁶	4.2×10 ⁶ 1.4×10 ⁶	2.1×10 ⁶ 5.1×10 ⁵	4.2×10 ⁶ 1.4×10 ⁶	2.6×10 ⁶ 7.21.4×10 ⁵	4.8×10 ⁷ 3.3×10 ⁶	3.9×10 ⁷ 1.5×10 ⁷	4.8×10 ⁷ 3.3×10 ⁶	5.0×10 ⁷ 1.9×10 ⁷	4.8×10 ⁷ 3.3×10 ⁶	5.8×10 ⁷ 2.1×10 ⁶

Table 3.32: Log conversion of Bacterial counts in biofilm formation by *S. mutans*: Blank nanoparticles

Log conversion of bacterial counts in biofilm formation by <i>S. mutans</i> : Blank nanoparticles										
		0 hours	6 hours exposure at mg/ml				24 hours exposure at mg/ml			
cultures	Repeat	ALL	control	3.125	1.56	0.78	control	3.125	1.56	0.78
ATCC 10923	1	5.0	6.5	6.2	6.3	6.3	7.3	6.9	6.9	6.7
	2	5.1	6.6	6.2	6.3	6.5	7.0	6.7	6.9	6.9
	3	5.3	6.7	6.3	6.4	6.5	7.3	6.7	6.8	6.9
SM1	1	5.3	6.7	6.3	6.3	6.5	7.9	7.5	7.7	7.7
	2	5.3	6.7	6.2	6.2	6.3	7.9	7.5	7.6	7.7
	3	5.7	6.8	6.4	6.5	6.5	7.9	7.5	7.5	7.6
SM6	1	5.7	6.3	6.0	6.1	6.2	8.0	7.7	7.7	7.8
	2	5.5	6.8	6.3	6.4	6.5	7.3	7.1	7.1	7.2
	3	5.0	6.4	6.0	6.3	6.4	7.5	7.3	7.5	7.6
	Mean ±SD	5.3 0.3	6.6 0.2	6.2 0.1	6.3 0.1	6.4 0.1	7.6 0.4	7.2 0.4	7.3 0.4	7.3 0.4

Table 3.33 shows the percentage reduction values obtained. The highest concentration of blank nanoparticles that reduced biofilm formation was 3.125 mg/ml. The reduction was 59.1% at 6 hours and 55.8% at 24 hours. The lowest concentration of blank nanoparticles that reduced biofilm formation was 0.78 mg/ml and the reduction was 35.5% at 6 hours and 33.8% at 24 hours. The statistical analysis for the comparison between control and the sub-inhibitory concentrations of blank nanoparticles showed that the blank nanoparticles significantly inhibited biofilm production by *S. mutans* at 6 hours and 24 hours with P value of <0.01 (Figure 3.28).

Table 3.33: The percentage reduction in biofilm production by *S. mutans* : Blank nanoparticles

Cultures <i>S. mutans</i>	Repeat	% Reduction in biofilm formation: Blank nanoparticles					
		6 hours exposure at mg/ml			24 hours exposure at mg/ml		
		3.125	1.56	0.78	3.125	1.56	0.78
ATCC 10923	1	54.3	42.9	37.1	58.9	52.8	45.0
	2	58.3	38.9	22.2	58.2	29.1	20.9
	3	58.3	45.8	31.3	56.7	42.5	38.3
SM1	1	62.0	56.0	38.0	58.8	43.8	37.5
	2	64.3	61.9	57.1	55.1	46.2	34.6
	3	59.7	54.8	45.2	56.4	51.3	41.0
SM6	1	52.4	42.9	28.6	52.1	42.7	36.5
	2	66.7	59.7	40.4	52.4	42.9	23.8
	3	56.0	36.0	20.0	54.0	30.0	26.0
	Mean ±SD	59.1 4.6	48.8 9.5	35.5 11.6	55.8 2.6	42.3 8.2	33.8 8.3

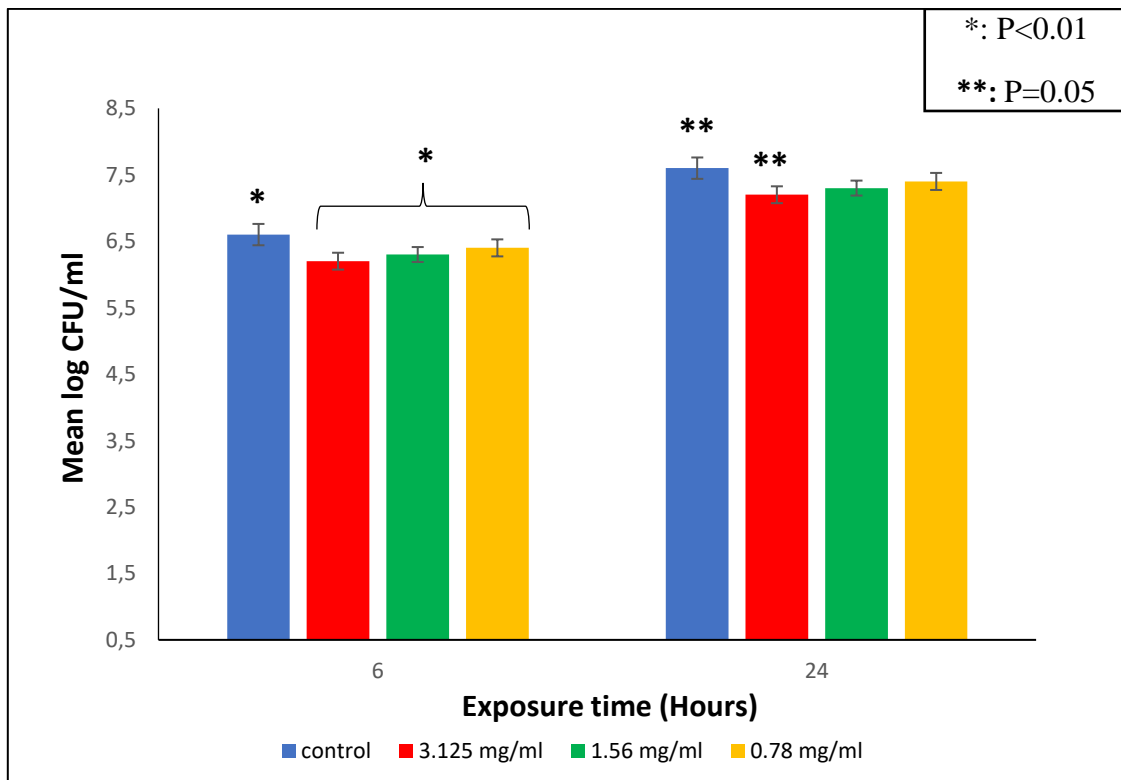


Figure 3.28: The effect of sub-inhibitory concentrations of blank nanoparticles on biofilm production by *S. mutans* after 6 and 24 hours of exposure

3.8.4: Summary of the effect of compounds on biofilm formation by *S. mutans*

The three sub-inhibitory concentrations of F 5.1, F 5.1 NPs and NPs significantly inhibited biofilm formation in *S. mutans*. However, the concentrations were different, highest concentration of NPs were required whereas lowest concentration of F 5.1 was required (NPs > F 5.1/NPs > F 5.1). This was the same trend as observed in MIC/MBC and acid production assay. The dose of subfraction F 5.1 in stabilized nanoparticles contained 4.4mg in 10mg of nanoparticles. This implies that, the three sub-inhibitory concentrations of the nanoparticles used contained less subfraction F 5.1 as compared to raw subfraction F 5.1 used. Therefore, loading the subfraction onto the nanoparticles improved biofilm reduction in *S. mutans*.

Table 3.34 highlights the statistical comparison of biofilm formation between tests and controls in the acid production assay.

Table 3.34: Statistical comparison between control and tests in biofilm formation by *S. mutans*

Compound	Exposure time	Comparison	P value
F 5.1	6 hours	Control to all concentrations (Overall)	<0.01
		Control to 0.39mg/ml	<0.01
		Control to 0.20mg/ml	<0.01
		Control to 0.10mg/ml	<0.01
	24 hours	Control to all concentrations (Overall)	<0.01
		Control to 0.39mg/ml	<0.01
		Control to 0.20mg/ml	<0.01
		Control to 0.10mg/ml	<0.01
F5.1 NPs	6 hours	Control to all concentrations (Overall)	<0.01
		Control to 0.78mg/ml	<0.01
		Control to 0.39 mg/ml	<0.01
		Control to 0.20mg/ml	<0.01
	24 hours	Control to all concentrations (Overall)	<0.01
		Control to 0.78mg/ml	<0.01
		Control to 0.39mg/ml	<0.01
		Control to 0.20mg/ml	<0.01
Blank NPs	6 hours	Control to all concentrations (Overall)	<0.01
		Control to 3.125mg/ml	<0.01
		Control to 1.56mg/ml	<0.01
		Control to 0.78mg/ml	0.01
	24 hours	Control to all concentrations (Overall)	0.24
		Control to 3.125mg/ml	0.05
		Control to 1.56mg/ml	0.15
		Control to 0.78mg/ml	0.24

3.9. Cytotoxicity study

The cytotoxicity effects of subfraction F 5.1, subfraction F 5.1 nanoparticles and blank nanoparticles were performed on normal human epithelial (HEP2) cells using MTT assay. Dose response graphs were constructed for all the tests as percentage cell viability.

For the screening process a threshold of 50% cell growth inhibition is used as a cut off for compound toxicity against cell lines is used.

Concentration used in the cytotoxicity study ranged from 500 µg/ml to 0.049 µg/ml (0.5 mg/ml-0.0004 mg/ml).

3.9.1. The effect of subfraction F 5.1 on the viability of cells

The results of the effect of subfraction F 5.1 on the viability of Hep 2 cells are shown in Table 3.35. The results were recorded in the form of absorbances and percentage inhibition. The effect of beneficial compounds against cell lines was calculated as the percentage inhibition using the following formula:

$$\% \text{ Growth inhibition} = 100 - \frac{\text{Mean OD of individual test group}}{\text{Mean OD of control group}} \times 100$$

The percentage cell growth inhibition in the presence of subfraction F 5.1 ranged from 89.32% (500 µg/ml) to 1.29% (0.49 µg/ml). The concentration of subfraction F 5.1 that reduced absorbance of treated cells by nearly 50% was 0.0625 mg/ml (62.5 µg/ml) with a calculated value of 50.24%. The absorbance of untreated cells was 0.412 and the absorbance of DMSO was 0.333 suggesting that DMSO has negligible effect on the cells. The absorbance of Triton X was 0.016 and media had absorbance of 0.016 and 0.028 respectively. The results were shown in the form of cell viability percentages in Figure 3.29

Table 3.35: Cytotoxicity assay absorption values of subfraction F 5.1

Test wells	Media only blank	DMSO control	Triton X +ve control	Untreated cells	500µ/ml	250µg/ml	125µg/ml	62.5µg/ml	31.25µg/ml	15.63µg/ml	7.81µg/ml	3.91µg/ml	1.95µg/ml	0.98µg/ml	0.49µg/ml
F5.1 Repeats	0.036	0.387	0.014	0.404	0.039	0.111	0.149	0.184	0.208	0.248	0.327	0.361	0.349	0.406	0.410
	0.024	0.324	0.015	0.415	0.042	0.127	0.156	0.137	0.219	0.284	0.315	0.344	0.373	0.428	0.390
	0.025	0.289	0.018	0.417	0.052	0.105	0.103	0.294	0.290	0.322	0.273	0.353	0.358	0.360	0.420
Mean	0.028	0.333	0.016	0.412	0.044	0.114	0.136	0.205	0.239	0.285	0.305	0.353	0.360	0.398	0.417
SD	0.001	0.050	0.002	0.007	0.007	0.011	0.029	0.081	0.045	0.037	0.028	0.009	0.012	0.035	0.015
%I	-	19.1	96.2	-	89.3	72.3	67.0	50.2	42.0	30.9	26.0	14.4	12.6	3.4	1.3

%I= Percentage inhibition

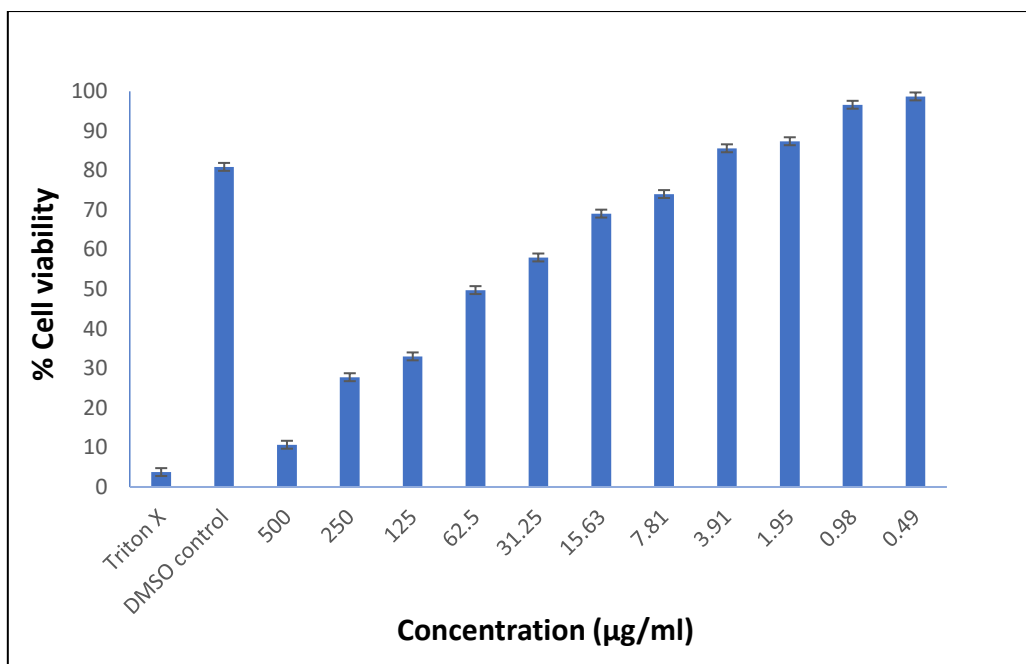


Figure 3.29: Viability of cells exposed to F 5.1 expressed as percentage

3.9.2. The effect of subfraction F 5.1 stabilized nanoparticles on the viability of cells

The results of the effect of subfraction F 5.1 nanoparticles on the viability of HEP2 cells is shown in Table 3.36. The results were recorded in the form of absorbance and percentage inhibition.

The effect of beneficial compounds against cell lines was calculated as the percentage inhibition using the following formula:

$$\% \text{ Growth inhibition} = 100 - \frac{\text{Mean OD of individual test group}}{\text{Mean OD of control group}} \times 100$$

The percentage cell growth inhibition in the presence of subfraction F 5.1 nanoparticles ranged from 92.96% (500 µg/ml) to 5.83% (0.49 µg/ml). The subfraction F 5.1 nanoparticles concentration that reduced absorbance of treated cells by nearly 50% was 0.0156mg/ml (15.63µg/ml) with a calculated value of 49.51%. The absorbance of untreated cells was 0.412 and the absorbance of DMSO was 0.333 suggesting that DMSO has negligible effect on the cells. The absorbance of Triton X was 0.016 and media had absorbance of 0.028. The results were shown in the form of cell viability percentages in Figure 3.30.

Table 3.36: Cytotoxicity assay absorption values of subfraction F 5.1 nanoparticles

Test wells	Media only blank	DMSO control	Triton X +ve control	Untreated cells	500 μ /ml	250 μ g/ml	125 μ g/ml	62.5 μ g/ml	31.25 μ g/ml	15.63 μ g/ml	7.81 μ g/ml	3.91 μ g/ml	1.95 μ g/ml	0.98 μ g/ml	0.49 μ g/ml
F5.1/NPs Repeats	0.036	0.387	0.014	0.404	0.029	0.041	0.091	0.121	0.168	0.198	0.220	0.278	0.304	0.328	0.391
	0.024	0.324	0.015	0.415	0.036	0.067	0.089	0.132	0.189	0.214	0.245	0.281	0.313	0.378	0.400
	0.025	0.289	0.018	0.417	0.022	0.045	0.085	0.125	0.169	0.212	0.264	0.293	0.325	0.351	0.374
Mean	0.028	0.333	0.016	0.412	0.029	0.051	0.088	0.126	0.175	0.208	0.243	0.284	0.314	0.352	0.388
SD	0.001	0.050	0.002	0.007	0.007	0.014	0.003	0.006	0.012	0.009	0.022	0.008	0.011	0.021	0.013
%I	-	19.1	96.2	-	93.0	87.6	78.6	69.4	57.5	49.5	41.0	31.1	23.8	14.6	5.8

%I= Percentage inhibition

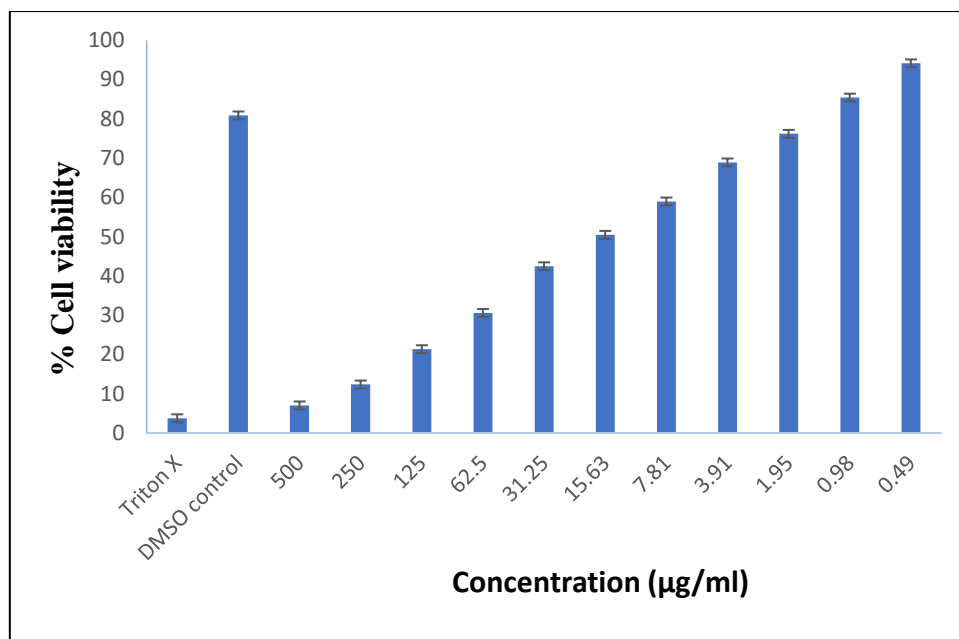


Figure 3.30: Viability of cells exposed to F 5.1 nanoparticles expressed as percentage

3.9.3 The effect of blank nanoparticles on the viability of cells.

The results of the effect of blank nanoparticles on the viability of HEP cells is shown in Table 3.37. The results were recorded in the form of absorbance and percentage inhibition.

The effect of beneficial compounds against cell lines was calculated as the percentage inhibition using the following formula:

$$\% \text{ Growth inhibition} = 100 - \frac{\text{Mean OD of individual test group}}{\text{Mean OD of control group}} \times 100$$

The percentage cell growth inhibition in the presence of blank nanoparticles ranged from 92.18% (500 µg/ml) to 4.93% (0.49 µg/ml). The blank nanoparticles concentration that reduced absorbance of treated cells by nearly 50% was 0.0039 mg/ml (31.25 µg/ml) with a calculated value of 48.92%. The absorbance of untreated cells was 0.507 and the absorbance of DMSO was 0.401 suggesting that DMSO has negligible effect on the cells. The absorbance of Triton X was 0.026 and media had absorbance of 0.023 respectively. The results were shown in the form of cell viability percentages in Figure 3.28.

Table 3.37: Cytotoxicity assay absorption values of blank nanoparticles

Test wells	Media only blank	Triton X +ve control	DMSO control	Untreated cells	500ug/ml 0.5mg	250ug/ml	125ug/ml	62.5ug/ml	31.25ug/ml	15.63ug/ml	7.81 ug/ml	3.91 ug/ml	1.95 ug/ml	0.98 ug/ml	0.49 ug/ml
Blank/NPS Repeats	0.022	0.024	0.397	0.534	0.041	0.067	0.099	0.122	0.158	0.199	0.238	0.296	0.401	0.441	0.471
	0.021	0.022	0.414	0.475	0.046	0.074	0.097	0.134	0.160	0.203	0.267	0.299	0.410	0.445	0.485
	0.025	0.031	0.409	0.511	0.032	0.075	0.095	0.132	0.159	0.215	0.272	0.321	0.378	0.474	0.490
Mean	0.023	0.026	0.401	0.507	0.040	0.072	0.097	0.129	0.159	0.206	0.259	0.305	0.396	0.453	0.482
SD	0.005	0.005	0.009	0.030	0.007	0.004	0.002	0.006	0.001	0.008	0.018	0.014	0.017	0.018	0.010
%I	-	94.8	19.7	-	92.2	85.8	80.9	74.6	68.6	59.4	48.9	39.8	21.9	10.7	4.9

%I= Percentage inhibition

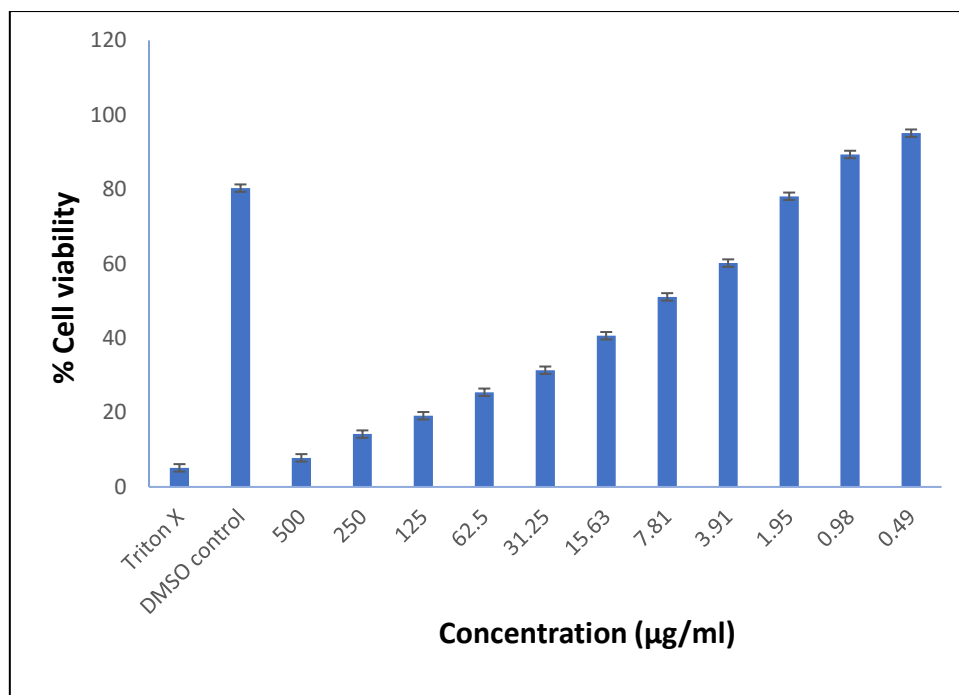


Figure 3.31: Viability of cells exposed to blank nanoparticles expressed as percentage

3.9.4. Summary of the cytotoxicity effects of compounds on Hep2 cells

The three compounds (F 5.1, F 5.1 NPs and NPs) showed minimal effects on the viability of Hep2 cells. The highest viability was observed with blank nanoparticles with calculated value of 51.1% at a concentration of 31.25 µg/ml. Subfraction F 5.1 stabilized nanoparticles had viability of 50.5% at a concentration of 15.63 µg/ml. Subfraction F 5.1 had viability of 49.8% at a concentration of 62.5 µg/ml.

CHAPTER 4

DISCUSSION

Dental caries is the most important infection in children and adults globally and it continues to be a major health problem. The significant role of socio-behavioural and environmental factors in oral disease and health is well evidenced in an extensive number of surveys (Abanto *et al.*, 2011). The impact of dental caries includes jeopardizing general health and increased morbidity and mortality. In school children, dental caries restricts activity at school due to many days absent from school. Other negative impacts on children's lives include chewing difficulties, decreased appetite, weight loss, sleeping difficulties, changes in behaviour and decrease in school performances (Abanto *et al.*, 2011). In adults, dental caries restricts activity at work and at home thereby creating an economic burden to the individual, family and society. It significantly diminishes the quality of life and extensive tooth loss may also restrict social contact and interaction. Normal daily activities are also restricted due to pain from untreated dental caries and sleep is also disturbed (Griffin *et al.*, 2012).

Many therapeutic agents containing antimicrobial agents have been used to prevent dental caries in the form of toothpaste and mouthwashes. Some of these therapeutic compounds are derived from plants. Plants and plant products have been used in many parts of the world, for example *Acokanthera oppositifolia*; *Albizia adianthifolia* (leaves and roots); *Annona senegalensis* (bark); *Barleria prionitis*; *Carissa bispinosa* (root); *Dicoma anomala* (root); several *Cassia*, *Acacia* and *Ficus* species, *Dodonaea viscosa jacq*, *Erythrina lysistemon Hutch* and *Zea mays* are used for toothache (Henly-Smith, 2012 and Akhalwaya *et al.*, 2018). Most of these plants have been used traditionally. However, it is important to validate the use of these plants using scientific experiments in order to maximise production of these plant products.

Dodonaea viscosa has been proven to have anti-*streptococcus mutans* activity and validated using scientific experiments. It was shown in studies that were conducted by Patel *et al.*, (2009) and Naidoo *et al.*, (2012) that the crude extract of *Dodonaea viscosa var. angustifolia* (DVA) was able to reduce acid production and biofilm production in *Streptococcus mutans* which are responsible for the pathogenesis of caries. In addition, the chemical (flavone) responsible for this beneficial effect has been identified (Ngabaza *et al.*, 2017). In this study

anticariogenic activity of flavone derived from DVA was enhanced using nanotechnology. In addition, the slow release of the flavone and the safety of the stabilised nanoparticles were established.

4.1. Fractionation of crude extract

Crude extract was obtained and fractionated using chromatography to obtain fraction 5. Subfraction F 5.1 was isolated from fraction 5 and selected for further analysis. Subfraction F5.1 was chosen as the main agent due to its antimicrobial activities. Subfraction F5.1 was found to have anti-*streptococcus mutans* activity, anti-acidogenic and anti-aciduric properties. The total yield of crude extract was 24.4 g (40.6%). In contrast, Ngabaza *et al*, (2017) obtained a yield of 11.4 g of crude extract which is approximately half of the yield obtained in this study. The difference could have been due to the number of extractions prepared in both studies. The extract was further separated to isolate the bioactive agent (subfraction F 5.1) which was identified by Ngabaza *et al*, (2017) as 5,6,8-Trihydroxy-7-methoxy-2-(4-methoxyphenyl)-4-H-chromen-4-one. Subfraction F5.1 was chosen as the main agent due to its antimicrobial activities. Subfraction F5.1 was found to have anti-*streptococcus mutans* activity, anti-acidogenic and anti-aciduric properties. The average total quantity of subfraction F 5.1 after separation was 1.8 g. This quantity was still comprised of a mixture of compounds.

4.2 Characterisation of subfraction F 5.1

Analysis of the flavone (subfraction F 5.1) on UV-vis spectroscopy showed two major peaks. Band A was observed at 334nm and band B at 270 nm. Similarly, these peaks were observed in regions similar to those found by Tsimogiannins, 2007 and Ngabaza *et al.*, 2017 with band A in the region of 310-350 nm and band B in the region of 250-290 nm.

Infrared spectroscopic analysis also confirmed bending and stretching vibrations that have been cited by Clark, 2000 to be present in flavone (during analysis of subfraction F 5.1). The flavone found in subfraction F 5.1 has previously been identified using nuclear magnetic resonance (NMR) as 5,6,8-Trihydroxy-7-⁴l -dimethoxyflavone (Ngabaza *et al.*, 2017). However, in this work, the flavone was not isolated in pure form and sufficient quantity to

allow for NMR analysis and because of this there was no attempt to further elucidation (using NMR).

Subfraction F 5.1 was analysed using gas chromatography-mass spectroscopy to confirm the molecular weight of the flavone. The spectrum showed four major peaks at 149.02 m/z, 279.16 m/z, 331.08 m/z and 391.28 m/z. The ionization peaks that identifies the subfraction F 5.1 was found to be m/z 331.0811 $[M+H]^+$ which is close to molecular weight of the identified compound. Similarly, Ngabaza *et al.*, (2017) found that the molecular weight of the flavone was 330.28 with ionization peak of m/z 326.9 $[M-3H]^-$.

4.3. Synthesis of Nanoparticles

To reduce or minimize undesirable interactions, a biodegradable nano-carrier has been developed for crude extract of *Dodonaea viscosa var. angustifolia* and subfraction F 5.1 containing the active flavone. A di-block copolymer of PLGA-PEG polymers was synthesised by ring opening polymerization of lactide and glycolide in the presence of PEG containing acetic acid terminal at the end of the chains. Two subgroups of PLGA with different molecular weights (lower-50:50 and higher-85:15) were used.

A total of ten nanoparticles were prepared with subfraction F 5.1 and crude extract loaded onto the surface of the polymeric nanoparticles and entrapped in the core of polymeric nanoparticles. The crude extract and subfraction F 5.1 were loaded onto the surface of PLGA-PEG copolymeric nanoparticles matrix using the double emulsion technique. In this study, the influence of pH and temperature were not varied during synthesis.

4.4. Characterisation of nanoparticles

4.4.1. UV-vis spectroscopy and FTIR

Blank nanoparticles and subfraction loaded nanoparticles were analysed. Blank nanoparticles showed a lower peak at wavelength of 278 nm. Subfraction loaded nanoparticles showed similar peaks to those observed with analysis of subfraction F 5.1, this suggests that subfraction F 5.1 was successfully loaded onto the surface of the nanoparticles.

Infrared spectroscopic analyses of PLGA-PEG copolymers in this study also showed pronounced stretching and bending vibrations that are similar to those observed in PLGA-PEG copolymers cited by Li *et al.*, (2001). The infrared spectroscopic analyses of loaded flavone nanoparticles showed peaks observed in the PLGA-PEG nanoparticles as well as the peaks observed in flavone. Similarly, Li *et al.*, (2001) and Alimohammadi *et al.*, (2012) observed peaks appearing in similar areas to those found in the study suggesting that the loading of nanoparticles was successful.

4.4.2. Particle size and morphology

Scanning electron micrographs and transmission electron micrographs did not show good quality pictures from which size and shape could be ascertained with accuracy. However, ImageJ analysis was done using subfraction F 5. 1 stabilized nanoparticles TEM micrograph. The mean size obtained from ImageJ analysis was in the form of diameter. The diameter was found to be 9.2 nm on the TEM micrograph obtained for PLGA-PEG subfraction F 5.1 stabilized nanoparticles. The size of the nanoparticles based on TEM appeared to be smaller than those obtained from dynamic light scattering measurements. This discrepancy could have been due to the test used for analysis of the sample, wherein the samples were not immersed in water (as their immersion could have resulted in water uptake and swelling resulting in a larger size observed) (Li *et al.*, 2002).

Scanning electron micrographs of PLGA-PEG nanoparticles showed relatively spherical morphology. Similarly, Alimohammadi *et al.*, (2012) observed spherical morphology on SEM and TEM micrographs of magnetic PLGA-based nanoparticles.

4.4.3. Zeta potential and size distribution (Poly Dispersity Index)

Zeta potential measurements provide an important criterion for the stability of colloid systems (Tantra *et al.*, 2010 and Zhang *et al.*, 2014). The concept of zeta potential has been used in cell biology to study cell biological activation, cell agglutination and cell adhesion which are related to cell surface charge properties (Zhang *et al.*, 2014). Zeta potential can potentially be used to predict the environmental impact of commercial nanoparticles as well as their effects on human health.

In this study, zeta potential was measured for copolymers, blank nanoparticles and subfraction F 5.1 stabilized nanoparticles dispersed in distilled water with different pH values. The stability of copolymers and nanoparticles in line with zeta potentials were measured as highly unstable to highly stable. Copolymers and blank nanoparticles had a similar trend of zeta potential. High instability was observed at pH 2, moderate stability was observed at pH 3 and high stability was observed at pH 12 in both copolymers and blank nanoparticles. Subfraction loaded nanoparticles had a similar trend with blank nanoparticles at pH 3 where the nanoparticles were moderately stable and pH 12 where the nanoparticles were highly stable. The difference at other pH values may be due to the addition of subfraction F 5.1 moieties. Dorati *et al.*, (2010) observed that gentamicin sulfate loaded nanoparticles had approximately neutral zeta potential in the range of +0.5-3.58mV corresponding to highly unstable suspensions, and this was due to the fact that these nanoparticles were lyophilized. The values obtained in their work, were considered suitable since it was shown in studies that neutral zeta potential positively affects antimicrobial activity (Dorati *et al.*, 2010).

Particle distribution in nanoparticles relates to the particle size distribution of the nanoparticles in particular the magnitude of the distribution. Monodispersity is observed with PDI value of 0.1 and below while polydispersity manifests a PDI of greater than 0.1. Values between 0.1 and 0.25 indicate a narrow size particle distribution (Tantra *et al.*, 2010). In this study, polydispersity was observed in blank nanoparticles and subfraction F 5.1 stabilized nanoparticles. Narrow distribution was observed in blank nanoparticle at pH 11 with PDI value of 0.2 and zeta size of 116.2 nm. Subfraction F 5.1 had narrow distribution at pH 11 with PDI value of 0.2 and zeta size of 169 nm.

A study done by Kashi *et al.*, (2012) reported mean particle size (z-average) of all nanoparticles prepared to be in the range of 85-7070 nm. According to the authors an acceptable size of PLGA-PEG nanoparticles less than 500 nm is suitable for clinical purposes. In this study, particle size (z-average) with sizes less than 500 nm were observed when blank nanoparticles were dispersed in distilled water at pH 2 (191.4 nm), pH 3 (235.1 nm), pH 4 (365.0 nm), pH 11 (85.2 nm) and pH 12 (116.2 nm). Subfraction F 5.1 stabilized nanoparticles with sizes less than 500 nm were observed when dispersed in distilled water with pH 2 (239.9 nm), pH 5 (284.6 nm), pH 6 (262.8 nm), pH 7 (189.8 nm), pH 11 (169.8 nm) and pH 12 (143.6 nm).

The results observed in TEM, SEM and Image J were smaller than those observed in zeta size analysis. The size difference may have been due to the hydrodynamic (water) effects in the results obtained in zeta size. The particles might swell up in solution thereby causing bigger sizes for zeta sizer analysis whereas for the analysis conducted using SEM and TEM the particles were not dissolved in water.

4.5. Drug entrapment analyses

4.5.1. Drug loading and drug entrapment

The percentage drug loading of PLGA-PEG was 43.5% and the encapsulation efficiency was 87.1%. The nanoparticles showed lower encapsulation efficiency. In contrast Li *et al*, (2001) found encapsulation efficiency of 48.6% with PLGA-PEG nanoparticles and 63.8% efficiency with PLGA chains. The difference may have been due to the difference in the amount of PLGA and PEG used. Li *et al*, (2001) used 10 g of PLGA and 2 g of PEG. However, in this study only 1.8 g PLGA and 0.2 g PEG were used. The amount of subfraction F 5.1 that was successfully loaded in 10 mg of nanoparticles was found to be 4.4 mg.

4.5.2. Release profiles of F 5.1 from nanoparticles

In vitro drug release assessment assumes a greater significance in serving as an indicator for drug product quality and performance. It is generally assumed that a drug is released by several processes such as diffusion through the polymer matrix, release by polymer degradation and solubilisation and diffusion through microchannels that exist in the polymer matrix or are formed by erosion (Li *et al.*, 2001). A standard curve was plotted in order to deduce an equation that will be used to calculate the concentration of subfraction F 5.1. This was used to determine the actual concentration of subfraction that would be released from the nanoparticle's matrix at different time intervals. The release of F 5.1 from the nanoparticles was slow and steady. Since the n-fickian mechanism states that a fickian diffusion method has the n-value being less or equal to 0.45, the release of F 5.1 at pH 7.4 meets the requirements of this model since the n-value was calculated to be 0.277 pointing to release through diffusion. The release of F 5.1 in pH 5.5 does not meet the requirement for the n-

fickian diffusion method since the n-value was calculated to be 0.713, pointing to a non-fickian diffusion method

The slow release of F 5.1 from F 5.1/NPs suggests that it was released by diffusion through the polymer matrix, where release could have been by polymer degradation or solubilisation and diffusion through microchannels that exist in the polymer matrix or are formed by erosion (Li *et al.*, 2001). Only 40% of the drug was released from the nanoparticles at 12 hours of incubation suggesting that more of the compound was still retained in the nanoparticles. Most of the subfraction F 5.1 flavone compound was released at pH 5.5 (60 % released), suggesting that these nanoparticles could be pH dependent. Li *et al.*, (2001) observed a high and faster release of BSA in PEG-PLGA nanoparticles compared to PLGA nanoparticles at 12 hours.

During the release profile study, subfraction F 5.1 was released steadily over time, at 5 hours of incubation 0.1 mg/ml of subfraction F 5.1 was released from the subfraction F 5.1 nanoparticles. At this concentration, the subfraction will be able to inhibit the virulence factors of *streptococcus mutans* (acid and biofilm production) since the minimum inhibitory concentrations used were 0.78 mg/ml, 0.39 mg/ml and 0.2 mg/ml. In addition, an *in vitro* release profile showed that it was released up to 12 hours at a neutral as well as at an acidic pH value. This suggests that F 5.1/NPs may provide long lasting anti-cariogenic effect.

Previous studies indicated that barrier devices impregnated with antibacterial drugs could decrease the risk of infection and contribute to increased gain of clinical attachment. The release profiles of Tetracycline, a commonly used antibacterial agent, which was successfully loaded onto PLGA membranes showed an initial burst phase in the first week followed by a sustained drug release over 14 days. This was desired for the needs of high antibiotic concentration in early phases of infection and enough dose of antibiotic during the whole healing process (Sun *et al.*, 2017). Another study showed that chlorhexidine conjugated chitosan nanoparticles release chlorhexidine quickly within 5 hours but thereafter drug was released in a controlled and slow manner for several hours (Chronopoulou *et al.*, 2016). Similarly, in this study a steady release was observed at 0-5 hours of incubation and over a period of time the release was sustained (6-12 hours). This implies that application of the nanoparticles at a higher concentration will kill *S. mutans*. Over time, the concentration will be diluted by saliva to sub-inhibitory concentrations and the flavone would be able to inhibit acid production and biofilm formation.

4.6. MIC/MBC

Crude and subfraction F 5.1 were shown to have anti-*streptococcus mutans* activity therefore, these compounds were used in the form of nanoparticles in order to enhance their activity. Among these nanoparticles, subfraction F 5.1 surface adsorbed nanoparticles had better MIC value (1.56 mg/ml) compared to the other nanoparticles that were prepared. Therefore, surface adsorbed F 5.1 was selected for further tests.

More MIC/MBC tests were done using the selected nanoparticles, which include subfraction surface adsorbed, blank nanoparticles and raw subfraction F 5.1. Subfraction F 5.1 had the highest MIC value of 0.78 mg/ml which doubled with subfraction F 5.1 nanoparticles, however the doses of subfraction F 5.1 were not the same. F 5.1 nanoparticles had MIC value of 1.56 mg/ml. The dose of subfraction F 5.1 in stabilized nanoparticles was not adjusted to be the same amount as the raw subfraction F 5.1. The dose of subfraction F 5.1 in stabilized nanoparticles contained 4.4 mg in 10 mg of nanoparticles. This implies that in 50 mg/ml starting concentration of nanoparticles 22 mg of subfraction was loaded therefore, encapsulation with nanoparticles improved the activity using lower concentrations. The quantity of F5.1 contained in the 1.56 mg/ml MIC value obtained for the subfraction stabilized nanoparticles was determined through calculation to be 0.7 mg/ml.

A study was done by *Kashi et al.*, (2012), they tested antibacterial activity of minocycline loaded PLGA nanoparticles and free minocycline against *Aggregatibacter actinomycetocomitans*, a causative agent for periodontal disease. The authors found that the MIC of minocycline-loaded nanoparticles (4 µg/ml) was two folds less than that of free minocycline (8 µg/ml) and the MBC value of minocycline-loaded nanoparticles (8 µg/ml) was also two folds less than that of free minocycline (16 µg/ml). However, the concentration of minocycline in nanoparticles was similar to that of free minocycline based on the actual drug loading of the nanoparticles which was used to provide equivalent concentration. Other researchers studied the effect of curcumin (a polyphenol) loaded PLGA nanoparticles (CUR-NPs) and curcumin-free nanoparticles (NPs). They found that cationic NPs with or without curcumin eradicated growth of three microorganisms including cariogenic bacteria (*S. mutans*, *C. albicans* and methicillin resistant *Staphylococcus aureus*) when treated with 130µM of NPs and CUR-NPs (*Gutierrez et al.*, 2017).

Blank nanoparticles prepared in this study also showed activity against *streptococcus mutans* with MIC value of 3.125 mg/ml. The MBC value was 6.25 mg/ml. These MIC/MBC values

were very high. Kashi *et al.*, (2012) and Dorati *et al.*, (2018) have shown that PLGA nanoparticles do not have any antimicrobial activity however, in these studies the test concentrations were very low. Kashi *et al.*, (2012) reported a concentration of 3.5µg/ml however, these nanoparticles did not consist of PEG polymer. Another study by Dorati *et al.*, (2018) reported lack of any antimicrobial activity when 20 µg/ml- 80 µg/ml of placebo (PLGA-PEG nanoparticles) were tested. However, Gutierrez *et al.*, (2017) showed that 130µM of PLGA-NPs eradicated growth of *S. mutans*, *C. albicans* and methicillin resistant *Staphylococcus aureus*. The difference in results between this study and other studies may have been due to the absence of PEG polymer in the nanoparticles that were prepared. PEG may have some effect towards inhibition of bacterial growth.

4.7. Acid production of subfraction 5.1 and prepared nanoparticles

Sub-inhibitory concentrations of subfraction F 5.1, subfraction F 5.1 stabilized nanoparticles and blank nanoparticles inhibited acid production in *S. mutans*. Acids are responsible for the demineralisation of enamel. The observed inhibition in acid production could have been due to the reaction between flavone and the bacterial enzymes in *S. mutans*. Because a study has shown that flavones and flavonols inhibit several enzymes, including glucosyltransferases and lactate dehydrogenase in *Streptococci species* including *Streptococcus mutans* (Koo *et al.*, 2002). GTFs catalyse the formation of soluble and insoluble α -linked glucans from sucrose and contribute significantly to the dental plaque matrix polysaccharide composition. Glucans facilitate attachment of *S. mutans* on to the teeth surface. Lactose dehydrogenase is known to produce lactic acid from pyruvate which leads to the production of acid. Flavones such as Apigenin derived from *Propolis* are known to inhibit bacterial enzymes, including glucosyltransferases and lactate dehydrogenase in *S. mutans* (Koo *et al.*, 2002). The exact mechanism by which Apigenin and related flavonoids inhibit glucosyltransferases and lactate dehydrogenase (GTF) activity is unknown, although the data reported provide some insights into the mode of their inhibitory action. It appears that inhibition of GTFs depends on the molecular structure of flavonoids and the physical state of the enzyme (Koo *et al.*, 2002). Catechin containing green tea has also been shown to interfere with acid production by inhibiting the bacterial enzyme lactate dehydrogenase which is responsible for the formation of lactic acid (Hamilton-Miller, 2001).

In the present study DVA flavone may have inhibited F-ATPase or lactate dehydrogenase which is responsible for the aciduric and acidogenic properties (Brown *et al.*, 1972 and Carlsson *et al.*, 1974). Glycolytic pathways are responsible for the conversion of glucose to pyruvate and subsequently into lactic acid. There are many catalytic enzymes involved in this conversion and F 5.1/NPs may have affected one of these enzymes. For example, widely used anticariogenic compound fluoride inhibits enzyme enolase which is responsible for the conversion of 2-phosphoglycerate to phosphoenolpyruvate and subsequent production of acid (Marsh and Martin, 2003). Blank nanoparticles also showed great anti-cariogenic effect, however the concentrations were high, and the mechanism of inhibition is not known.

4.8. Biofilm formation of subfraction 5.1 and the beneficial nanoparticles

Biofilms are characterised by dense clusters of bacterial cells and a multitude of different microorganisms embedded in an extra-cellular matrix which allows them to adhere to the surface and to communicate with each other within the matrix (Pandit *et al.*, 2011 and Akhalwaya *et al.*, 2018). Biofilm and extracellular polysaccharide production are also responsible for the development of dental caries.

Subfraction F 5.1 significantly inhibited biofilm formation at the lowest concentration of 0.1mg/ml. The reduction was 98.7% and 97.9% at 6 hours and 24 hours of exposure respectively. Similarly, Ngabaza *et al.*, (2018) reported that the flavone subfraction F 5.1 inhibited the effect of biofilm formation at a concentration of 0.05 mg/ml with reduction of 94% (6 hours) and 99% (24 hours). The slight difference in concentrations may have been due to availability of subfraction in higher amount or in its purest form.

The lowest concentration of F 5.1 stabilized nanoparticles that inhibited biofilm formation was 0.2 mg/ml, it inhibited biofilm formation by 84.0% at 6 hours and 85.8% at 24 hours. The dose of subfraction F 5.1 in stabilized nanoparticles was lower than that of raw subfraction F 5.1 compound therefore, encapsulation with nanoparticles improved biofilm inhibition.

Chemicals and plant derived compounds stabilised nanoparticles have been studied for their anti-biofilm activity. Free methylene blue as well as methylene blue anionic and cationic nanoparticles reduced bacterial viability of dental plaque/biofilm by 38%, 43% and 60.1%

respectively. The same study was done for photodynamic analysis in the presence of light. In the presence of light, free Methylene Blue, Methylene Blue loaded anionic and cationic nanoparticles reduced bacterial viability by approximately 37%, 42% and 48%. Mean log CFU levels for light and Methylene Blue loaded nanoparticles were not significantly different from those of free Methylene Blue alone (Klepac-Ceraj, 2011). Another study showed that curcumin loaded PLGA nanoparticles significantly reduced biofilm of *S. mutans*, *C. albicans* and methicillin resistant *Staphylococcus aureus* at a concentration of 130 μ M (Gutierrez *et al.*, 2017).

Blank nanoparticles showed activity against biofilm formation in *S. mutans* with the lowest concentration of 0.78 mg/ml. The inhibition was 35.5% and 33.8% at 6 hours and 24 hours respectively. However, most studies have shown that blank nanoparticles did not have any effect on the inhibition of biofilm formation. A study by Cheow *et al.*, (2010) showed that there was no difference in viable colony forming units (CFU) of the exposed biofilm cells after 6, 12 and 24 hours; suggesting that the viable CFU in blank nanoparticles (poly caprolactone/ poly DL-lactide-co-glycolide-PCL/PLGA prepared by nanoprecipitation and polycaprolactone/ poly DL-lactide-co-glycolide-PCL/PLGA ESE (emulsification-solvent-evaporation) was similar to experimental control. Therefore, blank nanoparticles did not alter the biofilm growth. In contrast, a study by Gutierrez *et al.*, (2017) showed that when *S. mutans* (grown as biofilm) was treated with PLGA nanoparticles without curcumin, the evaluation of biofilm was significantly lower than control. This suggests that PLGA nanoparticles had an effect on the growth of biofilm.

4.9. Cytotoxicity study of subfraction F 5.1 and the prepared nanoparticles

Cytotoxicity is an important measure in both evaluating the impact of nanomaterials on public health and developing them for various biomedical applications such as drug delivery. The effect of subfraction F 5.1, subfraction F 5.1 stabilized nanoparticles and blank nanoparticles were tested on normal Human hepatic epithelial (Hep2) cells. The absorption values were measured at a wavelength of 450 nm.

Subfraction F 5.1 concentration of 0.0625 mg/ml reduced absorbance of treated cells by nearly 50% with calculated value of 50.24% cell death. Ngabaza *et al.*, (2017) reported that a concentration of 0.03 mg/ml (subfraction F 5.1) reduced the absorbance of treated cells by

nearly 50% in relation to untreated cells (IC_{50}) with a calculated value of 48.35%. The concentration observed in their work is double what was found in this present study, which may have been due to greater quantity of the flavone component or having the flavone in its pure form.

The concentration of 0.0156 mg/ml subfraction F 5.1 nanoparticles reduced absorbance of treated cells by nearly 50% with calculated value of 49.51% cell death. Flavones have been shown not to have any cytotoxicity effect and the PLGA-PEG polymers have been approved for use by FDA (Makadia and Siegel, 2011). When the cytotoxicity of curcumin nanoparticles on normal oral keratinocytes in a study by Gutierrez *et al.*, (2017) was tested, they reported that the anionic formulations of the nanoparticles showed a similar cell viability percentage to the negative control group, demonstrating that the curcumin nanoparticles were not cytotoxic. However, cytotoxicity was observed with cationic nanoparticles loaded with curcumin which might have been due to the addition of various chemicals such as CTAB (cetyl trimethylammonium bromide). Cetyl trimethylammonium bromide is commonly used as an antibacterial cationic surfactant for its ability to inactivate bacteria (Salim *et al.*, 2013).

Blank nanoparticles reduced absorbance of treated cells by nearly 50% at a concentration of 0.0039 mg/ml with a calculated value of 48.92% cell death. Gutierrez *et al.*, (2017) reported that PLGA nanoparticles (without drug) showed a similar cell viability percentage to the negative control group, demonstrating that the nanoparticles were not cytotoxic.

Parameters such as composition, surface chemistry, surface charge and shape play an important role in affecting the toxicity of nanomaterials (Zhang *et al.*, 2017). Other parameters include electrostatic stature of the surface; morphology; and agglomeration status (Shin *et al.*, 2015).

The effect of toxicology of PLGA-PEG has been tested mostly on cancerous cells. The effect of shape of PLGA-PEG NPs were investigated on the physiological response on Human liver carcinoma cells (HepG2) cells (Zhang *et al.*, 2017). In the study they formed needle-shaped nanoparticles and introduced them to the cells. The needle shaped nanoparticles were found to induce physiological changes in cells which led to significant cytotoxicity. The concentration ranged from 5-250 $\mu\text{g/ml}$. The cytotoxicity increased with increase in concentration (cell viability decreased from 93% at concentration of 5 $\mu\text{g/ml}$ to around 56% at concentration of 250 $\mu\text{g/ml}$. Little toxicity was observed in cells that were fed with

spherical nanoparticles with cell viability of 84% at concentration of 250 µg/ml (Zhang *et al.*, 2017).

Cytotoxicity analysis of the prepared flavone stabilized nanoparticles on Hep2 cells revealed that the concentration (0.156 mg/ml) that reduced cell viability by 50% was lower than the MIC values (1.56 mg/ml), however it is not certain whether it was the effect of dead cells that was measured or the cumulative effect of the polymeric nanoparticles. The effect may have been due to agglomeration of the polymers, size and surface characteristics (Zhang *et al.*, 2017).

The sub-inhibitory concentrations (0.78, 0.39 and 0.2 mg/ml) showed inhibition of acid and biofilm formation, therefore if these nanoparticles are used at sub-inhibitory concentrations, they would be safe to use in the oral cavity. The sub-inhibitory concentrations would not be harmful since saliva would dilute the compound to concentrations that would still exert an effect. The amount of subfraction released observed over time was lower than the MIC value, this implies that over time the amount that will be released will not be harmful, it will be diluted by saliva and still exert its expected effect.

4.10. Clinical implications

Subfraction F 5.1 stabilized nanoparticles retained the known anticariogenic properties of subfraction F 5.1. The nanoparticles showed anti-*streptococcus mutans* activity, anti-biofilm and acidogenic properties at three sub-inhibitory concentrations. The release profiles of subfraction F 5.1 from the surface of the nanoparticle polymer matrix showed good substantivity (slow release and absorption) at 12 hours. More subfraction was still retained in the nanoparticles suggesting that the subfraction F 5.1 will continue being released for more than 12 hours. The amount of subfraction released over 5 hours was 0.10 mg/ml, this amount will be able to inhibit growth of *S. mutans*, acid production and biofilm formation. Therefore, PLGA-PEG subfraction F 5.1 stabilized nanoparticles can be used as anticariogenic agents. They can be incorporated in oral hygiene products such as toothpaste, mouthrinses and chewing gums. The use of nanoparticles will inhibit washing away effect by saliva, whereby nanoparticles will be absorbed into the oral mucosal cells and slowly be released inhibiting virulence factors of *S. mutans*. If the MIC or the sub-inhibitory concentrations are used in the development of these oral hygiene products, growth of *S. mutans* will be reduced and the

remaining bacterial cells will not be able to cause acid production and biofilm. Using these nanoparticles in toothpaste day and night would offer maximum protection against dental caries.

CHAPTER 5

5.1. CONCLUSION

Crude extract and subfraction F 5.1 from the plant *Dodonaea viscosa var. angustifolia* are well known to have anti-*streptococcus mutans* properties. Ten nanoparticles containing subfraction F 5.1 and crude extract were prepared and showed varying levels of antimicrobial activity against *S. mutans* with MIC values ranging from 25 mg/ml- 1.56 mg/ml. Among all the prepared nanoparticles, subfraction F 5.1 surface stabilized nanoparticles had higher antimicrobial activity which was selected for the further studies. At sub-inhibitory concentrations including low concentration of 0.2mg/ml, these nanoparticles inhibited biofilm formation and acid production in *S. mutans*. Great substantivity was also observed due to the slow release of the subfraction F 5.1 from the nanoparticles over time at physiological pH (7.4) and at cariogenic pH (5.5). Only 40-60% of subfraction F 5.1 was released at 12 hours, suggesting that more subfraction F 5.1 was still retained and therefore would continue being released after 12 hours. At the released concentrations, it will be able to inhibit the virulence factors of *S. mutans*. The toxicity study showed that F 5.1 surface stabilized nanoparticles were safe to be used.

If these nanoparticles containing flavone are used at MIC/MBC concentrations, they would be absorbed by the cells in the oral cavity and gradually release the flavone to the oral cavity. The released flavone will be diluted gradually with saliva in the oral cavity to sub-inhibitory concentrations and these will inhibit growth of *S. mutans*, acid production and biofilm production. This suggests that F 5.1/NPs if used in the form of oral hygiene products such as toothpaste and mouthwash, F 5.1/NPs may provide long lasting anti-cariogenic effect. Therefore, DVA derived flavone stabilized PLGA-PEG nanoparticles have potential to be used in the prevention of dental caries.

5.2. Limitations to the study

1. Ideally this study should be done in the presence of mix flora because dental biofilm contains variety of microorganisms. Studies such as biofilm assay should be done on mix flora. However, most preliminary studies are done on monoculture as it is difficult to study the effect of the virulence of any organism. *S. mutans* was used as the primary causative agent of dental caries.
2. The effect of the nanoparticles on extracellular polysaccharides which are produced by *S. mutans* was not studied due to limited study time. Extracellular polysaccharides produced by *S. mutans* play a role in biofilm development.
3. Yield of subfraction F 5.1 is affected during extraction and purification processes, thereby leading to little quantities obtained at the end of extraction process.
4. The method of synthesis and purification used may have affected the yield of subfraction F 5.1 nanoparticles obtained. The subfraction F 5.1, was loaded onto the surface of the nanoparticles. Some of it may have been washed away during purification by washing with distilled water.
5. The dose of subfraction F 5.1 in F 5.1 stabilized nanoparticles was not adjusted in order to have the same doses in plain subfraction and subfraction loaded onto the nanoparticles. This would have been ideal for the comparison tests between what happens when this subfraction is loaded onto the nanoparticles and when it is not loaded.
6. The sizes of the nanoparticles were bigger than expected. This might have been due to the fact that the nanoparticles seemed to aggregate forming clusters leading to observation of bigger sizes on TEM, SEM and Zeta sizer.
7. The cytotoxicity method used to study the effect of nanoparticles was through reading of the absorption values. The absorbances observed might have been of the nanoparticles and not of the cells. Therefore, the readings may have not been of dead cells, but the polymers used in the nanoparticles.
8. The release assay was done *in vitro*, conditions used to mimic the oral cavity was temperature of 37°C only, saliva was not used. Therefore, what we may have seen might not exactly be a representation of what would happen *in vivo*.

5.3. Future research

1. A study on the effect of the nanoparticles on other microorganisms that are also found in dental plaque would be ideal as dental plaque is composed of a variety of organisms.
2. Clinical trials would be ideal for studying the prepared nanoparticles by incorporating them into a mouth rinse, toothpaste or chewing gum to determine the efficacy in preventing dental caries. *In vitro* analysis does not provide a complete representation of what happens *in vivo*.
3. A study could be done to investigate the effect of the nanoparticles on enzymes that contribute to the pathogenicity of *S. mutans*. Enzymes like glucosyltransferase, F-ATPase and enolase.
4. A study on the methods of optimization of nanoparticles to get a desired size that will be able to penetrate the cells and not form aggregation clusters could be conducted.
5. The effect of the compound on the production of extracellular polysaccharides that contribute to development of dental plaque could be investigated.

CHAPTER 6

REFERENCES

- Abanto, J., Carvallo, T.S., Mendes, F.M., Wanderley, M.T., Bonecker, M., Raggio, D.P. 2011. Impact of oral diseases and disorders on oral health-related quality of life of preschool children. *Community Dentistry and Oral Epidemiology* 39, 105-14.
- Akhalwaya, S., Van Vuuren, S., Patel, M. 2018. An in vitro investigation of indigenous South African medicinal plants used to treat oral infections. *Journal of Ethnopharmacology* 210, 359-371.
- Alimohammadi, S., Salehi, R., Amini, N., Davaran, S. 2012. Synthesis and physicochemical characterization of biodegradable PLGA-based magnetic nanoparticles containing amoxicillin. *Bulletin of the Korean Chemistry Society* 33, 3225.
- Allaker, R.P. 2010. The use of nanoparticles to control biofilm formation. *Journal of Dental Research* 89, 1175-1186.
- Amerongen, A.V.N, Veerman, E.C.I. 2002. Saliva the defender of the cavity. *Oral diseases* 8, 12-22.
- Anbg, N.D. 2006. Australian plant common name database, Australian botanical gardens. *Department of the Environment and Heritage* 18, 4-6.
- Andre, R.F., Andrade, I.M., Silva-Lovato, C.H., Paranhos, H.F., Pimenta, F.C., Ito, I.Y. 2011. Prevalence of *mutans streptococci* isolated from complete dentures and their susceptibility to mouthrinses. *Brazilian Dental Journal* 22, 62-67.
- Banas, J.A., 2004. Virulence properties of *streptococcus mutans*. *Frontiers in Bioscience* 9, 1267-1277.
- Bhattacharjee, S.2018. DLS and zeta potential- What they are and what they are not. *Journal of controlled release* 235, 337-351

- Borel, T., Sabliov, C.M., 2014. Nano-delivery of bioactive components for food applications: types of delivery systems, properties, and their effect on ADME profiles and toxicity of nanoparticles. *Annual review Food and science technology* 5, 197–213.
- Brown, A.T., Wittenberger, C.L. 1972. Fructose-1.6-diphosphate-dependent lactate-dehydrogenase from a cariogenic *streptococcus* purification and regulatory properties. *Journal of Bacteriology* 110, 604-615.
- Carlsson, J., Griffith, C.J. 1974. Fermentation products and bacterial yields in glucose limited and nitrogen limited cultures of streptococci. *Archives of Oral Biology* 19, 1105-1109.
- Cheow, W.S., Wook, M., Hadinoyo, K. 2010. Antibacterial efficacy of inhalable levonofloxacin loaded polymeric nanoparticles against *E. coli* biofilm cells: The effect of antibiotic release profile. *Pharmaceutical Research* 27, 1597-1609.
- Chronopoulou, L., Nocca, G., Castagnola, M., Paludetti, G., Ortaggi, G., Sciubba, F., Bevilacqua, M., Lupi, A., Gambarini, G., Palocci, C. 2016. Chitosan based nanoparticles functionalised with peptidomimetic derivatives for oral drug delivery. *New Biotechnology* 33, 23-31.
- Clark, J. 2000. Interpreting an Infrared Spectrum. <http://www.chemguide.co.uk/analysis/ir/interpret.html>. Accessed on 20th October 2018.
- Danhier, F., Ansorena, E., Silva, J.M., Coco, R., Le Breton, A., Préat, V. 2012. PLGA-based nanoparticles: An overview of biomedical applications. *Journal of Controlled Release* 161, 505–522.
- Dodds, W.J.M., Johnson, A. D., Yeh, C. 2005. Health benefits of saliva: A review. *Journal of Dentistry* 33, 223-233.
- Dorati, R., DeTrizio, A., Spalla, M., Migliavacca, R., Pagani, L., Pisani, S., Chiesa, E., Conti, B., Modena, T, Genta, I.2018. Gentamicin sulfate PEG-PLGA-H nanoparticles: screening design and antimicrobial effect evaluation toward clinic bacterial isolates. *Nanomaterials (Basel)* 8, 37.
- Duarte, S., Koo H., Bowen, W.H., Hayacibara, M.F., Cury J.A., Ikegaki, M., Rosalen, P.L., 2003. Effect of a novel type of propolis and its chemical fractions on glucosyltransferases and

on growth and adherence of mutans streptococci. *Biological pharmaceutical bulletin* 26, 527-531.

- Engineer, C., Parikh, J., Raval, A. 2011. Review on hydrolytic degradation behaviour of biodegradable polymers from controlled drug delivery system. *Trends Biomaterial and Artificial Organs* 25, 79-85.
- Eloff, J.N. 1998. A sensitive and quick microplate method the minimum inhibition concentration of plant extracts for bacteria. *Planta medica* 64, 711-713.
- Featherstone, J.D.B. 2000. The science and practice of caries prevention. *Journal of the American Dental Association* 131, 887- 899.
- Ferrazzano, F.G., Amato, I., Ingenito, A., De Natale A, Pollio, A. 2009. Anti-cariogenic effects of polyphenols from plant stimulant beverages (cocoa, coffee and tea). *Fitorapia* 80, 255-262.
- Gentile, P., Chiono, V., Carmagnola, I., Hatton, P.V. 2014. An overview of poly lactic co-glycolic acid (PLGA)-based biomaterials for bone tissue engineering. *International Journal of Molecular Sciences* 15, 3640-3659.
- Getie, M., Gebre-Marima, T., Rietz, R., Ho`hne, C., Huschkad, C., Schmidtke, M., Abatef, A., Neubert, R.H.H. 2003. Evaluation of anti-microbial and anti-inflammatory activities of the medicinal plants *dodonaea viscosa*, *rumex nervosus* and *rumex abyssinicus*. *Fitorapia* 74, 139-143.
- Gold, J.A. 2008. The role of chlorhexidine in caries prevention. *Operative Dentistry* 33, 710-716.
- Griffin, S.O., Jones, J.A., Brunson, D., Griffin, P.M., Bailey, W. 2012. Burden of oral diseases among older adults and implications for public health priorities. *American Journal of Public Health* 102, 411-418.
- Gulube, Z., Patel, M. 2016. Effect of *punica granatum* on the virulence factors of cariogenic bacteria *streptococcus mutans*. *Microbial pathogenesis* 98, 45-49.

- Gutierrez, J.K.T., Zanatta, G.C., Ortega, A.L.M., Balastegui, M.I.C., Sanita, V.P., Pavarina, A.C., Barbugli, P.A., de Oliveira, E.G. 2017. Encapsulation of curcumin in polymeric nanoparticles for antimicrobial photodynamic therapy. *PLOS ONE* 12, 1-34.
- Hamilton-Miller, J.M. 2001. Anti-cariogenic properties of tea (*Camellia sinensis*). *Journal of Medical Microbiology* 50, 299-302.
- Harris, J.M., Chess, R.B. 2003. Effect of pegylation on pharmaceuticals. *Nature Reviews. Drug Discovery; London* 2, 214–221.
- Harshiny, M., Iswarya, C.H., Matheswaran, M. 2015. Biogenic synthesis of iron nanoparticles using amaranthus dubius leaf extract as a reducing agent. *Powder Technology* 286, 744–749.
- Helwitz, R.H., Ishmail, A., Pitts, N.B. 2007. Dental caries. *The Lancet* 369, 51-59.
- Hosseininasab, S., Pashaei-Asl, R., Khandaghi, A.A., Nasrabadi, H.T., Nejati-Koshki, K., Akbarzadeh, A., Joo, S.W, Hanifehpour, Y., Davaran, S. 2014. Synthesis, characterization, and invitro studies of PLGA-PEG nanoparticles of oral insulin delivery. *Chemical Biology and Drug Design* 84, 307-315.
- Iravani, S. 2011. Green synthesis of metal nanoparticles using plants. *Green Chemistry* 13, 2638–2650.
- Kashi, T.S.J., Eskandarion, S., Esfandyari-Manesh, M., Marashi, S.M.A., Samadi, N., Fatemi, S.M., Atyabi, F., Eshraghi, S., Dinarvand, R. 2012. Improved drug loading and antibacterial activity of minocycline-loaded PLGA nanoparticles prepared by solid/oil/water ion pairing method. *International Journal of Nanomedicine* 7, 221-234.
- Khan, R., Alam, F., Anwar, S., Khan, B.M., Shah, Z. 2012. Isolation of flavones from indigenous *Dodonaea viscosa*. *Journal of Chemical Society of Pakistan* 34, 195-200.
- Klepac-Ceraj, V., Patel, N., Song, X., Holewa, C., Patel, C., Kent, R., Amiji, M.M., Soukos, N.S. 2011. Photodynamic effects of methylene blue-loaded polymeric nanoparticles on dental plaque bacteria. *Lasers in Surgery and Medicine* 43, 600-606.

- Koo, H., Roselen, P.L., Cury, J.A., Park, Y.K., Bowen, W.H. 2002. Effects of compounds found in propolis on *streptococcus mutans* growth and on glucosyltransferase activity. *Antimicrobial Agents in Chemotherapy* 46, 1302-1309.
- Kumari, A., Yadav, S.K., Yadav, S.C., 2010. Biodegradable polymeric nanoparticles-based drug delivery systems. *Colloids and Surfaces B: Biointerfaces* 75, 1-18.
- Leonarduzzi, G., Testa, G., Sottero, B., Gamba, P., Poli, G. 2010. Design and development of nanovehicle-based delivery systems for preventive or therapeutic supplementation with flavonoids. *Current Medicinal Chemistry* 17, 74-95.
- Lewinski, N., Colvin, V., Drezek, R. 2008. Cytotoxicity of nanoparticles. *Small* 4, 26–49.
- Li, Y., Pei, Y., Zhang, X., Gu, Z., Zhou, Z., Yuan, W., Zhou, J., Zhu, J., Gao, X. 2001. PEGylated PLGA nanoparticles as protein carriers: synthesis, preparation and biodistribution in rats. *Journal of Control Release* 71, 203-211.
- Li, Y., Boone, E., El-Sayed, M.A. 2002. Size effects of PVP-Pd nanoparticles on catalytic Suzuki reactions in aqueous solution. *Langmuir* 18, 4921-4925.
- Limsong, J., Benjavongkulchai, E., Kuvatanasuchati, J. 2004. Inhibitory effect of some herbal extracts on adherence of *Streptococcus mutans*. *Journal of Ethnopharmacology* 92, 281-289.
- Locatelli, E., Franchini, M.C. 2012. Biodegradable PLGA-*b*-PEG polymeric nanoparticles: synthesis, properties, and nanomedical applications as drug delivery system. *Journal of Nanoparticle Research* 14, 1316.
- Löe, H. 2000. Oral hygiene in the prevention of caries and periodontal disease. *International Dental Journal* 50, 129-139.
- Loesche, W.J. 1986. Role of *Streptococcus mutans* in human dental decay. *Microbiological reviews* 50, 353-380.
- Makadia, H. K., Siegel, S. J. (2011). Poly lactic-*co*-glycolic acid (PLGA) as biodegradable controlled drug delivery carrier. *Polymers (Basel)* 3, 1377-1397.

- Marsh, P., Martin, M.V. 2003. Oral microbiology. 4th edition. Wright Edinburgh London New York Oxford Philadelphia St Louis Sydney Toronto.
- Menon, L.U., Varma, B., Kumaran, P., Xavier, A.M., Govinda, B.S., Kumar, S.J. 2018. Efficacy of a calcium sucrose phosphate-based toothpaste in elevating the level of calcium, phosphate ions in saliva and reducing plaque: A clinical trial. *Contemporary Clinical Dentistry* 9, 151–157.
- Metwalli, K.H., Khan, S.A., Krom, B.P., Jabra-Rizk, M.A. 2013. *Streptococcus mutans*, *Candida albicans*, and the human mouth: A sticky situation. *PLOS Pathogens* 9, 1-5.
- Nagavarma, B.V.V., Hemant, K.S.Y., Ayaz, A., Vasudha, L.S., Shivakumar, H.G. 2012. Different techniques for preparation of polymeric nanoparticles- A review. *Asian Journal of Pharmaceutical and clinical Research* 5, 16-16.
- Naidoo, R., Patel, M., Gulube, Z., Fenyvesi, I. 2012. Inhibitory activity of *Dodonaea viscosa* var. *angustifolia* extract against *Streptococcus mutans* and its biofilm. *Journal of Ethnopharmacology* 144, 171-174.
- Nalina, T., Rahim, Z. H. A. 2007. The crude aqueous extract of *Piper betle* L. and its antibacterial effect towards *Streptococcus mutans*. *American Journal of Biotechnology and Biochemistry* 3, 10-15.
- Nassar, H.M., Gregory, R.L. 2017. Biofilm sensitivity of seven *streptococcus mutans* strains to different fluoride levels. *Journal of Oral Microbiology* 9, 1328265.
- Ngabaza, T., Johnson, M.M., Moeno, S., Patel, M. 2017. Identification of 5,6,8-trihydroxy-7-methoxy-2-(4-methoxyphenyl)-4H-chromen-4-one with antimicrobial activity from *dodonaea viscosa* var. *angustifolia*. *South African Journal of Botany* 112, 48-53.
- Ngabaza, T., Moeno, S., Patel, M. 2018. Anti-acidogenic and anti-biofilm activity 5,6,8-trihydroxy-7-methoxy-2-(4-methoxyphenyl)-4H-chromen-4-one. *Microbial Pathogenesis* 123, 149-152.
- Ngwuluka, N. C., Pillay, V., Choonara, Y. E., Modi, G., Naidoo, D., du Toit, L., Kumar, P., Ndesendo, V. M. K., Khan, R. A. 2011. Fabrication, modelling and characterization of multi-

crosslinked methacrylate copolymeric nanoparticles for oral drug delivery. *International Journal of Molecular Sciences* 12, 6194-6225.

- O'Toole, G., Kaplan, H.B., Kolter, R. 2000. Biofilm formation as microbial development. *Annual Review of Microbiology* 54, 49-79.
- Palombo, E.A., 2011. Traditional medicinal plant extracts and natural products with activity against oral bacteria: potential application in the prevention and treatment of oral diseases. *Evidence Based Complementary Alternative Medicine* 2011, 1-15.
- Panche, N., Diwan, A. D., Chandra, S. R. 2016. Flavonoids: an overview. *Journal of Nutritional Science* 5, 1-15.
- Pandit, S., Kim, J., Jung, K., Chang, K., Jeon, J. 2011. Effect of sodium fluoride on the virulence factors and composition of *S. mutans* biofilm. *Archives of oral biology* 56, 643-649.
- Patel, M., Coogan, M.M. 2008. Antifungal activity of plant *Dodonaea viscosa* var. *angustifolia* on candida albicans from HIV infected patients. *Journal of Ethnopharmacology* 118, 173-176.
- Patel, M., Gulube, Z., Dutton, M. 2009. The effect of *Dodonaea viscosa* var. *angustifolia* on *candida albicans* proteinase and phospholipase production and adherence to oral epithelial cells. *Journal of Ethnopharmacology* 124, 562-565.
- Petersen, P.E., Bourgeois, D., Ogawa, H., Estupinan-Day, S., Ndiaye, C. 2005. The global burden of oral diseases and risks to oral health. *Bulletin of the World Health Organisation* 83, 661-669.
- Puy, C.L. 2006. Saliva in maintaining oral health and as an aid to diagnosis. *Medicina Oral, Patologia Oral y Cirugia Bucal* 11, 449-455.
- Rani, M.S., Pippalla, R.S., Mohan, K. 2009. *Dodonaea viscosa* linn.-an overview. *Journal of pharmaceutical research and health care* 1, 97-112.

- Salim, M.M., Ahmad, N., Malek, N., Ramli, N.I., Aishah, S., Hanim, M., Hamdan, S. 2013. Antibacterial activity of CTAB-modified Zeolite NaY with different CTAB loading. *The International Conference and Workshops on Basic and Applied Sciences and 11th Regional Annual Fundamental Science seminar*.
- Savithramma, N., Linga, Rao M., Rukmini, K., Suvarnalatha devi, P. 2011. Antimicrobial activity of silver nanoparticles synthesized by using medicinal plants. *Journal of international chemical technology Research* 3, 1394-1402.
- Seleem, D., Pardi, V., Murata, R.M. 2017. Review of flavonoids: A diverse group of natural compounds with anti-*candida albicans* activity in vitro. *Archives of Oral Biology*. 76, 76-83.
- Sima, C.P.C., Dashpera, S.G., Reynolds, E.C. 2016. Oral microbial biofilm models and their application to the testing of Anticariogenic agents. *Journal of Dentistry* 50, 1-11.
- Singh, R., Lillard, J.W. 2009. Nanoparticle-based targeted drug delivery. *Experimental and Molecular Pathology* 86, 215-223.
- Singh, S. 2011. Dental caries in South Africa: Implications for oral health planning. *South African Journal of Epidemiology and Infection* 26, 259-261.
- Singh, M, Kaur, M., Silakari, O. 2014. An important scaffold for medicinal chemistry. *European Journal of Medicinal Chemistry* 84, 206-239.
- Stephan, R.M., Miller, B.F. 1943. A quantitative method for evaluating physical and chemical agents which modify production of acids in bacterial plaques on human teeth. *Journal of Dental Research* 22, 45-51.
- Sun, X., Xu, Chun., Wu, G., Ye, O., Wang, C. 2017. Poly (lactic-co-glycolic acid): Applications and future prospects for periodontal regeneration. *Polymers* 9, 189.
- Takahashi, N. 2005. Microbial ecosystem in the oral cavity: metabolic diversity in an ecological niche and its relationship with oral diseases. *International Congress Series* 1284, 103-112.

- Tantra, R., Schulze, P., Quincey, P. 2010. Effect of nanoparticle concentration on zeta potential measurement results and reproducibility. *Particuology* 8, 279-285.
- Tanzer, J.M., Livingston, J., Thompson, A.M. 2001. The microbiology of primary dental caries in humans. *Journal of Dental Education* 65, 1028-1037.
- Tapsoba, H., Deschamps J. 2006. Use of medicinal plants for the treatment of oral diseases in Burkina Faso. *Journal of Ethnopharmacology* 104, 68-78.
- Teffo, L.S., Aderogba, M.A., Eloff, J.N. 2010. Antibacterial and antioxidant activities of four kaempferol methyl ethers isolated from *dodonaea* Jacq. var. *angustifolia* leaf extracts. *South African Journal of Botany* 76, 25-29.
- Touger-Decker, R., Van Loveren, C., 2003. Sugars and dental caries. *American journal of clinical nutrition* 78, 88-92.
- Tuberoso, C.I.G., Montoro, P., Piacente, S., Corona, G., Deiana, M., Dessì, M.A., Pizza, C., and Cabras, P. 2009. Flavonoid characterization and antioxidant activity of hydroalcoholic extracts from *Achillea ligustica*. *Journal of Pharmaceutical Biomedical Analysis* 50, 440-448.
- Umamaheswaril, P., Basha, S.K., Narasimhamurthy, C.V., 2015. GC-MS analysis of *Dodonaea viscosa* (l), leaf extract. *Advance Research Journal of Biological Sciences and Molecular Techniques* 1, 1-7.
- Virlan, M.J.R., Miricescu, D., Totan, A., Greabu, M., Tanase, C., Sabliov, C.M., Caruntu, C., Calenic, B. 2015. Current uses of poly (lactic-co-glycolic acid) in the dental field: a comprehensive review. *Journal of Chemistry* 2015, 1-12.
- Wang, Y., Dave, R.N., Pfeffer, R., 2014. Polymer coating/encapsulation of nanoparticles using a supercritical anti-solvent process. *The Journal of Supercritical Fluids* 28, 85-99.
- Wang, Y., Li, P., Tran, T.T., Zhang, J., Kong, L. 2016. Manufacturing techniques and surface engineering of polymer-based nanoparticles for targeted drug delivery to cancer. *Nanomaterials (Basel)* 6, 26.

- Whiley, R.A., Beighton, D. 1998. Current classification of oral streptococci. *Oral microbiology and immunology* 13, 193-216.
- Xiao, J., Zuo, Y., Liu, Y., Li, J., Hao, Y., Zhou, X. 2007. Effects of *Nidus vespae* extract and chemical fractions on glucosyltransferases, adherence and biofilm formation of *Streptococcus mutans*. *Archives of Oral Biology* 52, 869-875.
- Zabokova-Bilbilova, E., Bajraktarova, B., Sotirovska-Ivkovska, A. 2007. A field analysis of buffer value of bicarbonate in saliva. *Balkan Journal of Stomatology*, 11, 167-170.
- Zhang, K., Tang, X., Zhang, J., Lu, W., Lin, X., Zhang, Y., Tian, B., Yang, H., He, H. 2014. PEG-PLGA copolymers: Their structure and structure-influenced drug delivery applications. *Journal of Controlled Release* 183, 77-86.
- Zhang, B., Lung, P. S., Zhao, S., Chu, Z., Chrzanowski, Li, Q. 2017. Shape dependent cytotoxicity of PLGA-PEG nanoparticles on human cells. *Scientific Reports* 7, 7315.
- Zero, D.T., Fontana, M., Martínez-Mier, E.A., Ferreira-Zandoná, A., Ando, M., González Cabezas, C., Bayne, S. 2009. The biology, prevention, diagnosis and treatment of dental caries: scientific advances in the United States. *The Journal of the American Dental Association* 140, 25-34.
- Zonyane, S., Van Vuuren, S.F., Makunga, N.P. 2013. Antimicrobial interactions of Khoi-San poly-herbal remedies with emphasis on the combination; *Agathosma crenulata*, *Dodonaea viscosa* and *Eucalyptus globulus*. *Journal of Ethnopharmacology* 148, 144-151.

CHAPTER 7

APPENDICES

Appendix I: Preparation of media and its composition

Tryptone soya broth

30g Tryptone soya broth

1000ml Distilled water

Thirty grams of Tryptone broth was dissolved in distilled water and boiled for 1minute thereafter the media was autoclaved at 121°C for 15minutes.

5% Sucrose broth

30g Tryptone

0.6g Sucrose

1000ml Distilled water

The solids products (39g tryptone and 0.6g sucrose) were first boiled in 500ml distilled water to dissolve thereafter the remaining water was added to the mixture and boiled then autoclaved at 121°C for 15minutes.

Blood agar

39g Columbia agar (Oxoid Ltd, UK)

1000ml Distilled water

5g Sterile defibrinated blood

Thirty-nine grams of Columbia agar base was suspended in 1000ml of distilled water. The suspension was boiled to dissolve the powder completely. It was sterilized by autoclaving at 121°C for 10minutes. The media was then allowed to cool to 50°C, then 5% sterile

defibrinated blood was added. The media was then poured into petri dishes and allowed to set. The plates were then refrigerated.

Human cell culture medium (DMEM)

88%	Dulbeco's modified eagles's medium
10%	Fetal calf serum
1%	L-glutamine
1%	Streptomycin
1%	Penicillin

Dulbeco's modified eagle's medium was supplemented with 10% fetal calf serum, 1% L-glutamine and antibiotics (1% streptomycin and 1% penicillin).

Phosphate buffered saline

8g	Sodium chloride
0.24g	Potassium hydrogen phosphate
0.2g	Potassium chloride
1.44g	Sodium hydrogen phosphate
800ml	Distilled water

Sodium chloride, potassium hydrogen phosphate, potassium chloride, sodium hydrogen phosphate were suspended in 800ml distilled water and autoclaved at 121°C for 15 minutes.

1X Trypsin-EDTA solution

0.05%	Trypsin
0.5Mm	EDTA
1X	Phosphate suffered saline

Semi-solid media

1.125g Columbia agar base

100ml Distilled water

Columbia agar base (42g) media was dissolved in 100ml of distilled water, boiled and autoclaved at 121°C for 15minutes.

Appendix II: Ethical clearance letter

Human Research Ethics Committee (Medical) 50 years 1966 – 2016

Research Office Secretariat: Faculty of Health Sciences, Phillip Tobias Building, 3rd Floor, Office 301, 29 Princess of Wales Terrace, Parktown, 2193 Tel +27 (0)11-717-1252 /1234/2656/2700
Private Bag 3, Wits 2050, email: zanele.ndlovu@wits.ac.za
Office email: hrec-medical.researchoffice@wits.ac.za
Website: www.wits.ac.za/research/about-our-research/ethics-and-research-integrity/



Ref: W-CJ-170713-2

13/07/2017

TO WHOM IT MAY CONCERN:

Waiver: This certifies that the following research does not require clearance from the Human Research Ethics Committee (Medical).

Investigators: Miss M A Sebelemetja (student no. 1819566), Prof M Patel, Dr S Moeno.

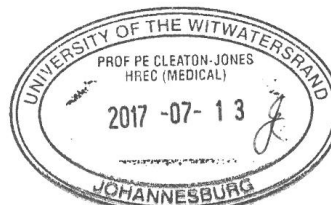
Project title: Anticariogenic properties of *Dodonaea viscosa* var. *augustifolia* derived flavone stabilised nanoparticles.

Reason: This laboratory study uses bacterial cultures of *Streptococcus mutans* and oral epithelial cells. The cultures of *Streptococcus mutans* were isolated in a previous study M10205. There are no human participants.

A handwritten signature in black ink, appearing to read 'Peter Cleaton-Jones'.

Professor Peter Cleaton-Jones

Chair: Human Research Ethics Committee (Medical)



Copy – HREC (Medical) Secretariat: Zanele Ndlovu, Rhulani Mkansi, Lebo Moeng.

Appendix III: Modification of Ethical clearance waiver

UNIVERSITY OF THE
WITWATERSRAND,
JOHANNESBURG



HUMAN RESEARCH ETHICS COMMITTEE
(MEDICAL)

18 February 2019

Mpho Sebelemetja

Sent by email to: 1819566@students.wits.ac.za

Dear Mpho Sebelemetja

Re: Protocol Ref No: W-CJ-17013-2

Protocol Title: Anticariogenic properties of *Dodonaea viscosa* var. *angustifolia* derived flavone stabilised nanoparticles

Principal Investigator: Mpho Sebelemetja et al

Protocol Amendment: Modification of cells used

This letter serves to confirm that the Chairperson of the Human Research Ethics Committee (Medical) has approved the protocol amendment for the above-mentioned protocol, as detailed in your letter, dated 21 January 2018.

The following documents were received:

- Summary Letter
- Waiver certificate

Thank you for keeping us informed and updated.

Yours Sincerely,

A handwritten signature in blue ink, appearing to read 'J. Ndlangamandla', written over a dotted line.

Mr Joshua Ndlangamandla
Administrative Officer
Human Research Ethics Committee (Medical)



Appendix IV: Cell count worksheet

APPENDIX 1: CELL COUNT WORKSHEET FOR SEEDING CELLS

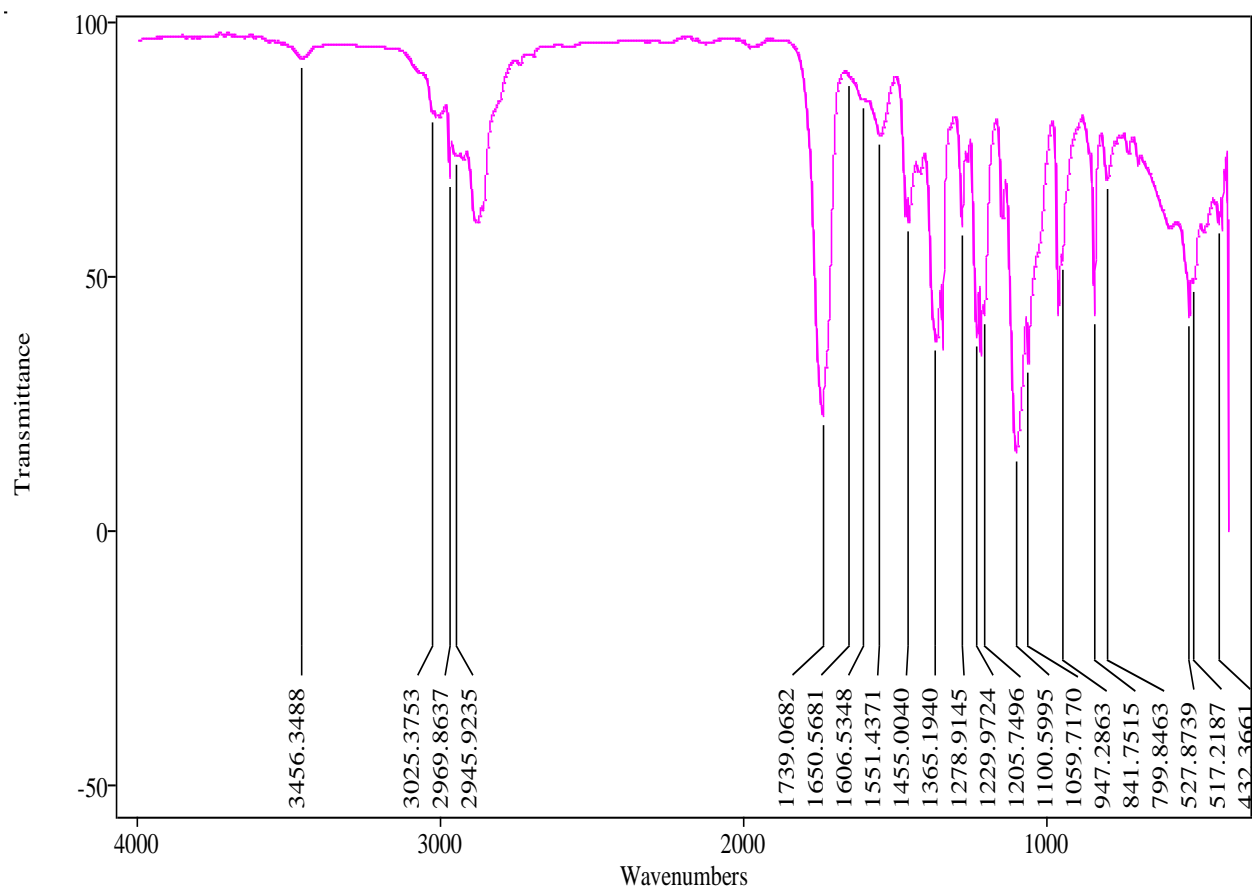
Cell type <u>Hep 2</u>									
Passage number <u>46</u>									
<p>Viable (a, c, e, & g) & non-viable (b, d, f, h) cells per square</p> <p>- Count the 4 outer squares and record readings accordingly</p>	<table border="1"> <tr> <td>a-viable 49</td> <td>b-non-viable 7</td> <td>c-viable 51</td> <td>d-non-viable 7</td> </tr> <tr> <td>e-viable 63</td> <td>f-non-viable 12</td> <td>g-viable 70</td> <td>h-non-viable 12</td> </tr> </table>	a-viable 49	b-non-viable 7	c-viable 51	d-non-viable 7	e-viable 63	f-non-viable 12	g-viable 70	h-non-viable 12
a-viable 49	b-non-viable 7	c-viable 51	d-non-viable 7						
e-viable 63	f-non-viable 12	g-viable 70	h-non-viable 12						
<p>Calculation of viability</p> <p>= Total viable cells (a+c+e+g) / total cells (a+b+c+d+e+f+g+h) x 100</p> <p>* Suitable viability is 80%</p>	<p>(total viable) $\frac{233}{271}$</p> <p>(total)</p> <p><u>86</u> %</p>								
<p>Cell count (cells/ml)</p> <p>= Total viable / 4 squares</p> <p>x 2 (Trypan dilution) x 10⁴ (surface area)</p>	<p>= $\frac{233}{4} \times 2 \times 10^4$</p> <p>= <u>116.5 x 10⁴</u> cells / ml</p>								
<p>Required cells for seeding (i.e. cell dilutions)</p> <p>Dilution = Want $\frac{5 \times 10^4}{116.5 \times 10^4}$</p> <p>= <u>23.3</u></p>	<p><u>1.0</u> l/s Cell suspension</p> <p>+</p> <p>$\frac{23.3}{230.3} \times 116.5$ Growth media</p> <p>= $\frac{23.3}{230.3} \times 116.5$</p>								
Name / signature	<u>Nenolia Mombane</u>								
Date	<u>10.10.2018</u>								

In the event of a dispute concerning this document, the electronic version stored on Q-Pulse will be deemed to be the correct version

National Health Laboratory Service- All rights reserved

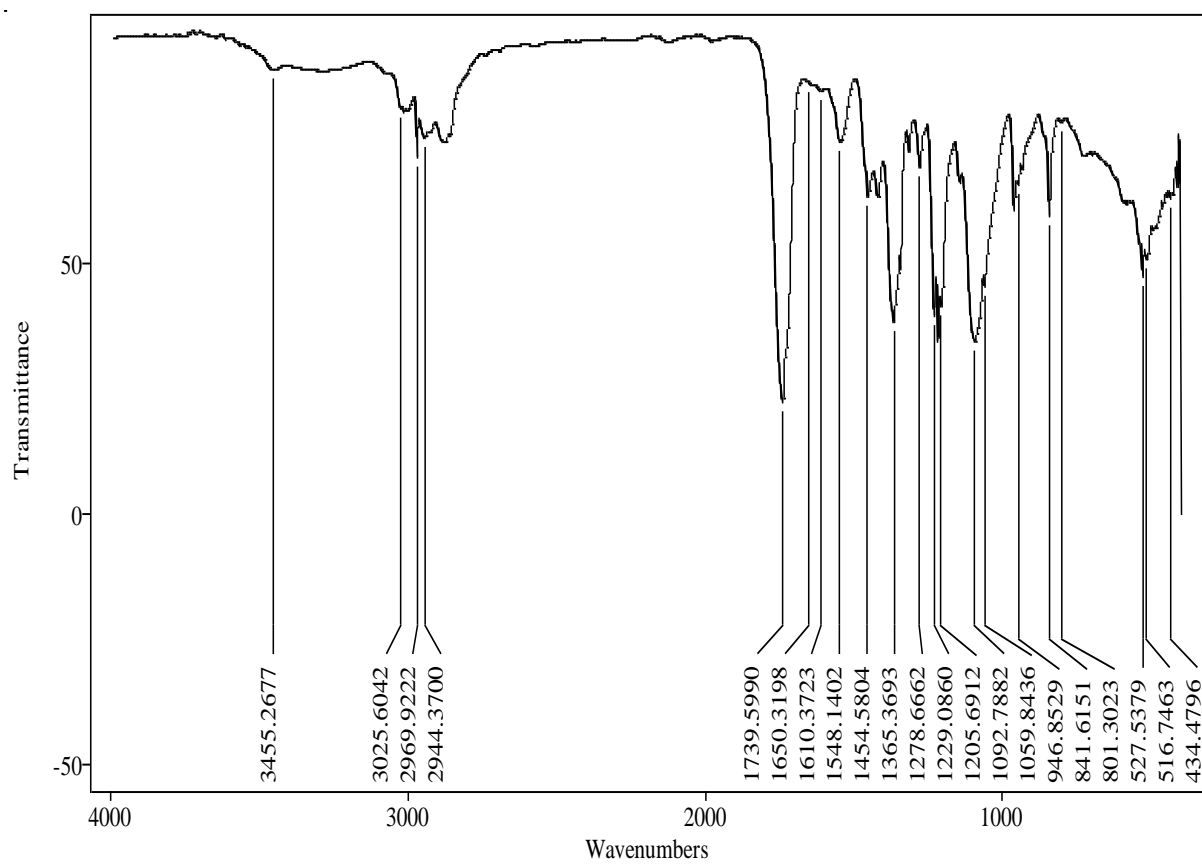
Appendix V: Fourier Transform Infrared spectroscopy analyses PLGA-PEG Copolymers

Sample Filename	PLGA-PEG Copolymer.CSV
File Title	Column 1
Date	Tue Dec 18 12:47:11 2018



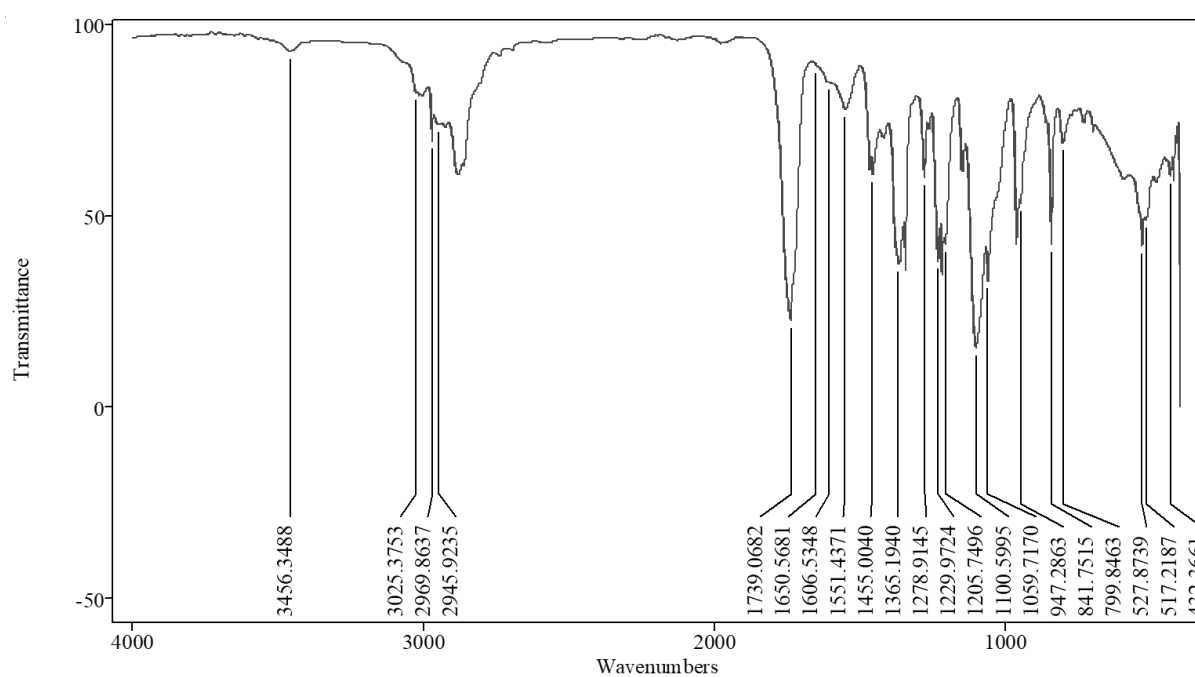
Appendix VI: Fourier Transform Infrared spectroscopy analyses F5.1

Sample Filename	F5.1.CSV
File Title	Column 1
Date	Tue Dec 18 12:49:38 2018



Appendix VII: Fourier Transform Infrared spectroscopy analyses of Blank nanoparticles

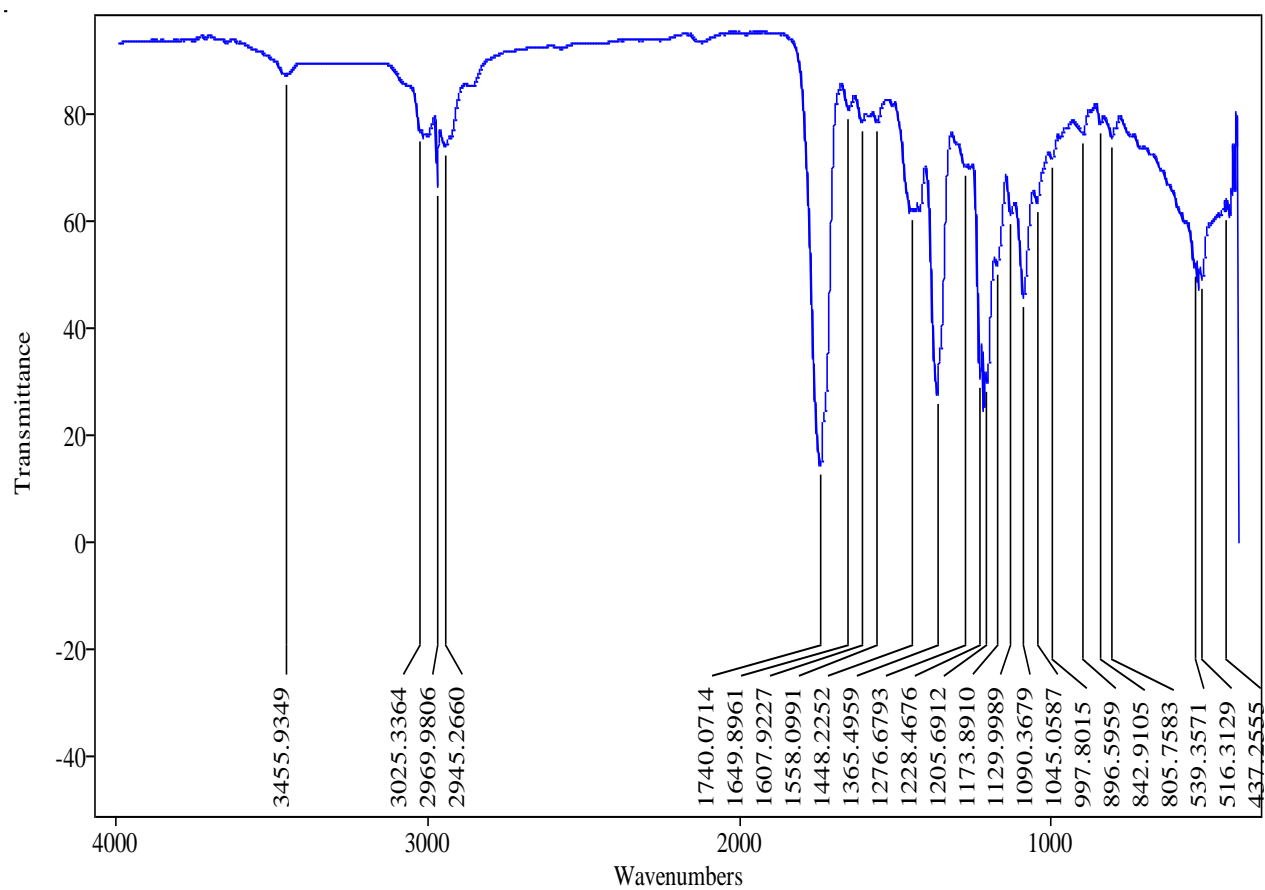
Sample Filename	PLGA-PEG Blank.CSV
File Title	Column 1
Date	Tue Dec 18 12:37:11 2018



Appendix VIII: Fourier Transform Infrared spectroscopy analyses PLGA-PEG

F5.1NPs

Sample Filename	PLGA-PEG F5.1NPs.CSV
File Title	Column 1
Date	Tue Dec 18 12:38:55 2018



Appendix IX: Abstract for the conference presentation

Anticariogenic properties of *Dodonaea viscosa* var. *angustifolia* flavone stabilized nanoparticles

Mpho Sebelemetja¹, Sharon Moeno¹, Mrudula Patel¹

¹Department of Oral Biological Sciences, School of Oral Health Sciences, University of The Witwatersrand, South Africa.

Abstract

Introduction: Dental caries is the most important oral infection. It is caused by *Streptococcus mutans* due to its ability to form biofilm and the production of acids in the oral cavity. Many oral hygiene products containing antimicrobial chemicals are used to control and prevent dental caries. Medicinal plants have been investigated for their ability to prevent dental caries. *Dodonaea viscosa* var. *angustifolia*, has been found to have this property. However, beneficial concentrations are difficult to maintain in the oral cavity due to continual saliva flow which can be overcome using nanotechnology. **Aim:** The aim of this study was to investigate the anticariogenic and slow release properties of *Dodonaea viscosa* var. *angustifolia* (DVA) derived flavone stabilized polymeric nanoparticles. **Methods:** Crude extract prepared from DVA leaves was fractionated to produce subfractions and the beneficial subfraction (F5.1) was identified.

Polymeric nanoparticles (PLGA-PEG) were prepared, stabilized with the DVA subfraction (F5.1/NPs) and characterized. Anti-*streptococcus mutans* and anti-acidogenic properties were determined.

The subfraction release profile (substantivity) was determined. Results were analyzed using the Wilcoxon sum test (Mann-Whitney). **Results:** The results showed that subfraction stabilized nanoparticles had anti-*streptococcus mutans* property with a median MIC value of 1.56 mg/ml. Subinhibitory concentrations of these nanoparticles significantly reduced the acid production in *S. mutans* ($p < 0.02$). The retention and slow release of the beneficial compound was detected up to 12 hours, reaching 0.1 mg/ml concentration at pH 7.4 after 4 hours and at pH 5.5 after 5 hours. **In conclusion**, the DVA flavone containing subfraction stabilized nanoparticles showed anticariogenic activity with improved substantivity. Therefore, it has potential to be used to control dental caries.

Key words: *S. mutans*; caries; acidogenicity; *D. angustifolia*; flavone; nanoparticles; PLGA-PEG